ORAU TEAM
Dose Reconstruction
Project for NIOSH

Oak Ridge Associated Universities | NV5|Dade Moeller | MJW Technical Services

DOE Review Release 04/12/2021

Breathing Zone to General Area Air Concentration Ratios in Small Workrooms	ORAUT-RPRT-0097	Rev. 00
	Effective Date:	03/29/2021
	Supersedes:	None

Subject Expert(s): Brian P. Gleckler and Thomas R. LaBone

Document Owner Approval:	Signature on File Brian P. Gleckler, Document Owner	Approval Date:	03/24/2021
Concurrence:	Pat McCloskey Signature on File for Michael S. Kubiak, Objective 4 Manager	Concurrence Date:	03/24/2021
Concurrence:	Vickie S. Short Signature on File for Kate Kimpan, Project Director	Concurrence Date:	03/29/2021
Approval:	Signature on File Timothy D. Taulbee, Associate Director for Science	Approval Date:	03/29/2021

FOR DOCUMENTS MARKED AS A TOTAL REWRITE, REVISION, OR PAGE CHANGE, REPLACE THE PRIOR REVISION AND DISCARD / DESTROY ALL COPIES OF THE PRIOR REVISION.

☒ New ☐ Total Rewrite ☐ Revision ☐ Page Change

PUBLICATION RECORD

EFFECTIVE DATE	REVISION NUMBER	DESCRIPTION
03/29/2021	00	New document initiated to evaluate the data from several air sampling studies performed in small workrooms. The air sample data were evaluated in terms of breathing zone air concentrations and air concentrations measured from general area air samplers. A statistical evaluation of the potential ratios of the breathing zone air concentrations and the general area air concentrations is presented in this document. Incorporates formal internal and NIOSH review comments. Training required: As determined by the Objective Manager. Initiated by Brian P. Gleckler.

TABLE OF CONTENTS

LIST OF TABLES

LIST OF FIGURES

FIGURE   **TITLE**   **PAGE**

ACRONYMS AND ABBREVIATIONS

AC	air change
AMAD	activity median aerodynamic diameter
AWE	atomic weapons employer
BD	breathing zone dilution factor
BZ	breathing zone
CAM	continuous air monitor
CEA	Commissariat à l'Énergie Atomique
cfm	cubic feet per minute
cm	centimeter
CMAD	count median aerodynamic diameter
DOE	U.S. Department of Energy
ft	foot
g	gram
GA	general area
GM	geometric mean
GSD	geometric standard deviation
hr	hour
in.	inch
kg	kilogram
LANL	Los Alamos National Laboratory
LPC	laser particle counter
m	meter
min	minute
mm	millimeter
MMAD	mass median aerodynamic diameter
NIOSH	National Institute for Occupational Safety and Health
ORAU	Oak Ridge Associated Universities
PAS	personal air sampler
ROS	regression on order statistics
s	second
SAS	stationary air sampler
SRDB Ref ID	Site Research Database Reference Identification (number)
SRS	Savannah River Site
µCi	microcurie
µg	microgram
µm	micrometer

1.0 PURPOSE AND SCOPE

The purpose of this report is to evaluate the relationship between the general area (GA) and breathing zone (BZ) air concentrations for small workrooms and to determine if adjustments to the GA air concentrations are necessary to make them equivalent to the BZ air concentrations in a small workroom. Therefore, the scope of the report is limited to small workrooms. Air concentrations that are representative of the air breathed by the workers (i.e., BZ air concentrations) are needed to assess inhalation intakes of those workers when bioassay data are not available. Application of the BZ:GA ratio information within this report should be justified on a case-by-case basis, as discussed in Sections 2.0 and 11.0.

In this report, the term "workroom" refers to a work location having a single discernable airspace. Similarly, the term "test room" refers to a mockup of a real or hypothetical work location having a single discernable airspace. As used in this report, the term "significant" means "practically significant" as opposed to "statistically significant." In other words, in this report "significant" means that the difference (effect size) is large enough to influence how a parameter is used or treated in practice. In addition, the relationships between BZ and GA air concentrations were evaluated in terms of BZ:GA air concentration ratios, which are abbreviated as BZ:GA ratios throughout the remainder of this report.

2.0 INTRODUCTION

In any workroom where there is complete air mixing, the concentration of respirable airborne radioactive material would be homogeneous throughout the airspace. In such a room, the air concentration measured at any location within the room would be the same, and there would be no significant difference between the BZ air concentration and the GA air concentration. However, complete air mixing is rarely possible or practical, for a number of reasons, which results in differences between the air concentrations measured at various locations throughout the room. When the mixing of the air in the room becomes less and less complete, the variability between air concentrations throughout the room increases, resulting in a distribution of BZ:GA ratios. As mixing becomes less complete, the central tendency of this distribution (the median) can shift away from 1 and the spread of the distribution (the geometric standard deviation [GSD]) can increase. When the median of the BZ:GA ratio distribution becomes significantly greater than 1 or the GSD becomes large, the GA air concentration should be adjusted to account for the increased uncertainty in the BZ air concentration.

As indicated in Section 1.0, the use of the BZ:GA ratio information in this report is intended to be justified on a case-by-case basis. Because there are so many potential parameters and scenarios that could have a significant effect on the BZ and GA air concentrations for a given workroom, it is important for the user of this BZ:GA ratio information to justify its use for their specific application.

The subsections below identify the key parameters that were considered when evaluating the relationship between the GA and BZ air concentrations for this report. Those parameters could be grouped into two groups: (1) ones that affect the level of mixing of an aerosol and (2) ones that only affect the BZ:GA ratio. Section 3.0 and the sections discussing the evaluated studies provide the details about how these parameters were addressed for the purposes of this report.

2.1 PARAMETERS AFFECTING LEVEL OF MIXING

The parameters that affect the level of mixing are important because less mixing tends to lead to larger air concentration gradients, which have a significant and direct effect on BZ:GA ratios and the GA air concentrations in a workroom. When looking to apply BZ:GA ratios to GA air concentrations to make them equivalent to BZ air concentrations, the analysis should consider the parameters that

affected the level of mixing in both the source of the BZ:GA ratios and for the room where the GA air samples were collected. Ideally, the parameters affecting the level of mixing for the source of the BZ:GA ratios would be comparable to the location where the GA air samples were collected. Unfortunately, that is often impractical or impossible, unless the BZ:GA ratios were based on the same room and conditions that the GA air samples were collected in. However, using BZ:GA ratios that have a basis that encompasses the parameters for the room where the GA air samples were collected is one of the next best options. Proper determination and application of BZ:GA ratios supports good decision-making about potential inhalation intakes of workers and associated steps to protect worker health.

The level of mixing of an aerosol within a workroom is dependent on a large number of parameters. However, the following four parameters tend to affect the level of mixing the most: (1) the size of the room, (2) the particle size distribution of the aerosol, (3) the ventilation rate, and (4) room complexity. The following subsections address each of these potentially significant parameters in more detail.

2.1.1   Size of the Room

Total workroom or air space volume is a key parameter that usually influences how much an aerosol can or cannot be dispersed. However, with the exception of rooms where elevated releases above the typical breathing zone can occur, a room's height is usually less of a factor influencing the aerosol concentration than its other dimensions, because of gravitational settling. Therefore, in most instances room sizes can be compared in terms of area for determining applicability of the BZ:GA ratio information in this report to a specific room. For the purposes of this report, elevated releases are considered to be above the typical BZ elevations and can include releases originating at a lower elevation that are propelled above the typical BZ elevations (e.g., jet releases, over-pressurization releases, aerosol plumes lofted by heat source etc.).

2.1.2   Particle Size Distribution of the Aerosol

Because only respirable size particles (i.e., those particles with aerodynamic diameters smaller than about 20 μm [ICRP 2015]) contribute to inhalation intakes, only the respirable fraction of an aerosol is of interest for assessing the inhalation intakes of workers. Therefore, the ideal air sample measurements for assessing a worker's inhalation exposure would discriminate against collecting nonrespirable particles. However, most routine air sampling systems used at atomic weapons employer (AWE) and U.S. Department of Energy (DOE) sites (including the DOE predecessor agencies) did not include particle sizing or particle discrimination devices to eliminate the nonrespirable particles from being collected on the air sample. Because of that, most air samples collected at AWE and DOE sites included both the respirable and nonrespirable particles that were present. The presence of larger nonrespirable particles on any air sample being used to estimate a worker's inhalation intake, whether it is a BZ or GA air sample, could result in an unreasonable overestimate of the worker's intake.

In addition, air samples collected closer to the release location are more likely to collect larger nonrespirable particles, because the larger particles do not travel with air currents as far as the smaller respirable particles. One of the major causes of that is the terminal settling velocity for different size particles because the terminal settling velocity increases rapidly with particle size. For particles of the same composition, the terminal settling velocity increases proportionally to the square of the particle diameter (Hinds 1982, p. 35). Based on that, a 10-μm diameter particle has a terminal settling velocity that is 100 times faster than a 1-μm diameter particle. A nonrespirable 100-μm particle would settle 10,000 times faster than a 1-μm diameter particle. Even though there can be a number of potential causes or contributing causes to the discrepancies between BZ and GA air concentrations, the presence of nonrespirable particles is often a cause of discrepancy between BZ and GA air concentrations.

2.1.3   Ventilation Rate

The ventilation rate in terms of air changes (ACs) per unit time, usually in units of AC/hr, is a removal constant for the aerosol within a workroom. This removal constant is directly related to the depletion of the aerosol from an acute, constant, or variable release of aerosol and can be used to estimate the average air concentration at different points in time when the release quantity (instantaneous/puff releases) or release rate (longer term releases) along with several other parameters are known. This can be done using linear first-order kinetics equations as described in Skrable (1974). However, those kinetics calculations are based on a simple model that does not account for factors encountered in more complex rooms (e.g., air streaming, dead air spaces, eddy currents, etc.).

2.1.4   Room Complexity

Factors contributing to the complexity of a workroom include room layout, obstructions, heat sources, room ventilation inlet and outlet locations, local exhaust locations, and general flow directions. All of these affect the airflow patterns and level of mixing within a room. These things tend to cause air streaming, dead air spaces, eddy currents, etc. within a room, which result in larger air concentration gradients. The more complex a room is, the more likely one is to encounter larger air concentration gradients.

In combination with air velocity, the direction of the incoming and outgoing air can have a significant effect on the level of mixing. In some situations, this can enhance the level of mixing; in other situations this can cause extreme air concentration gradients within a workroom. It should be noted that ventilation systems designed to minimize worker exposures often cause the largest air concentration gradients and vice versa. In most instances, only the flow rates are typically known when assessing past events and information about the room air vent sizes and orientations (directions) are often unknown. Therefore, it is often impossible to assess how these two aspects of the ventilation would have affected the BZ and GA air concentrations during past events.

More recently, much more sophisticated computational fluid dynamics models have been used to model aerosol releases and the resulting air concentrations throughout a workroom over a period of interest. The computational fluid dynamics models can provide air concentration estimates in three dimensions. However, those more sophisticated models require a detailed knowledge of the room being evaluated. When reconstructing worker exposures that occurred in the past, many of the needed details on the rooms where exposures occurred are unknown, making it impossible to adequately model those areas to determine what the air concentration gradients were. Therefore, the use of BZ:GA ratios as a means for accounting for the differences between BZ and GA air concentrations is one of the next best options.

2.2   PARAMETERS ONLY AFFECTING BZ:GA RATIOS

The parameters discussed in this section do not have any effect on the level of mixing but can have a significant effect on the BZ:GA ratio distribution. As discussed in the following subsections, two parameters that could have the most impact on the BZ and GA samples and resulting BZ:GA ratio distribution are sampler and release locations and low number concentrations of dominant aerosol particles.

In addition to the parameters discussed in the sections below, there are numerous other parameters and factors that can affect the differences between the measured BZ and GA air concentrations, but most of them have to do with issues or errors associated with the collection and analysis of the individual air samples (e.g., not accounting for natural radioactivity, self-shielding of activity on a sample, sample contamination, sample flow rates, etc.). The subject of sample collection, sample analysis, and their potential measurement errors is a major subject and beyond the scope of this

report. Therefore, it is assumed that the user of this report is already familiar with that subject and no further details are provided here. When details about the collection and analysis of individual samples are available, those parameters should also be considered when evaluating the relationship between the GA and BZ air concentrations. However, in documented air sampling studies, such details about individual samples are usually not included in the reports on the studies. When those details are unavailable, it should be reasonable to assume that there were no significant and unresolved sample collection or analysis issues or errors with the reported air sample data.

2.2.1   Sampler and Release Locations

When mixing is not complete, which is often the case, the following three spatial parameters and their locations, in relation to each other and in relation to the location of workroom ventilation inlets and outlets and obstructions, can have a significant effect on the BZ:GA ratio distribution: (1) the location of the worker (i.e., the BZ location), (2) the GA air sampler location, and (3) the location of the release point for the radioactive material. Therefore, when evaluating the differences between BZ and GA air concentrations, consideration should be given to where these three things were located in relation to each other. It is also important to understand any work activities that may cause the worker to position their direct breathing zone much closer to a source than their BZ sampler, for example, within an equipment enclosure or local ventilation shroud during an inspection or maintenance operation.

2.2.2   Low Number Concentrations of Dominant Aerosol Particles

Low numbers of airborne radioactive particles in a workroom are normally a good thing and a desirable condition for the workplace atmosphere. However, when those low-in-number radioactive particles have a relatively high specific activity and radiotoxicity (i.e., what will be referred to for the purposes of this report as "dominant particles"), that condition can become very problematic and have a very adverse effect on the ability to collect meaningful and reproducible air samples. When the numbers of the radioactive particles are too low, both BZ and GA air sampling becomes a stochastic process versus a deterministic process because there just are not enough radioactive particles to go around (Scott, Hoover, and Newton 1997; Scott and Fencl 1999; Scott et al. 2001; Aden and Scott 2003). In a discussion about personal air samplers (PASs), Strong (1988) indicated that "the personal air sampler behaves as a statistical sampling device when operated in an environment having only a few to a few tens of particles per m^3." Because this normally is not a significant issue of concern for lower specific activity and less radiotoxic particles, the following discussions are only relevant to situations when the low-in-number radioactive particles have a relatively high specific activity and radiotoxicity.

Discussions of the dominant particle phenomena have predominately been found in the reports for air sampling studies in the United Kingdom during the 1960s, such as in Sherwood (1966), and Lister (1967), and later in Jones et al. (1983). A few more recent references to these phenomena have been found in studies in the United States. Munyon and Lee (2002), a study evaluated for this report, includes a brief discussion on the "... dominant or single particle phenomena...." Other reports from the Lovelace Respiratory Research Institute address the difficulties of assessing the intakes and internal doses from the inhalation of dominant particles, which are referred to as the stochastic exposure paradigm and stochastic intake paradigm in those reports (Scott and Fencl 1999; Scott et al. 2001; Aden and Scott 2003). The available literature also indicates that dominant particles have a relatively high specific activity and are relatively few in number in comparison with the other particles in the radioactive aerosol being dispersed (Sherwood 1966; Lister 1967; Scott et al. 2001; Munyon and Lee 2002; Aden and Scott 2003). Fortunately, there is nothing to indicate the dominant particle phenomena was widespread, and most of the known radiological workrooms that had air sampling issues attributable to the presence of dominant particles were in the United Kingdom.

The presence of dominant particles can normally only be confirmed by autoradiograph analysis of the air samples, which is not a routine type of analysis. At best, autoradiographs are sometimes performed as part of a special air sampling study. Therefore, it is unlikely that any dominant particle information will be available for a given workroom.

The presence of dominant particles makes the following two scenarios likely, neither of which include an air sample that is representative of the air that was inhaled by the worker. Further, the more the low-in-number particles are dispersed from their point of origin in a workroom, the farther apart they are and the more likely these two scenarios become. An indication that these two scenarios might have occurred at a facility is when there is a lack of correlation between the air sample results and the bioassay results from that facility, which was one of the observations reported in Jones et al. (1983).

1. A dominant particle was collected on the air sample when the worker did not inhale one (i.e., no intake occurred). When air sample results are being used to estimate worker intakes, this scenario results in significant intakes being assessed when none actually occurred. For particles of the same material, radionuclide composition, and specific activity, the scale of that overestimate is proportional to the difference in the volumes of the dominant particles. Therefore, the overestimation can increase dramatically as the size of the dominant particle increases. For example, a single 10-μm diameter dominant particle on an air sample will yield an intake overestimate that is 1,000 times greater than the overestimated intake from a single 1-μm diameter dominant particle.

2. The worker inhales a dominant particle but one was not collected on the air sample. When this scenario occurs, the air sample fails to detect a potentially significant intake and any intakes based on that air sample result are underestimated.

Because of these two scenarios and because of the stochastic nature of sampling airborne radioactive particles that are low in number, air sample data from workrooms with dominant particles are very unreliable. If an air sample result from an area with dominant particles is needed to assess worker exposures, Scott and Fencl (1999) indicates that intake distributions can and should be calculated to account for the stochastic nature associated with sampling and inhaling those particles. However, based on that guidance, one would need to know many details about the dominant particles in a given room to perform the intake distribution calculations, and much of that information is often unavailable for performing retrospective dose reconstructions. Therefore, the Oak Ridge Associated Universities (ORAU) Team does not recommend using air sample data from workrooms known to have dominant particles for developing BZ:GA ratios.

3.0 STUDIES EVALUATED

This report evaluates the air sample data from the five air sampling studies discussed in Sections 4.0 through 8.0. The rooms in each of those studies are considered to be small rooms. The room size information for the evaluated studies is provided in Table 3-1. The room sizes in the evaluated studies ranged from 17.6 m^2 to 105 m^2 (190 ft^2 to 1,130 ft^2).

As the workroom size increases beyond the sizes in Table 3-1, there is a point where it will no longer be appropriate to use the BZ:GA ratio information in this report. Conversely, as the workroom size decreases below the sizes in Table 3-1, there is likely a point where the BZ and GA air concentrations are equivalent and no adjustment to the GA air concentration is needed. It is beyond the scope of this report to determine where those points are. The more a workroom size exceeds the room sizes in the evaluated studies, the more difficult it will be to conclude that the BZ:GA ratio information in this report is applicable to that room.

Table 3-1. Room sizes for the evaluated studies.

Study	Room dimensions[a] (m, ft)	Room area (m², ft²)	Room volume[b] (m³, ft³)
Gonzales et al. (1974)	6.1 × 6.1 × 2.4, 20 × 20 × 8	37.2, 400	89.3, 3,200
Charuau (1987)	15 × 7 × 4.5, 49 × 23 × 15	105.0, 1,130	472.5, 16,686
Munyon and Lee (2002)	4.9 × 3.6 × 2.4, 16 × 12 × 8	17.6, 190	42.3, 1,495
Scripsick et al. (1979b)	9.0 × 6.3 × 4.1, 30 × 21 × 13	56.7, 610	232.5, 8,211
Whicker and Moxley (2001)[c]	6 × 4 × 3, 20 × 13 × 10	24.0, 258	72.0, 2,542

a. The dimensions are provided in terms of length × width × height.
b. This room volume is the overall room volume, and does not account for large obstructions in the room such as equipment and gloveboxes. Therefore, it might not represent the actual volume of the airspace.
c. Room dimensions for the Whicker and Moxley (2001) study were obtained from Whicker, Rodgers, and Moxley (2003).

In addition, because only respirable size particles contribute to inhalation intakes, only studies with documented aerosol sizes that are considered respirable were evaluated for this report. The presence of larger nonrespirable particles on any air sample being used to estimate a worker's intake, whether it is a BZ or GA air sample, would result in a significant overestimate of the worker's intake. Air samples collected closer to the release location are more likely to collect larger nonrespirable particles, because those particles do not travel as far as the smaller respirable particles. Even though there can be a number of potential causes or contributing causes to the discrepancies between BZ and GA air concentrations, the presence of nonrespirable particles is also often the cause of the discrepancies between BZ and GA air concentrations, which would influence the BZ:GA ratios. Therefore, the inclusion of studies with air sample data that potentially included particles of sizes much larger than the respirable size range could generate BZ:GA ratios that would cause an unreasonable overestimate of the workers' intakes. Table 3-2 summarizes the particle size distributions associated with each of the evaluated studies.

Table 3-2. Summary of the particle size distributions for each study.[a]

Study	Particle size distributions	Reported units
Gonzales et al. (1974)	GM 0.64 to 0.86 µm, GSD 1.48 to 1.49	MMAD
Charuau (1987)	Gas, 2.3 µm, and 10.5 µm	MMAD
Munyon and Lee (2002)	GM 3.0 µm, GSD 2.4	AMAD
Scripsick et al. (1979a, 1979b)	GM 0.35 µm, GSD 2.1	CMAD[b]
Whicker and Moxley (2001)	GM 0.3 µm, GSD <2	Not provided

a. AMAD = activity median aerodynamic diameter; CMAD = count median aerodynamic diameter; GM = geometric mean; MMAD = mass median aerodynamic diameter.
b. Based on the Hatch-Choate conversion equations in Hinds (1982), a CMAD of 0.35 µm is equivalent to a MMAD of 1.83 µm, and shares the same GSD of 2.1.

With the exception of Whicker and Moxley (2001), all units for the particle sizes were reported in terms of aerodynamic diameter, which is an equivalent diameter versus an actual physical diameter. Because most aerosol particles are not spherical, particle diameters are typically reported in equivalent diameters, based on one or more properties of the particle. Aerodynamic diameter is defined as the diameter of a unit density (ρ_p = 1 g/cm³) sphere that has the same settling velocity as the particle (Hinds 1982). Particles with the same aerodynamic diameter are aerodynamically indistinguishable from other particles of different size, shape, and density (Hinds 1982). Note that the particle size units were not provided for the Whicker and Moxley (2001) study, and the study does not indicate how the particle size distribution was measured. Given that the aerosol was a nontoxic oil

(dioctyl sebacate) (Whicker and Moxley 2001), the particles were likely close to being spherical in shape. That combined with the density of dioctyl sebacate, which is 0.9 g/cm³, would indicate that the reported particle size in Whicker and Moxley (2001) was likely equivalent to an aerodynamic diameter.

As indicated Section 2.2.2, air sample data from rooms with dominant particles was very unreliable and should not be used to assess worker exposures or for developing BZ:GA ratios. Because the dominant particle issue is only applicable to radioactive particles, this issue is not applicable to studies that only involved nonradioactive aerosols. Of the five evaluated studies, Munyon and Lee (2002) was the only one that involved radioactive aerosols. It was therefore the only evaluated study potentially affected by the dominant particle issue. However, Munyon and Lee (2002, p. 7) indicated that autoradiographs were performed on some of the air samples, and that "none of them exhibited a dominant or single particle phenomena." Therefore, dominant particles were not considered to be an issue for any of the five studies that were evaluated for this report.

The approaches taken for the evaluations in this report do not rely on a specific definition for the location of the BZ. With the exception of the Munyon and Lee (2002) study, the BZ locations were designated by the authors of this report, since no actual workers were present during the other evaluated studies. In Munyon and Lee, the BZ sampling locations were the lapel samplers on the workers who were present during the radiological work activity. In the broadest definition, the BZ can be defined as any location within a volume of air that has a concentration that is representative of the air being inhaled by a worker. Usually, the BZ is limited to the air volume that is in close proximity to a worker's head or face. For the studies with no workers present, the BZ locations were designated based on sampling height and potential worker locations with air sample data. More information regarding the designation of BZ locations is provided in the following paragraphs and in the sections for each specific study.

Because the location of the worker, GA air sampler, and release point are often unknown and can have a significant effect on the BZ:GA ratio distributions, a method was devised to eliminate the need to know those exact locations. It was decided that there were only two main worker location scenarios that needed to be evaluated, which were in terms of where the worker was in relation to the release point. For those scenarios, the possible GA sampler locations could be anywhere in the room but were usually limited to the GA sampling locations in the evaluated studies.

Worker Location Scenarios

- Scenario 1. Assumes the worker (BZ location) was always located at the same *X,Y* coordinates in the room as the release point (i.e., colocated worker and release point).

- Scenario 2. Assumes the worker (BZ location) was not necessarily located at the same *X,Y* coordinates in the room as the release point (i.e., variable worker location relative to the release point).

Scenario 1 represents what is typically the worst-case scenario because it normally yields the highest BZ:GA ratios. In most instances, this scenario only applies to acute exposures because the workers often move around and are not always located at the release point.

Scenario 2 was created because most radiological processing areas have multiple workstations and multiple workers moving around in each room rather than one worker being at a single stationary location for an entire work shift. For Scenario 2, it was assumed that the potential BZ locations had the same probability of being anywhere in the room.

Evaluations based on Scenarios 1 and 2 represent a wide variety of the possible BZ and GA location combinations for these two scenarios, thereby eliminating the need to know the worker location in

relation to the GA location. To adjust the site-specific GA air concentrations to make them equivalent to BZ air concentrations, the analysis need only decide which of the two scenarios best represents the worker's location relative to the release point for a given exposure scenario.

When possible, the two BZ location scenarios above were evaluated for each study. The Munyon and Lee (2002) study was the only one in which both scenarios could not be evaluated because that study was based on a real work activity and personal air samples from real workers versus being based on a simulated study.

4.0   GONZALES ET AL. STUDY

Gonzales et al. (1974), *Relationship Between Air Sampling Data from Glove Box Work Areas and Inhalation Risk to the Worker*, was performed by Los Alamos National Laboratory (LANL). This study was an experiment to evaluate aerosol dispersal patterns from a simulated glovebox leak in a mockup of a plutonium work area.

4.1   EXPERIMENT DESCRIPTION

In Gonzales et al. (1974), plutonium releases were simulated using a nonradioactive tracer aerosol in a 20- by 20- by 8-ft tall (6.10- by 6.10- by 2.4-m tall) test room with a single glovebox at one end of the room. To produce submicron tracer aerosol, an air-operated dioctyl phthalate aerosol generator with a single jet impactor was placed inside the glovebox. The generated aerosol particle sizes ranged from a mass median aerodynamic diameter (MMAD) of 0.640 to 0.86 μm, with a GSD of 1.48 to 1.49. The release point was created by covering one glove port with an aluminum plate with a 1/8-in. (3.2-mm) hole drilled into the center, allowing the aerosol to escape from the glovebox into the room (Gonzales et al).

A three-dimensional Cartesian coordinate system was established to define air sampling locations relative to the aerosol release point (i.e., the aerosol release point is the point of origin for the coordinate system). The test room and the coordinate system for the experiment are depicted in Figure 4-1. In Figure 4-1, the three axes are depicted as "horizontal (H)," "longitudinal (L)," and "vertical (V)" axes, which are equivalent to the more commonly used X, Y, and Z axes. For descriptive purposes, when facing the glovebox, the wall behind it is considered to be the back wall. Therefore, the glovebox is considered to be in the back of the room and against the back wall. Based on the scale in Figure 4-1, the aerosol release point was approximately 3.75 ft (1.143 m) above the floor and 1.5 ft (0.457 m) from the back wall, because the glovebox has a longitudinal depth of approximately 1.5 ft (0.457 m) (ORAUT 2019a). Room aerosol concentrations were measured with a light-scattering photometer at several locations during each test to determine the aerosol dispersal patterns from a given test scheme (Gonzales et al. 1974). It should also be noted that nothing was placed in the room to simulate any obstructions, such as those that would be caused by workers or equipment in the room (i.e., the room was empty except for the glovebox and air sampler).
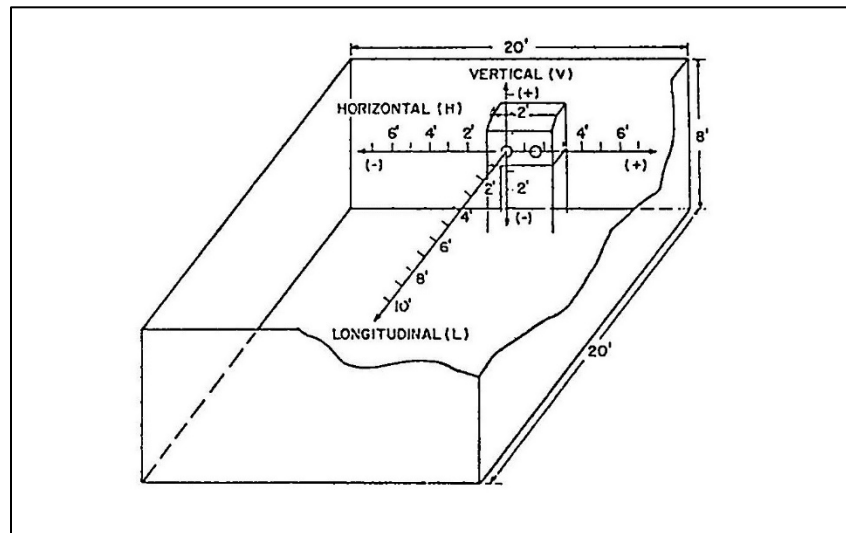
Figure 4-1. Coordinate system used for positioning sampling
probe (Gonzales et al. 1974, p. 6).

The test schemes were defined under the following ventilation conditions: 6, 9, and 12 room air changes per hour (AC/hr) for each of three different airflow directions (0°, 90°, and 180°) relative to the aerosol leak flow direction. For the 0° orientation, room air entered from behind the glovebox and flowed in the same direction as the aerosol leak. For the 90° orientation, room air entered from one side of the room perpendicular to the leak flow direction. For the 180° orientation, room air entered from the wall opposite the glovebox and flowed in the opposite direction from the leak flow. The room was designed to have room air enter and exit the room via inlet and outlet plenums. The plenums covered the entire width of each wall. From the inlet plenum, the entering air was uniformly distributed across the entire wall through 1/8-in. (3.2-mm) holes spaced 1 in. (2.54 cm) apart. The outlet plenum was similarly constructed (Gonzales et al. 1974).

4.2   REPORTED RESULTS AND CONCLUSIONS

Approximately 640 air concentration measurements were taken for this study, and those measurements were used to generate 44 graphs depicting iso-concentration curves, but only 18 of those were presented in Gonzales et al. (1974). However, Gonzales et al. indicated that the 18 selected graphs were representative of data and conclusions drawn from all of the graphs. For the purposes of this report, the 18 graphs in Figures 2 through 19 of Gonzales et al. have been reorganized and provided in Attachment A as Figures A-1 through A-8. The concentrations in the iso-concentration graphs are presented as a percentage of the air concentrations measured at the aerosol release point.

In relation to Figures 2 through 19 from Gonzales et al. (1974), it should be noted that those figures do not depict the entire area of the test room depicted in Figure 4-1 above. The dimensions of the test room were 20- by 20-ft (6.10- by 6.10-m), but Figures 2 through 19 only depict a 16- by 14-ft (4.88- by 4.27-m) area in that room. In addition, Figures 2 through 19 only provide iso-concentration data for a 10- by 14-ft (3.05- by 4.27-m) area (the monitored area) in the depicted area. To illustrate that, Figure 4-2 is an example of one of the iso-concentration graphs, specifically Figure 4 from Gonzales et al., with an added red box to depict the monitored area. Figure 4-2 contains another added notation to point out the release location for all of the tests.

The Discussion Section in Gonzales et al. (1974, p. 13) reported that "under all conditions of ventilation, aerosol concentrations ranging up to 4.0% occurred in the probable breathing zones", which were defined as an elevation of leak-level to 1 ft (0.30 m) above leak-level (i.e., approximately

3.75 to 4.75 ft [1.143 to 1.448 m] above the floor [ORAUT 2019a]) and distances 4 to 10 ft (1.22 to 3.05 m) from the leak source. However, Figures 4 and 17 in Gonzales et al., which are redisplayed in Attachment A (see Figures A-1 and A-7), contradict that statement, because the 4.1% to 10% aerosol concentration range extends into the longitudinal distance range of 4 to 10 ft (1.22 to 3.05 m). Contrary to what was indicated in Gonzales et al., the ORAU Team does not consider the leak-level to be a good representation of a probable BZ elevation in a process area, because the worker would have needed to be bent over or sitting for the majority of their time in the process area. The ORAU Team considers the 1- and 2-ft above leak-level elevations to be better representations of the probable BZ elevations, which are equivalent to approximately 4.75 and 5.75 ft (1.448 and 1.753 m) above the floor. All of the available iso-concentration graphs in Gonzales et al. are redisplayed in Attachment A. Because the graphs indicate that the aerosol concentrations decline as the elevation in the test room increases, it can also be concluded that the aerosol concentrations for the entire room were 4.0% or less for elevations of 1-ft above leak-level and higher. That is equivalent to 4.75 ft (1.448 m) above the floor and higher, and it represents the upper 3.25 ft (1.143 m) of the entire room volume.
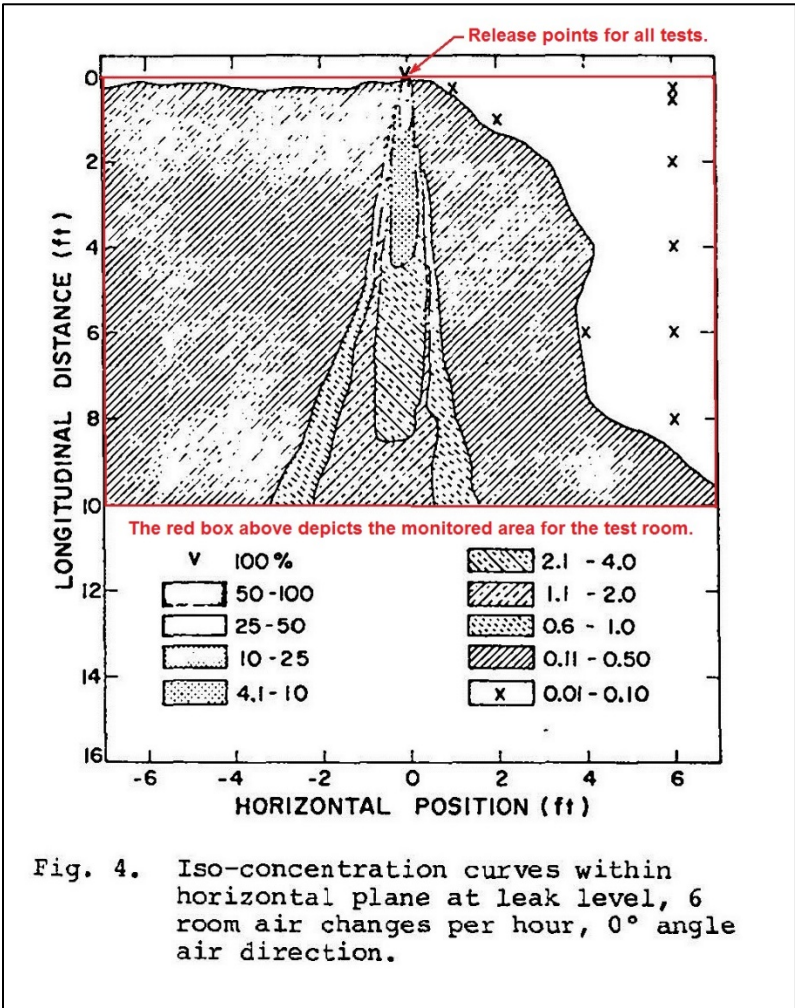
Figure 4-2. Example iso-concentration graph from Gonzales et al. (1974, p. 9).

Gonzales et al. (1974) also reported that the BZ air concentrations ranged from 0.11% to 10.0%, that the fixed room air sampler concentrations ranged from 0.04% to 0.6%, and that these data represented a maximum potential ratio of BZ to fixed room air concentrations of 250:1 (10.0% to 0.04%). However, the reported BZ:GA ratio of 250:1 is highly unlikely for the following reasons:

1. For a glovebox work station, the BZ would normally be higher than the leak-level (i.e., higher than 3.75 ft [1.143 m] above the floor), and the leak-level should not be considered as being in the BZ;

2. The ratio is based on the extremes of multiple graphs (i.e., different test schemes) versus the ranges in a single graph; and

3. The air concentrations in the graphs are reported in ranges, and the ratios are based on only the highest BZ result and the lowest fixed sampler result for a given range.

Because of this, the ORAU Team has reevaluated the air sampling data reported in Gonzales et al. (1974).

4.3   REEVALUATION OF GONZALES ET AL. STUDY DATA

The ORAU Team has reevaluated the graphical air sampling data in the Gonzales et al. (1974) study using four different scenarios. Those four scenarios were created from a combination of the two different worker location scenarios (Scenarios 1 and 2, described above) and two different sampler location scenarios, which are described below and identified as Scenarios A and B. This reevaluation depicts the differences between potential BZ and GA air concentrations in terms of BZ:GA air concentration ratios.

4.3.1   Bases and Assumptions for the Reevaluation

For most radiological processing areas, the majority of the processing work took place on bench tops, in hoods, and in gloveboxes. Radiological work involving kneeling or significant bending was probably limited to activities that only accounted for a small fraction of a worker's time in the processing areas. Therefore, the BZ elevation for most radiological processing areas would have been predominantly above the leak-level elevation in the Gonzales et al. (1974) study. Therefore, this reevaluation only used the nine iso-concentration graphs for the 1- and 2-ft (0.30- and 0.61-m) above leak-level elevations (i.e., elevations of 4.75 and 5.75 ft [1.448 and 1.753 m] above the floor). In addition, comparisons of the potential BZ air concentrations to the GA air concentrations were performed for the same elevation and the same test scenario (i.e., same AC rate and air direction).

For the other studies that were evaluated in this report, the GA air sampler locations were based on actual measurement locations. Unlike those studies, the iso-concentration graphs in Gonzales et al. (1974) made the air concentrations within any point of the monitored area of the test room known, which theoretically allowed for an infinite number of potential GA and BZ air sampler locations to be evaluated. As a result, any location within the monitored area in the test room could be designated as a potential GA air sampler location, which allowed for the evaluation of some additional scenarios for the GA sampler locations. Three potential GA sampler location scenarios are defined below. However, as discussed below, it was not feasible to evaluate the third scenario (Scenario C). Therefore, only Scenarios A and B were actually used to evaluate the data from Gonzales et al.

Sampler Location Scenarios

- Scenario A. Assumes the hypothetical GA air samplers had an equal probability of being located anywhere in the test room.

- Scenario B. Assumes the hypothetical GA air samplers were potentially located anywhere in the test room with the exception of the middle of the test room. The exclusion area for the hypothetical GA air sampler locations was defined as a 4- by 6-ft (1.2- by 1.8-m) area in the middle of the test room, which is depicted in Figure 4-3.

- Scenario C. Assumes the hypothetical GA air samplers were always located downstream of the release point and near the outlet plenum for the ventilation.
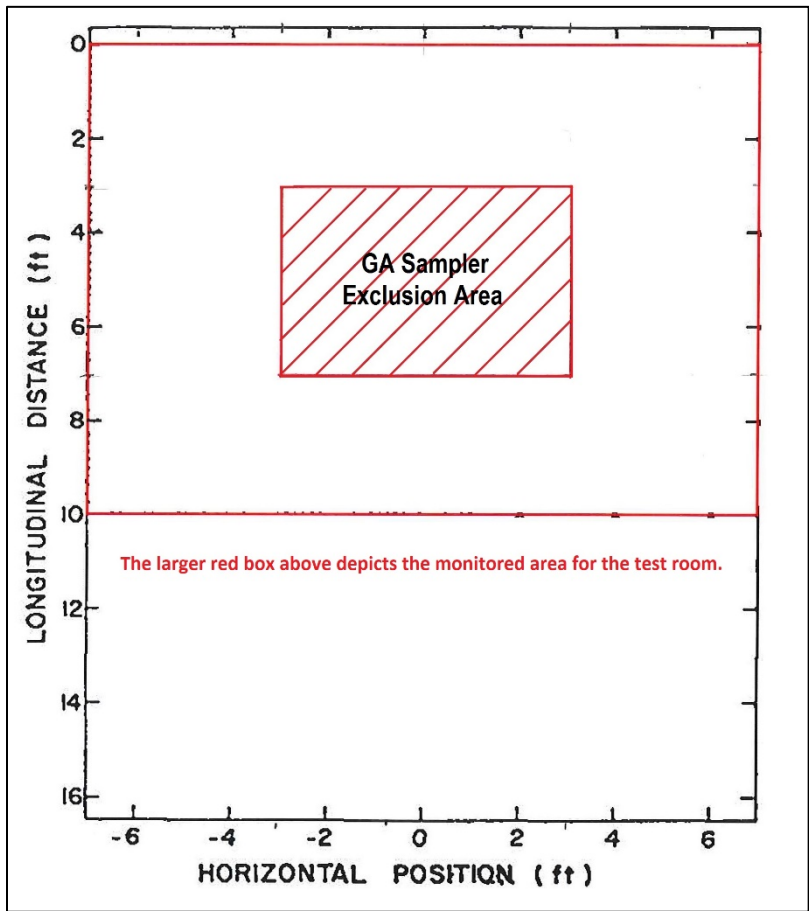
Figure 4-3. Sampler exclusion area for hypothetical GA air sampler locations for Scenario B (ORAUT 2019b).

Scenario A represents the potential GA sampler locations when there were no restrictions on where the sampler could be located.

Scenario B was created to evaluate another plausible scenario for the GA air sampler locations. Because the middle of a radiological processing area is often an unlikely location for a GA air sampler and because the highest air concentrations in the Gonzales et al. (1974) study tended to occur in the middle of the test room, there was concern that the assumptions used for the worker location Scenario 1 (i.e., colocated worker and release point) could underestimate the potential BZ:GA ratios. Therefore, a second scenario was evaluated and its results were compared to the results from the first scenario. GA air samplers are often located along the perimeters of the radiological processing areas

for the following reasons: (1) the locations for power outlets are normally along the outer walls, (2) the length of the power cord on the air samplers, and (3) keeping the GA air samplers out of primary traffic areas, which are often the middle of the room.

Scenario C was intended to evaluate a common placement scenario for GA air samplers. Often GA air samplers are placed downstream of where the radiological work is being performed, which helps to ensure that a release event is detected. Unfortunately, limitations in the iso-concentration graphs from Gonzales et al. (1974) prevented Scenario C from being evaluated. As discussed above and as shown in Attachment A, the iso-concentration graphs do not go all the way to the front and back walls of the test room. Additionally, the only thing that is known about the outlet plenum configurations for the ventilation were that they extended across the entire width of the wall. No information regarding the vertical aspects of those configurations was provided. As a result, determining the downstream air concentrations near the outlet plenum for the 0° and 180° orientations was not feasible. For the test room in Gonzales et al., the 180° orientation would have been the most likely airflow direction in a properly designed radiological workroom (i.e., where the radiological source term is between the workers and the workroom's ventilation outlet, such that the potentially contaminated air would be pulled away from the worker locations).

Combining the hypothetical BZ location and hypothetical GA air sampler location scenarios above resulted in a total of four scenarios being evaluated for Gonzales et al. (1974) (i.e., Scenarios 1A, 1B, 2A, and 2B). The following are the combined scenario definitions:

- Scenario 1A. Assumes the worker (BZ location) was always at the same X,Y coordinates in the test room as the release point, and assumes the GA air samplers had an equal probability of being located anywhere in the room.

- Scenario 1B. Assumes the worker (BZ location) was always at the same X,Y coordinates in the test room as the release point, and assumes the potential GA air samplers were potentially located anywhere in the room with the exception of the middle of the room. The exclusion area for the potential GA sampler locations was defined as a 4- by 6-ft (1.2- by 1.8-m) area in the middle of the room.

- Scenario 2A. Assumes the worker (BZ location) was not necessarily located at the same X,Y coordinates in the test room as the release point, and assumes GA air samplers had an equal probability of being located anywhere in the room.

- Scenario 2B. Assumes the worker (BZ location) was not necessarily located at the same X,Y coordinates in the test room as the release point, and assumes the potential GA air samplers were potentially located anywhere in the room with the exception of the middle of the room. The exclusion area for the potential GA sampler locations was defined as a 4- by 6-ft (1.2- by 1.8-m) area in the middle of the room.

Each of the nine iso-concentration graphs for the 1- and 2-ft (0.30- and 0.61-m) above leak-level elevations was evaluated for the four scenarios above. This resulted in a total of 36 BZ:GA ratio distributions being generated for the Gonzales et al. (1974) study.

4.3.2 Probabilities for Hypothetical BZ Locations and GA Sampling Locations

By dividing the areas for each potential air concentration region by the total monitored area in the test room, the resulting region area fractions are equivalent to the probability that a randomly located worker (i.e., BZ location) or GA air sampler was in a given air concentration region. Because the location of the worker and the GA air sampler can be treated as two independent events, the probability of a given BZ location and GA air sampler location combination would be the product of the

probabilities for each location. Using Figure 4-4 to illustrate this, the probability of the worker being in concentration region 3 (R3) while the GA air sampler was in concentration region 2 (R2) would be 0.1870 × 0.2548 = 0.0476. The areas for each concentration region in each iso-concentration graph were measured using the Measurement Log feature in Adobe Photoshop CC 20.00 Release (ORAUT 2019c). Because those areas were being used only to calculate unitless area fractions, the units for the area measurements were done in terms of pixels. Using this approach, probabilities for a BZ:GA air concentration ratio for every potential BZ location and GA air sampler location combination could be calculated and evaluated.

Fig. 12. Iso-concentration curves through horizontal plane 1 ft above leak level, 12 room air changes per hour, 90° angle air direction.

NOTE: The units for the areas are arbitrary, since only the area fractions are being used.
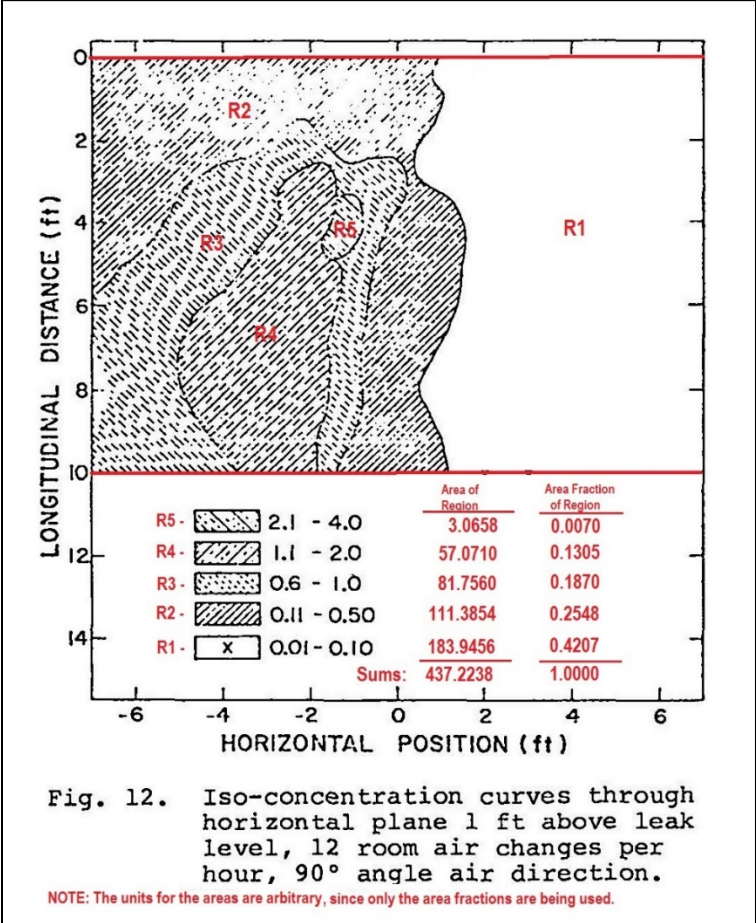
Figure 4-4. Illustration of area fraction calculations (ORAUT 2019d).

For this reevaluation, the air concentration regions in the iso-concentration graphs have been defined in Table 4-1.

Table 4-1. Defining air concentration regions for iso-concentration graphs.

Concentration region	Concentration range
R1	0.01–0.10
R2	0.11–0.50
R3	0.60–1.00
R4	1.10–2.00
R5	2.10–4.00

In Attachment B, Figures B-1 through B-4 provide summaries of the calculated area fractions for Scenarios 1A, 1B, 2A, and 2B. As indicated in Attachment B, the details regarding how the area fractions were calculated are provided in ORAUT (2019c).

4.3.3   Statistical Evaluation of the Data

The area fractions for the concentration regions presented in Section 4.3.2 were used to calculate the probabilities for each potential BZ:GA ratio combination. Because the air concentration regions are represented by a range of potential air concentration values, values within each air concentration range were randomly generated using a Monte Carlo simulation and a uniform distribution with limits equal to the lower and upper limits of the range (ORAUT 2020). To facilitate those calculations, the concentration ranges for the five concentration regions given in Table 4-1 were adjusted to make the lower limit of each range equal to the upper limit of the previous range as shown in Table 4-2.

Table 4-2. Adjusted air concentration ranges for probability calculations.

Concentration region	Concentration range
R1	0.01–0.10
R2	0.10–0.50
R3	0.50–1.00
R4	1.00–2.00
R5	2.00–4.00

As indicated in Section 4.3.1, four scenarios (i.e., Scenarios 1A, 1B, 2A, and 2B) were evaluated based on the data from the 9 iso-concentration graphs for the 1- and 2-ft (0.30- and 0.61-m) above leak-level elevations. This resulted in a total of 36 BZ:GA ratio distributions being generated for the Gonzales et al. (1974) study. In Figure 4-5, all 36 BZ:GA ratio distributions are presented in a scatter plot. The data point colors in Figure 4-5 represent the three ventilation airflow directions (i.e., red = 0°, blue = 90°, and black =180°). The data point shapes represent the four scenarios that were evaluated (i.e., solid square = Scenario 1A, open square = Scenario 1B, solid circle = Scenario 2A, and open circle = Scenario 2B) (ORAUT 2020).
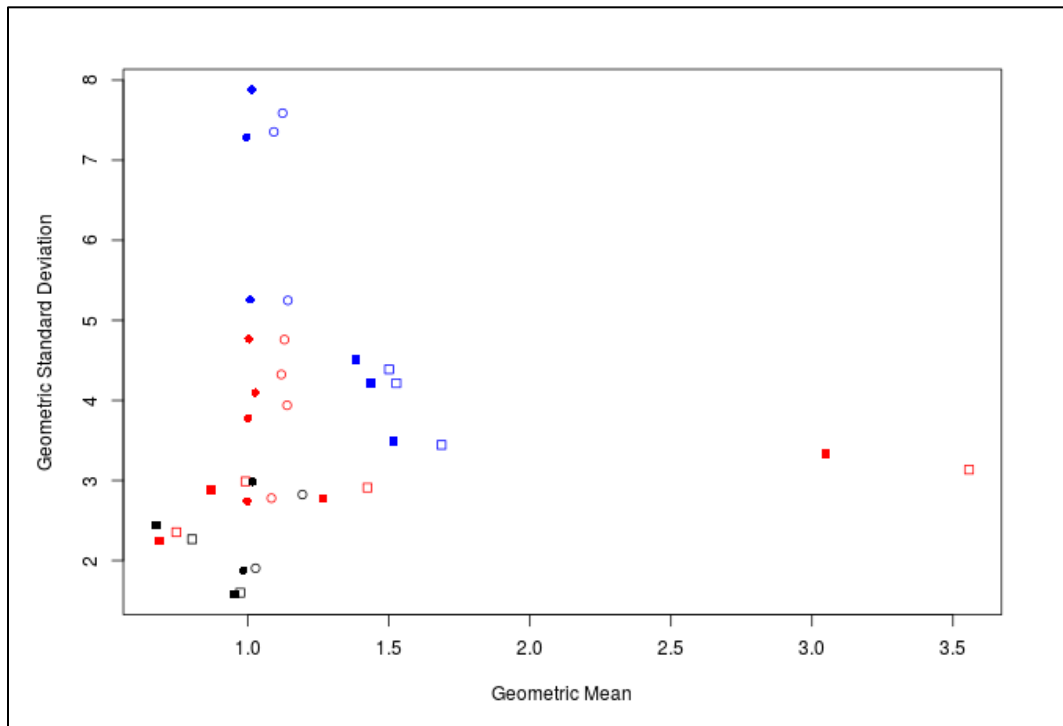
Figure 4-5. Scatter plot of all 36 results from Gonzales et al. (1974) (ORAUT 2020).

The solid and open squares, representing Scenarios 1A and 1B, at the far right of Figure 4-5 appear to be outliers in the dataset. Both data points are associated with Figure 5 in Gonzales et al. (1974). A review of the area fractions for those figures (see Figures B-1 and B-2 in Attachment B) indicates that Figure 5 in Gonzales et al. has a significantly larger GA area fraction for concentration region R1 than the other figures in Gonzales et al. That coupled with the fixed BZ location that was used for Scenarios 1A and 1B appears to be the cause for the higher geometric means (GMs) for those data points.

Figure 4-6 presents just the 18 data points associated with Scenario 1 (i.e., both Scenarios 1A and 1B), which was when the worker was always at the same X,Y coordinates as the release point. Figure 4-7 presents just the 18 data points associated with Scenario 2 (i.e., both Scenarios 2A and 2B), which is when the worker was not necessarily at the same X,Y coordinates as the release point. In these two figures, the data point colors and shapes represent the same things as in Figure 4-5.

The scatter plots indicate that the uncertainties for the 90° ventilation airflow direction are generally higher than the other directions, with the 180° ventilation airflow direction generally having the lowest uncertainties. That relationship is even more noticeable for Scenario 2 (see Figure 4-7). For Scenario 1, when one ignores the outliers at the far right, the GMs even appear to have a similar relationship to the uncertainties in regards to ventilation airflow direction.

The scatter plots also indicate that the differences between Scenarios A and B are generally just a slightly higher GM for Scenario B. As indicated in Section 4.3.1, there was a concern that Scenario A could underestimate the potential BZ:GA ratios when Scenario B would be a more realistic scenario for the test room in Gonzales et al. (1974). Though that appears to be true, the underestimate is considered to be too small to justify evaluating and developing separate BZ:GA ratios for Scenarios A and B. Therefore, Scenarios A and B were grouped together, to help minimize the number of BZ:GA ratio models being evaluated in this report. Because Scenarios A and B are both plausible GA

sampler location scenarios, it was decided to include both scenarios in the evaluation of the Gonzales et al. study versus just using Scenario B.

Figure 4-6. Scatter plot of Scenario 1 results from Gonzales et al. (1974) (ORAUT 2020).

Figure 4-7. Scatter plot of Scenario 2 results from Gonzales et al. (1974) (ORAUT 2020).

Because the data generated from Gonzales et al. (1974) was much more substantial than the other studies being evaluated and because it was the only study that evaluated different ventilation airflow directions, it was decided to weight the Gonzales et al. data more heavily by generating separate BZ:GA ratio models for each ventilation airflow direction (ventilation scheme). That resulted in a total of six models to represent the Gonzales et al. study (i.e., three Scenario 1 models and three Scenario 2 models). It should be noted that the generation of separate BZ:GA ratio models for each ventilation scheme is only being done as a weighting mechanism. The ORAU Team does not plan to develop any BZ:GA ratios to be applied to specific ventilation airflow directions, because the airflow direction observations made for this data may only be applicable to simple workrooms with simple ventilation flow patterns. In addition, needed details about the ventilation system and airflow patterns are often unknown for workrooms at other sites, which means there would be few scenarios where BZ:GA ratios for specific ventilation airflow directions could be used. It is also desirable to keep the final number of BZ:GA ratio models to a minimum.

As indicated above, the 18 Scenario 1A and 1B models were combined into three Scenario 1 models, one for each ventilation scheme. Similarly, the 18 Scenario 2A and 2B models were combined into three Scenario 2 models, one for each ventilation scheme. Table 4-3 identifies the figures in Gonzales et al. (1974) that were used to generate the datasets for evaluating Scenario 1 and Scenario 2 for each ventilation scheme. All of those figures are redisplayed in Attachment A. Then a lognormal model was fit to each dataset using regression on order statistics (ROS), generating a GM and GSD for each model. The six combined models were used to represent the Gonzales et al. study for the combined evaluations in Section 9.0. In the quantile-quantile plots below, the quantiles are from the fitted lognormal distribution, and the horizontal lines are the 50th, 84th, and 95th percentiles for the plotted data (ORAUT 2020). The plots for the Scenario 1 results are presented below in Section 4.3.3.1 (Figures 4-8 to 4-10), and the plots for the Scenario 2 results are presented below in Section 4.3.3.2 (Figures 4-11 to 4-13).

Table 4-3. Gonzales et al. (1974) figures used to evaluate each ventilation scheme.

Ventilation scheme	Figures used
0°	5, 6, 7, and 8
90°	12, 13, and 14
180°	18 and 19

4.3.3.1   Scenario 1 Results: Colocated Worker and Release Point
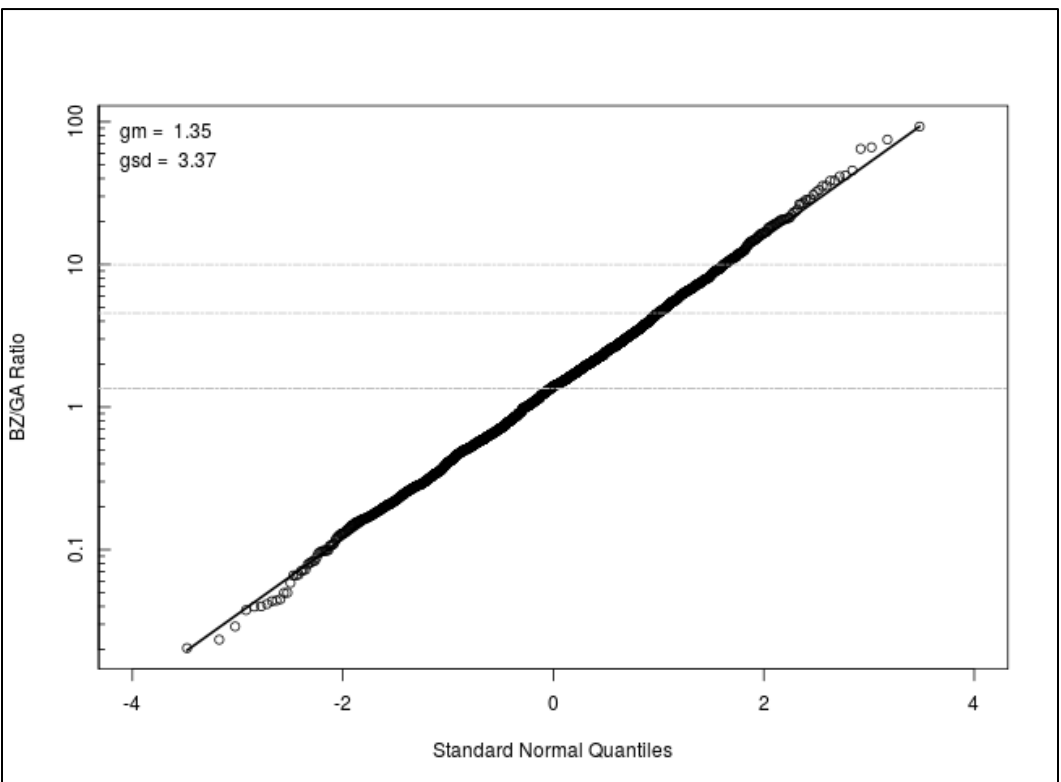
Figure 4-8. Model for Scenario 1 with 0° airflow direction (ORAUT 2020).
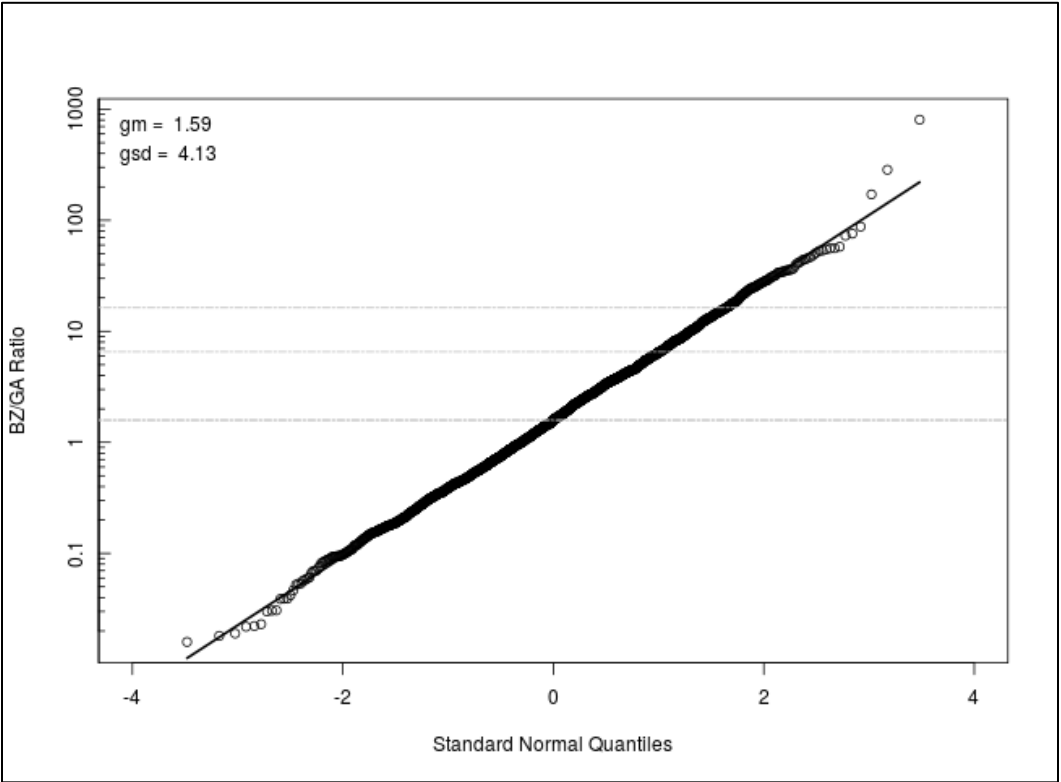
Figure 4-9. Model for Scenario 1 with 90° airflow direction (ORAUT 2020).
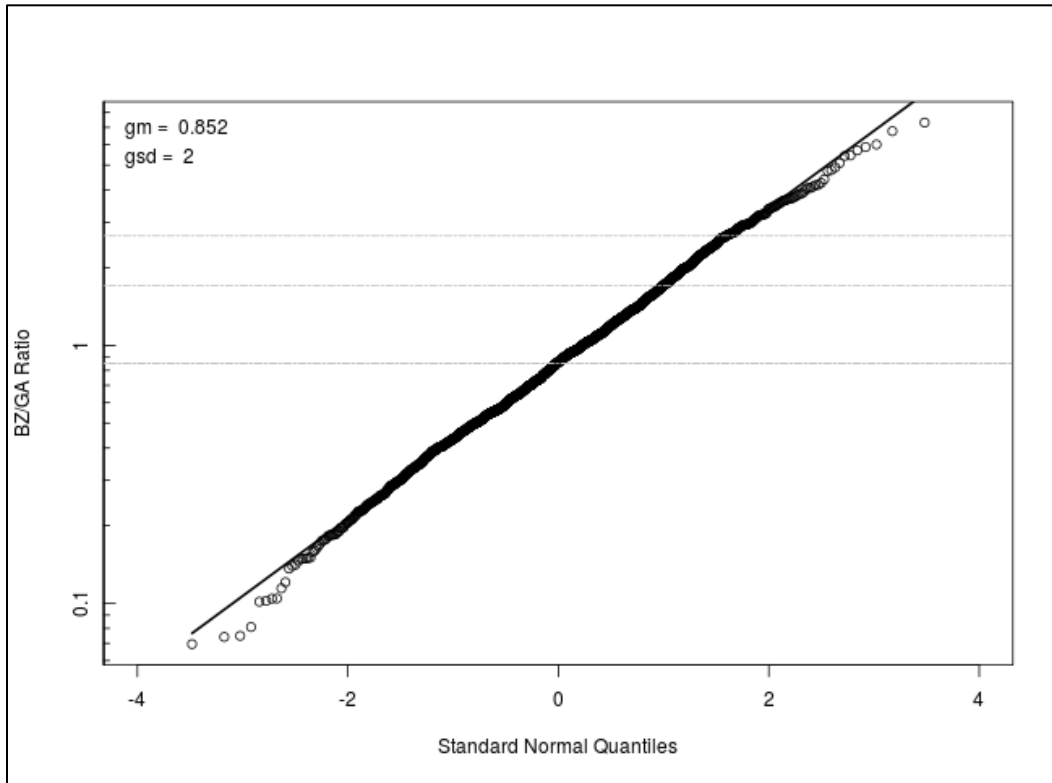
Figure 4-10. Model for Scenario 1 with 180° airflow direction (ORAUT 2020).

4.3.3.2   Scenario 2 Results: Variable Worker Location Relative to the Release Point
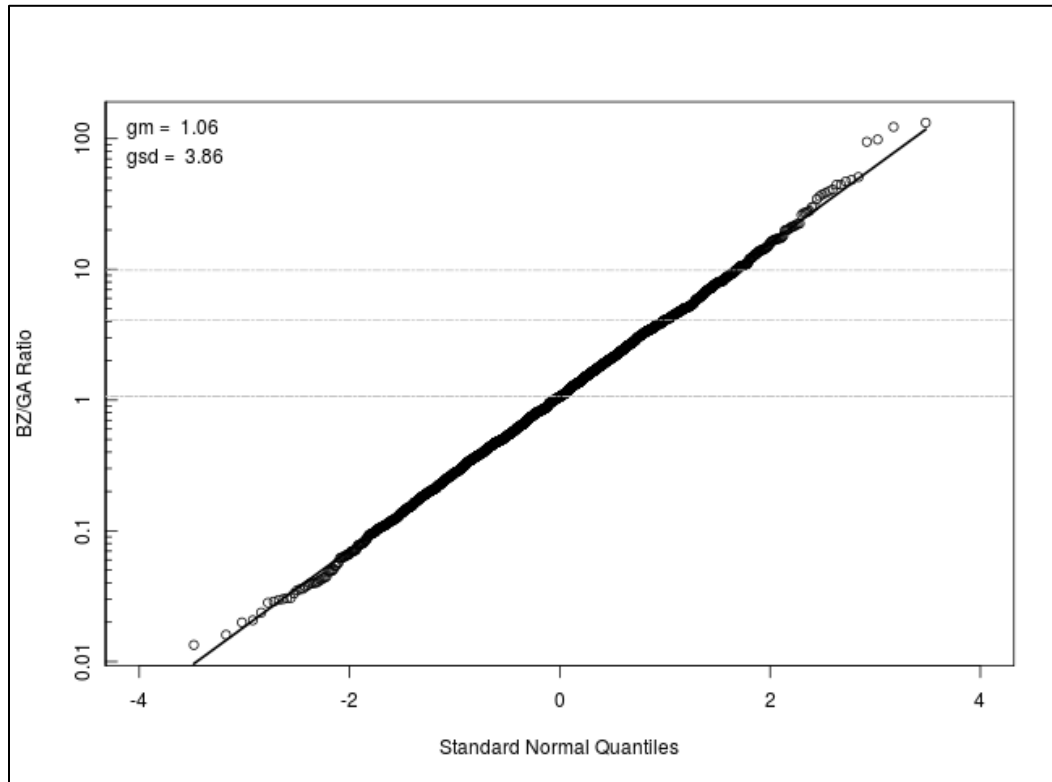
Figure 4-11. Model for Scenario 2 with 0° airflow direction (ORAUT 2020).
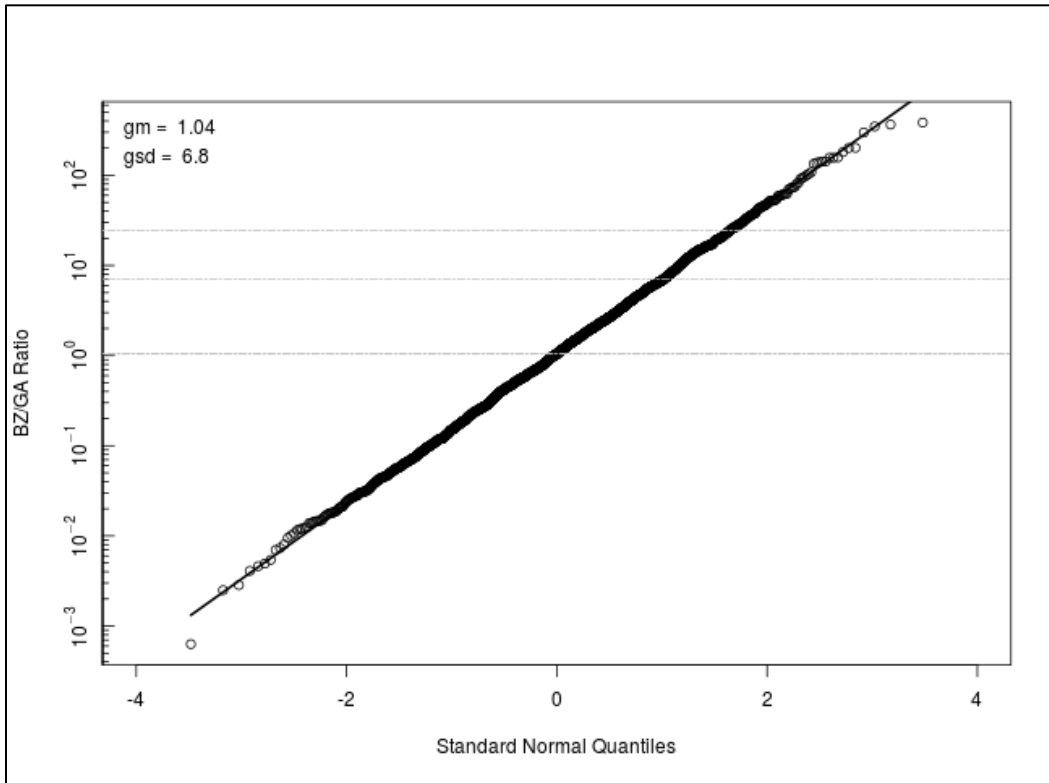
Figure 4-12. Model for Scenario 2 with 90° airflow direction (ORAUT 2020).
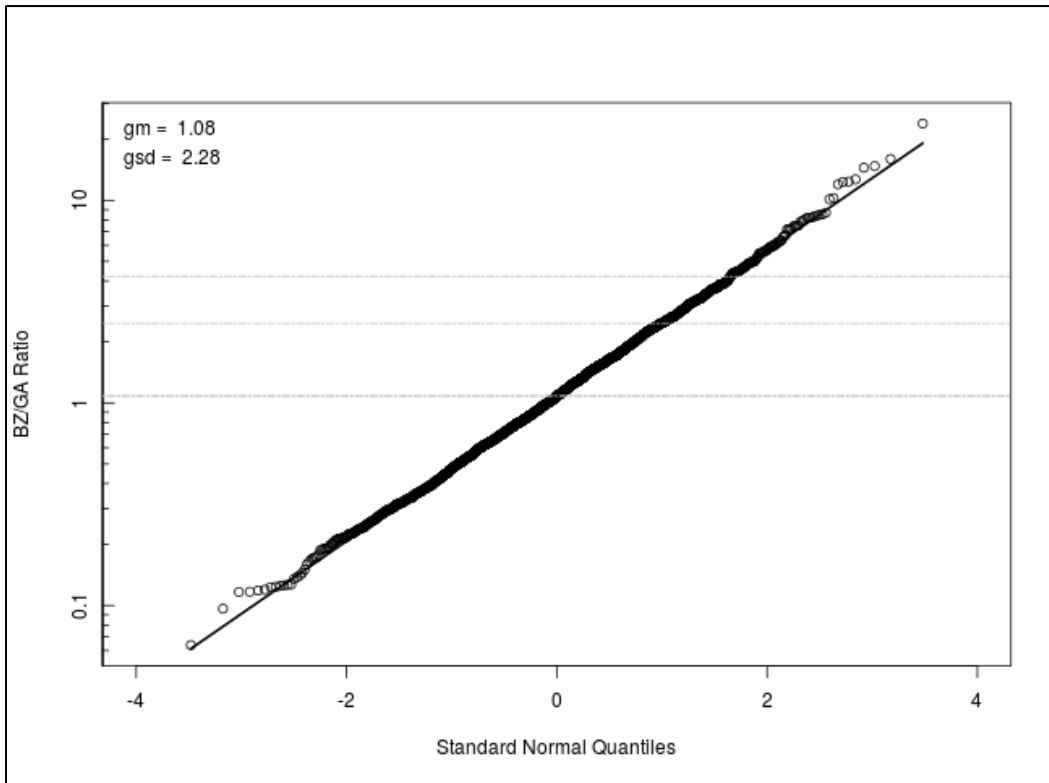
Figure 4-13. Model for Scenario 2 with 180° airflow direction (ORAUT 2020).

4.3.3.3 Summary of Scenario 1 and Scenario 2 Results

Table 4-4 summarizes the results from Section 4.3.3.1 for Scenario 1.

Table 4-4. Summary of the Scenario 1 BZ:GA ratio distributions for Gonzales et al. (1974).

Scenario	BZ:GA ratio GM	BZ:GA ratio GSD
Scenario 1 with 0° airflow direction	1.35	3.37
Scenario 1 with 90° airflow direction	1.59	4.13
Scenario 1 with 180° airflow direction	0.852	2.00

Table 4-5 summarizes the results from Section 4.3.3.2 for Scenario 2.

Table 4-5. Summary of the Scenario 2 BZ:GA ratio distributions for Gonzales et al. (1974).

Scenario	BZ:GA ratio GM	BZ:GA ratio GSD
Scenario 2 with 0° airflow direction	1.06	3.86
Scenario 2 with 90° airflow direction	1.04	6.80
Scenario 2 with 180° airflow direction	1.08	2.28

5.0 CHARUAU STUDY

The results of a French study (Charuau 1987), which was presented at the DOE Workshop on Workplace Aerosol Sampling in October 1985, were published as part of the proceedings for that workshop. The purpose of that study, which was performed by the Commissariat à l'Énergie Atomique (CEA), was to design and assess a personal monitor to optimize the occupational monitoring in plutonium laboratories. However, the part involving a contamination transfer study was of interest for this evaluation.

Charuau (1987) only provides the results for one contamination transfer study; however, it indicates that CEA specialists had completed several other ventilation and transfer studies. Therefore, information from other similar CEA studies might be available elsewhere but any such information was not found during the preparation of this report.

5.1 CONTAMINATION TRANSFER STUDY DESCRIPTION AND RESULTS

In Charuau (1987), plutonium releases were simulated using nonradioactive tracer gas and tracer aerosol (helium gas and a fluorescent aerosol) in a 15- by 7- by 4.5-m tall (49- by 23- by 15-ft tall) laboratory with multiple gloveboxes and workstations. Figure 5-1 provides a diagram of this laboratory, the inlet and outlet locations for the ventilation system, and the results from the study. During the study, the average ventilation rate was 10 AC/hr. Filtered air was blown into the workroom by three different diffusers arranged along the ceiling, and air was extracted from the room through 10 vents low on the walls (Charuau 1987). In Figure 5-1, the diffusers are the circular features with the outward pointing arrows, and the exhaust vents are the openings in the top and bottom walls with arrows pointing at them. The arrows represent the airflow direction. The room was reported to have no great ventilation dissymmetry and no dead zones (Charuau 1987).

Points of measurement	D1	D2	D3	D4	D5	D6	D7	D8	D9	D10
T_C helium	2.5	1.3	1.4	1.1	1.0	1.0	1.0	1.0	1.0	2.2
T_C aerosols 2.3 µm	2.7	1.5	1.0	0.7	0.5	0.6	0.5	/	0.7	1.4
T_C aerosols 10.5 µm	1.0	0.3	0.2	0.1	0.09	0.06	0.1	0.08	0.2	0.03
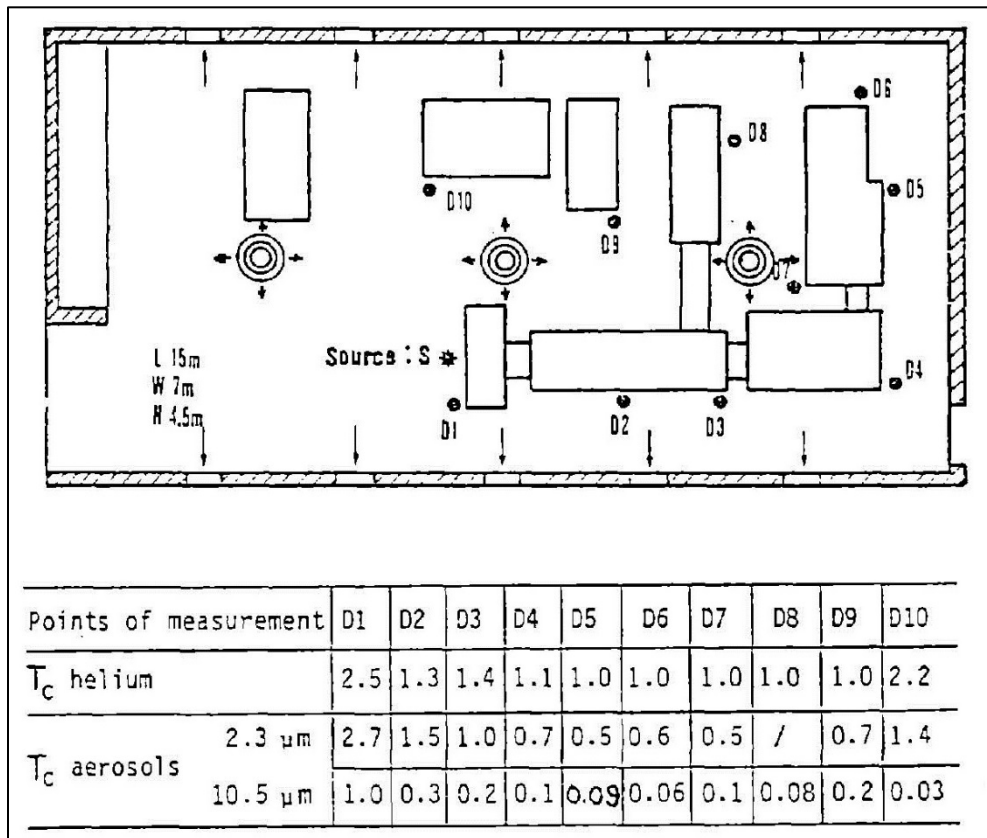
Figure 5-1. Plutonium laboratory and transfer study results (Charuau 1987, p. 174).

The generated aerosols consisted of two particle size groups, one with MMAD of 2.3 µm and the other with MMAD of 10.5 µm. The testing appears to have been conducted in multiple stages with a continuous emission of helium and then a continuous emission of each aerosol group (i.e., the 2.3-µm group and the 10.5-µm group) (Charuau 1987). Because the study did not include discussion about a sampling device with particle sizing capabilities and referred to "aerosols" in the plural form, it was assumed that the 2.3- and 10.5-µm particles were generated separately in two different parts of the study.

Air concentrations were measured at 10 locations in the workroom identified as D1 through D10 in Figure 5-1. The location of the gas and aerosol release point is identified as "Source: S". The release point and sampling locations were all at an elevation of 1.5 m (4.9 ft) above the floor (Charuau 1987).

The results for this study were reported in terms of transfer coefficient T_C in s/m^3. The transfer coefficient is the ratio of the locally measured concentration of gas (m^3/m^3) or aerosols (kg/m^3) to the emission flux from the source of gas (m^3/s) or aerosols (kg/s) (Charuau 1987).

5.2   EVALUATION OF THE CHARUAU STUDY DATA

The two BZ location scenarios described at the end of Section 3.0 were used to evaluate the potential differences between the BZ and GA air concentrations in the Charuau (1987) study. The following describes how Scenario 1 and Scenario 2 were evaluated using the data from Figure 5-1. For each scenario, a lognormal model was fit to the dataset for that scenario using ROS, generating a GM and GSD for each model.

5.2.1   Scenario 1 Evaluation: Colocated Worker and Release Point

As indicated above, air sampler location D1 was designated as the only BZ location to evaluate the BZ location scenario for Scenario 1 because it was the only sampling location near the release point. Then each of the 10 air sampling locations (D1 through D10) were evaluated as potential GA air sampler locations to generate a single BZ:GA ratio data point for each of the three types of tracer gas or aerosol used in Charuau (1987). This resulted in three separate datasets for Scenario 1 (i.e., one for gas, one for the 2.3-µm aerosol, and one for the 10.5-µm aerosol). Each of the three datasets would have contained nine BZ:GA ratio data points, but there were no data for the 2.3-µm aerosol at location D8 (see Figure 5-1). Therefore, only eight BZ:GA ratio data points could be generated for the 2.3-µm aerosol dataset. A lognormal model fit was then performed on each of the resulting three datasets, using ROS (ORAUT 2020).

Figures 5-2 through 5-4 present each of the three datasets for Scenario 1 in the form of a quantile-quantile plot. In the quantile-quantile plots below, the quantiles are from the fitted lognormal distribution, and the horizontal lines are the 50th, 84th, and 95th percentiles for the plotted data (ORAUT 2020).
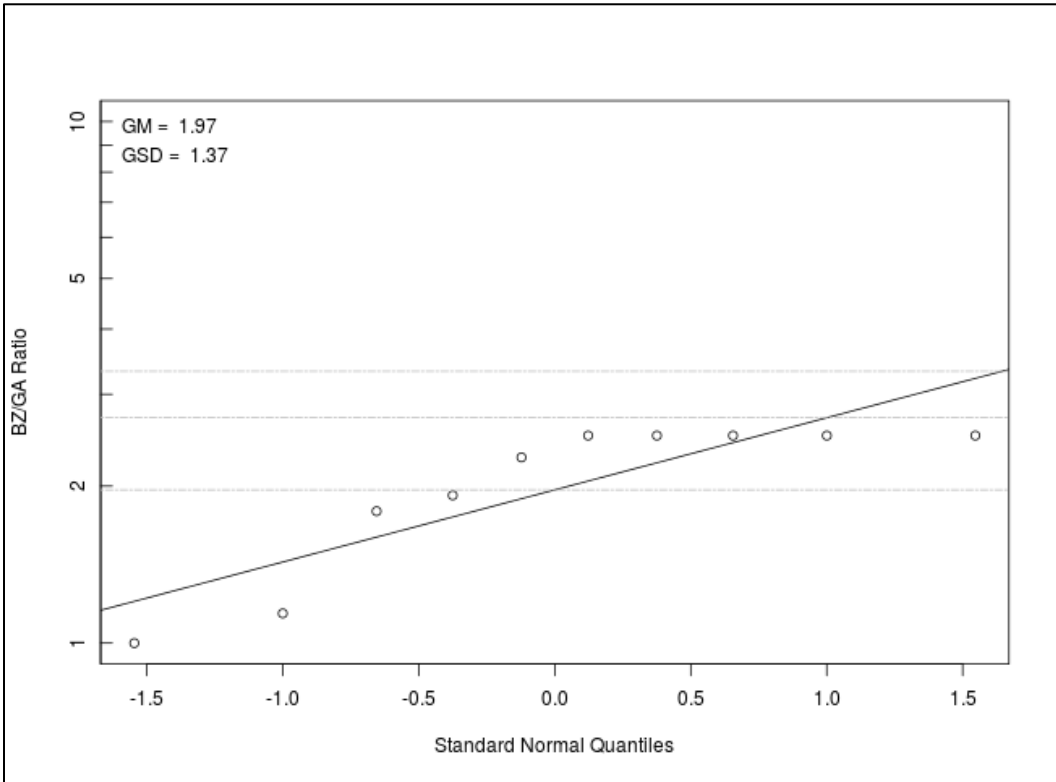
Figure 5-2. Model for Scenario 1 for gas (ORAUT 2020).
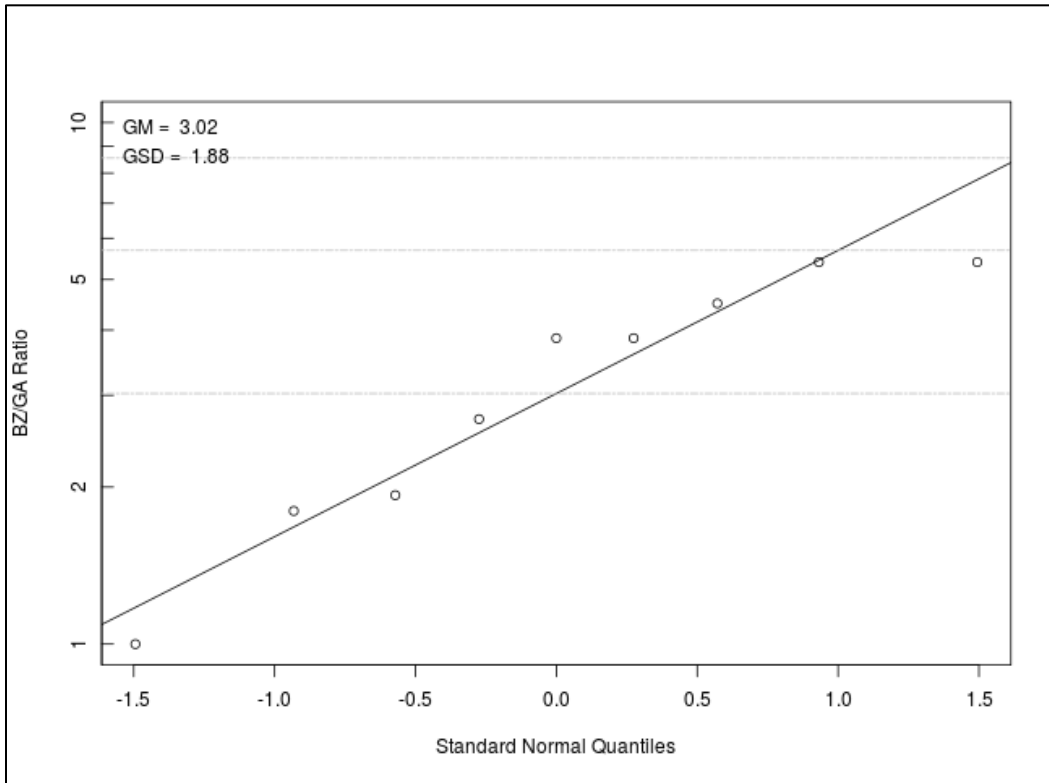
Figure 5-3. Model for Scenario 1 for 2.3-μm aerosols (ORAUT 2020).
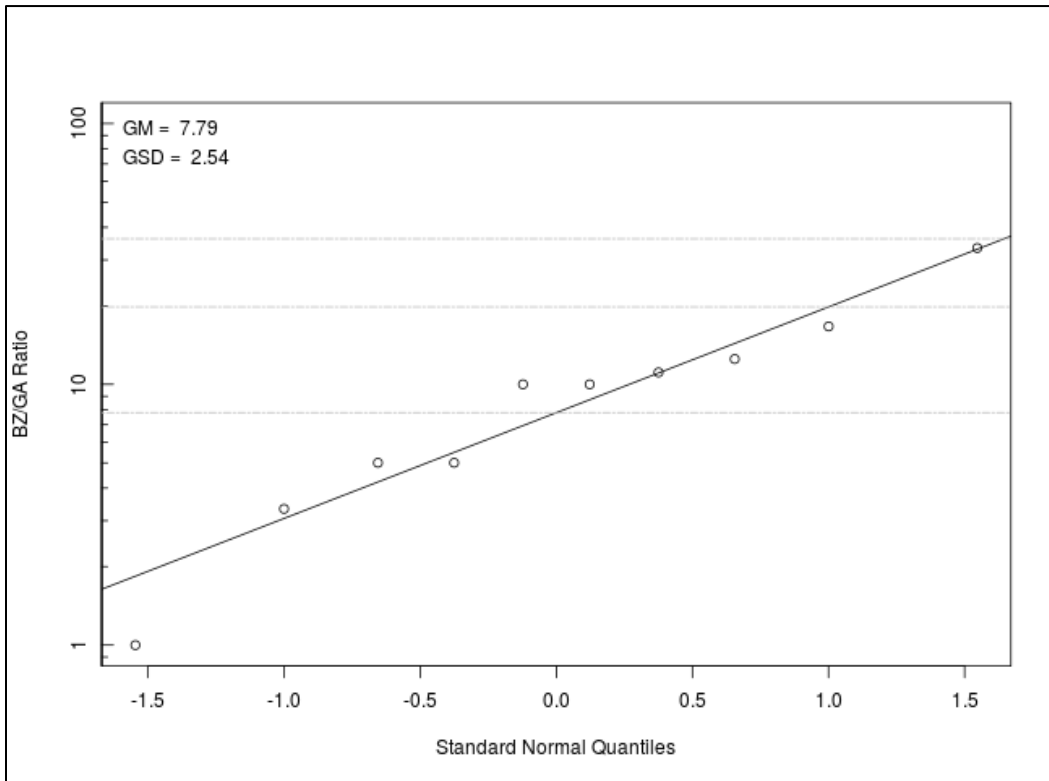
Figure 5-4. Model for Scenario 1 for 10.5-μm aerosols (ORAUT 2020).

5.2.2   Scenario 2 Evaluation: Variable Worker Location Relative to the Release Point

Air sampler locations D1 through D10 were each designated in turn as the BZ location to evaluate the BZ location scenario for Scenario 2. Then, for each BZ location designation, each of the 10 air sampling locations was evaluated as potential GA sampler locations to generate a single BZ:GA ratio dataset for each of the three types of tracer gas or aerosol used in Charuau (1987). This would have generated 30 BZ:GA ratio datasets for Scenario 2, but there were no data for the 2.3-µm aerosol at location D8 (see Figure 5-1). Therefore, only 29 BZ:GA ratio datasets could be generated for Scenario 2. A lognormal model fit was then performed on each of the 29 BZ:GA ratio datasets using ROS (ORAUT 2020).

The 29 lognormal models were then grouped by tracer gas or aerosol type, resulting in 9 lognormal models in the 2.3-µm aerosol group and 10 lognormal models in the other two groups. Each of the three groups of lognormal models were then combined using Monte Carlo simulation to create a single Scenario 2 dataset for each type of tracer gas or aerosol (i.e., one for gas, one for the 2.3-µm aerosol, and one for the 10.5-µm aerosol). A lognormal model fit was then performed on each of the resulting three datasets using ROS (ORAUT 2020).

Figures 5-5 through 5-7 present each of the combined datasets for Scenario 2 in the form of a quantile-quantile plot. In the quantile-quantile plots below, the horizontal lines are the 50th, 84th, and 95th percentiles for the plotted data (ORAUT 2020).
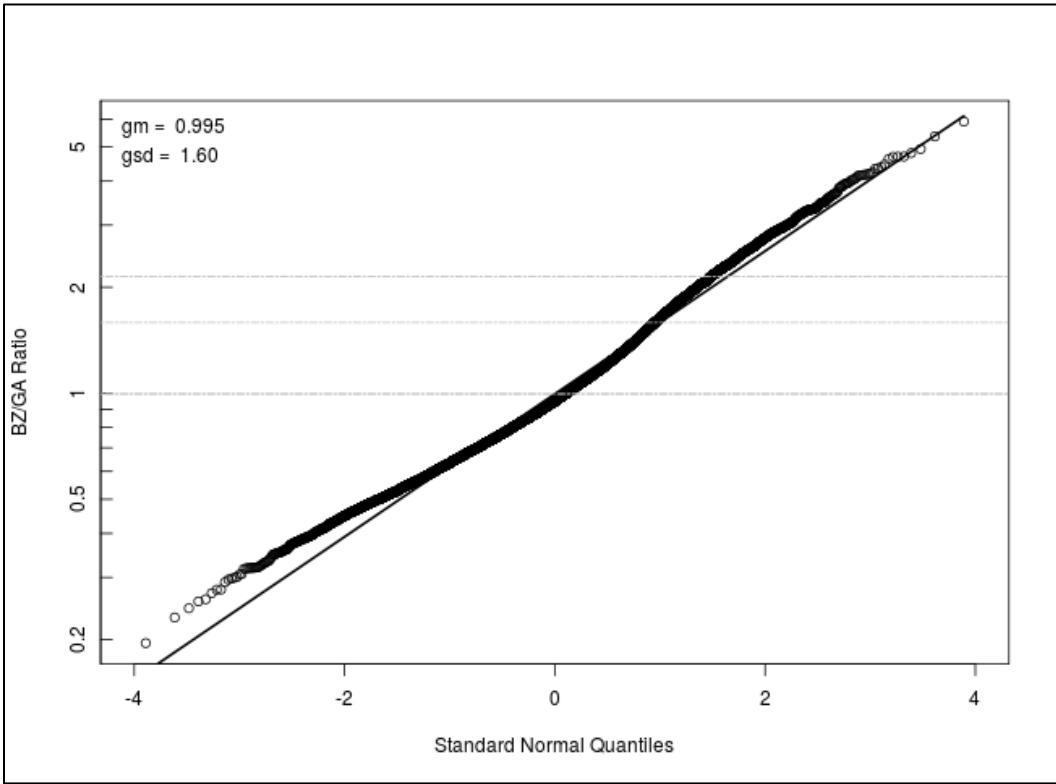
Figure 5-5. Model for Scenario 2 for gas (ORAUT 2020).
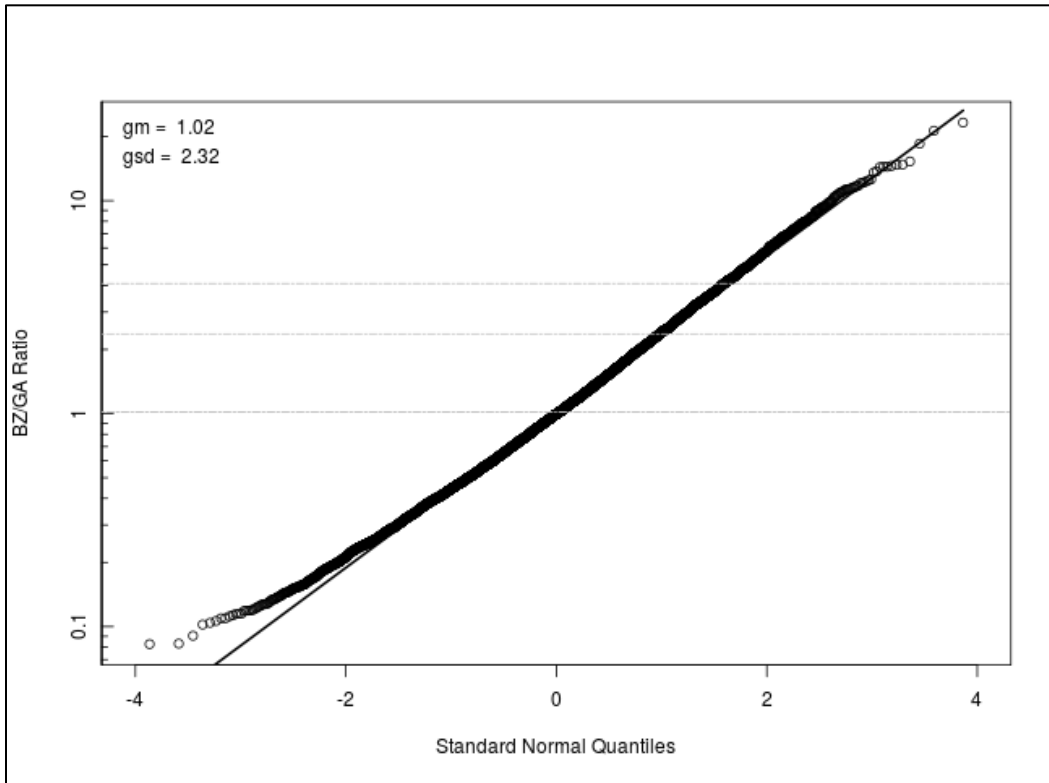
Figure 5-6. Model for Scenario 2 for 2.3-µm aerosols (ORAUT 2020).
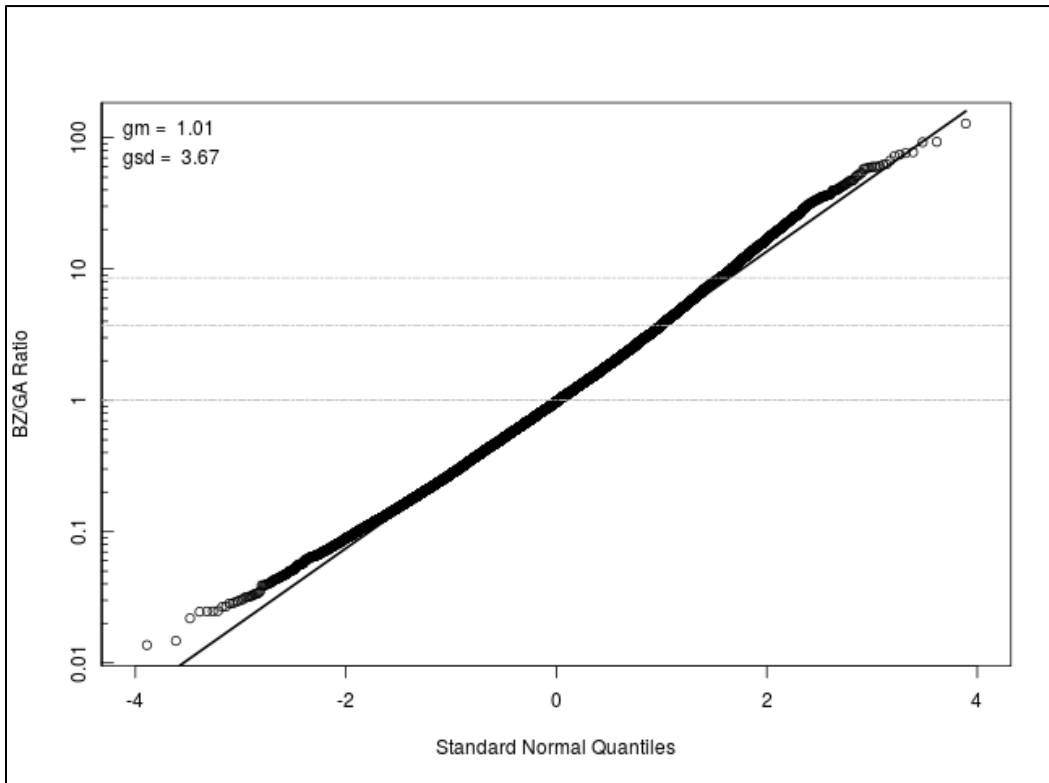
Figure 5-7. Model for Scenario 2 for 10.5-µm aerosols (ORAUT 2020).

5.2.3 Summary of Scenario 1 and Scenario 2 Results

Table 5-1 summarizes the results for Scenario 1, and Table 5-2 summarizes the results for Scenario 2.

Table 5-1. Summary of Charuau (1987) BZ:GA ratio distributions for Scenario 1.

Gas/aerosol	BZ:GA ratio GM	BZ:GA ratio GSD
Gas (helium)	1.97	1.37
2.3-µm aerosol	3.02	1.88
10.5-µm aerosol	7.79	2.54

Table 5-2. Summary of Charuau (1987) BZ:GA ratio distributions for Scenario 2.

Gas/aerosol	BZ:GA ratio GM	BZ:GA ratio GSD
Gas (helium)	0.995	1.60
2.3-µm aerosol	1.02	2.32
10.5-µm aerosol	1.01	3.67

The Charuau (1987) study was the only identified study that had data for different particle sizes. The data in Tables 5-1 and 5-2 show that particle size has a significant effect on the BZ:GA ratios even within the respirable particle size range. It is generally understood that larger particles do not travel as far as smaller size particles. The data for Scenario 1 (Table 5-1) provide a good demonstration of that. It also illustrates the importance of knowing the particle sizes when evaluating the differences between BZ and GA air concentrations for Scenario 1 (i.e., when the BZ is near the release location). For Scenario 2, the effect particle size has on the BZ:GA ratio is more complicated but less significant, because the BZ location is not always closer to the release point than the GA location. At this time, the ORAU Team has no recommendations regarding the use of particle size specific BZ:GA ratios and does not intend to use the particle size specific information in this section.

5.2.4 Combined Scenario 1 and 2 Results for Aerosols

For comparing the Charuau study to the other studies, only the aerosol datasets for the 2.3-µm and 10.5-µm aerosols were of interest. Therefore, the lognormal models for the 2.3-µm and 10.5-µm aerosols were combined, to create a single lognormal model for each scenario (i.e., one for Scenario 1 and one for Scenario 2). Monte Carlo simulation was used to create the combined aerosol datasets. A lognormal model fit was then performed on each of the resulting aerosol datasets using ROS (ORAUT 2020).

For Scenario 1 (colocated worker and release point), the two lognormal models for the 2.3-µm and 10.5-µm aerosols were combined using Monte Carlo simulation to create a single Scenario 1 dataset. A lognormal model fit was then performed on the new Scenario 1 dataset using ROS (ORAUT 2020). The combined Scenario 1 aerosol plot is provided as Figure 5-8.

For Scenario 2 (variable worker location relative to the release point), the 9 lognormal models for the 2.3-µm aerosols and the 10 lognormal models for 10.5-µm aerosols were combined using Monte Carlo simulation to create a single Scenario 2 dataset. A lognormal model fit was then performed on the new Scenario 2 dataset using ROS (ORAUT 2020). The combined Scenario 2 aerosol plot is provided as Figure 5-9.

Table 5-3 summarizes the combined BZ:GA ratio distributions for the aerosols, which will be compared to the other evaluated studies.
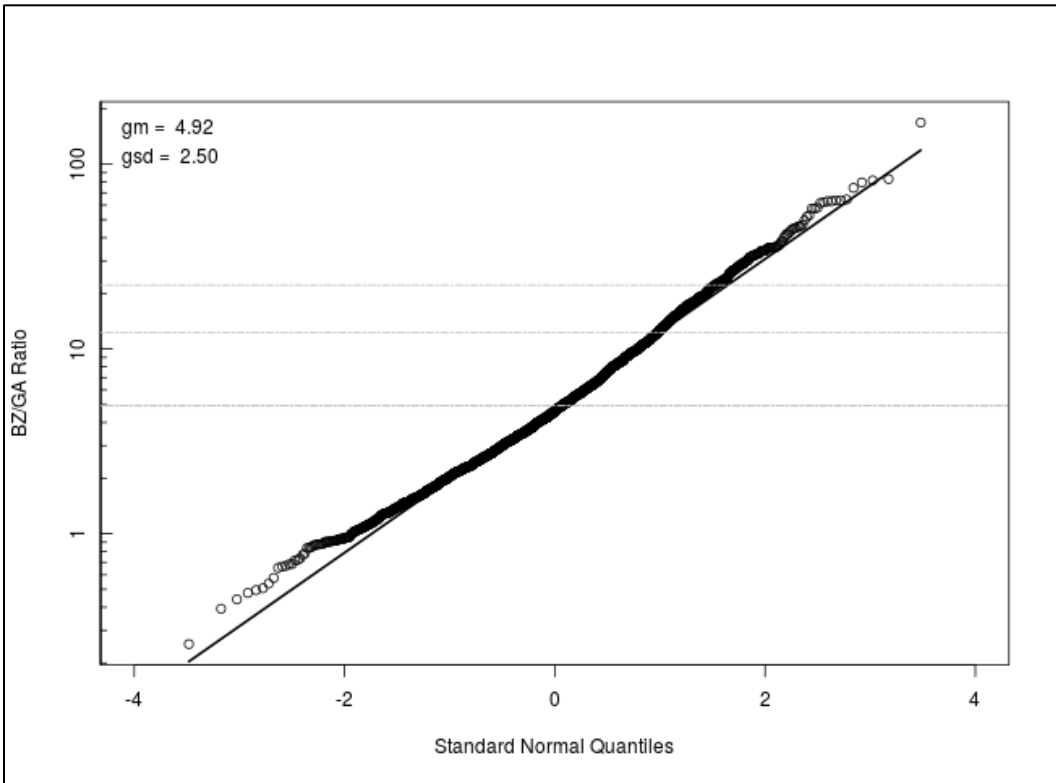
Figure 5-8. Combined model for Scenario 1 for aerosols (ORAUT 2020).
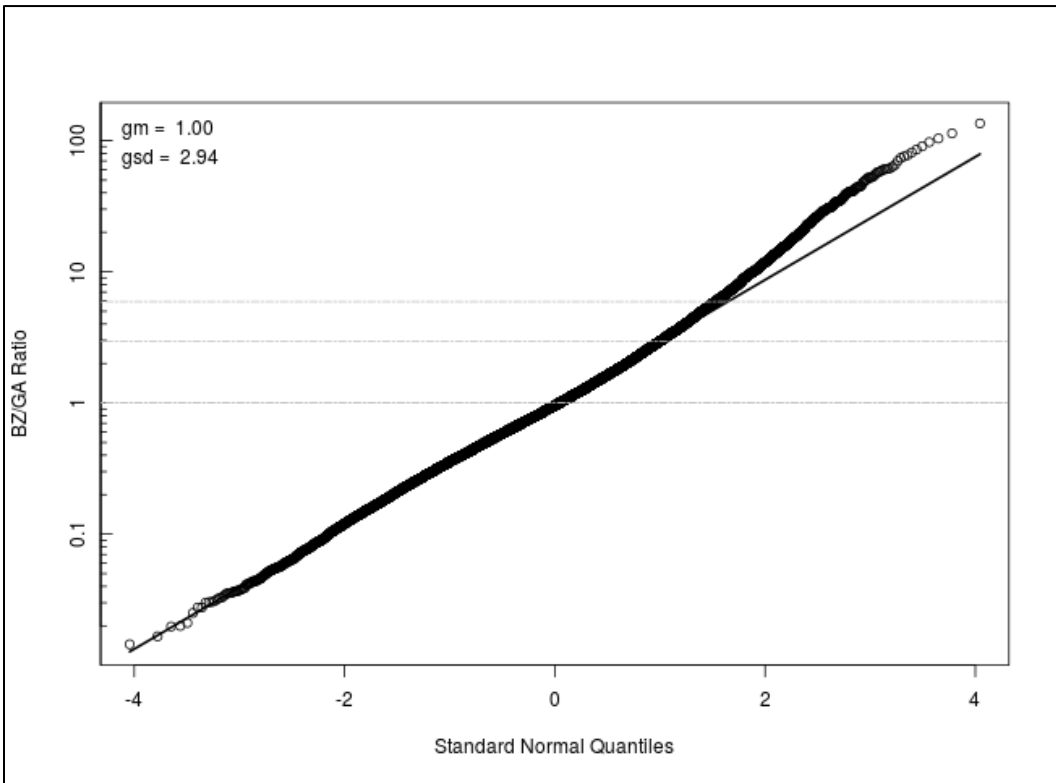
Figure 5-9. Combined model for Scenario 2 for aerosols (ORAUT 2020).

Table 5-3. Summary of the combined BZ:GA ratio distributions for aerosols.

Scenario	BZ:GA ratio GM	BZ:GA ratio GSD
Scenario 1 for aerosols	4.92	2.50
Scenario 2 for aerosols	1.00	2.94

6.0   MUNYON AND LEE STUDY

Workplace air sampling was performed during the decommissioning of a previously active plutonium glovebox facility at Argonne National Laboratory-East. Approximately 60 gloveboxes were included in the scope of the decommissioning project (Munyon and Lee 2002). The primary purposes of the study included (1) describing the relative response between the stationary air samplers (SASs) and PASs, (2) reporting on the results from a set of aerosol particle sizing measurements, and (3) summarizing some general observations about the spatial distribution of radioactive particles that were collected on air sampling filters and the degree to which gross alpha measurements were affected by alpha particle absorption phenomena. The portion of this study addressing the relative response between the SASs and PASs was the primary interest for this report.

6.1   DESCRIPTION OF THE STUDY

The decommissioning operations were performed in an 8.5- by 3.6- by 2.4-m tall (28- by 12- by 8-ft tall) enclosure of prefabricated stainless-steel panels. A drawing of the containment enclosure floorplan, consisting of a workroom and airlock area, is provided in Figure 6-1. The workroom portion of that enclosure had dimensions of 4.9- by 3.6- by 2.4-m tall (16- by 12- by 8-ft tall), which corresponds to a room air volume of 42.34 m^3 (1,495 ft^3). Four air exhaust vents were installed in the workroom; two along the west wall and two moveable aerosol capture hoods that were suspended from the ceiling. The workroom exhaust rate was reported to be approximately 64 m^3/min (2,260 cfm) and was reported to have an AC rate of 90 AC/hr (Munyon and Lee 2002). A portable vacuum system with high-efficiency particulate air filters was used in close proximity to the cutting operations to minimize the dispersal of aerosols. A photograph of the exterior of the enclosure, as viewed from the personnel and equipment entrance side of the enclosure (i.e., the east side), is provided in Figure 6-2. Figure 6-3 is a photograph of the interior of the enclosure's workroom, which shows the two movable aerosol capture hoods along with the west and north SASs (Munyon and Lee 2002).

PASs were used to measure BZ activity concentrations of workers engaged in size-reducing work on the contaminated gloveboxes. SASs were used to measure the work area activity concentrations and test their application in providing representative sampling of BZ activity concentrations (Munyon and Lee 2002). Based on Figures 6-2 and 6-3, the sampling heads for the SASs appear to be positioned at an elevation of 4.5 ft above the floor, which is within the typical BZ elevation. Both the SAS and PAS air filters were removed after each 4-hour work-shift and counted 24 hours later using a gas-flow proportional counter. The air samples were recounted 1 week later, which allowed for the decay of short-lived radon progeny. The contribution of the radon progeny to the initial gross alpha count rate was quite small, typically less than 10% (Munyon and Lee 2002).
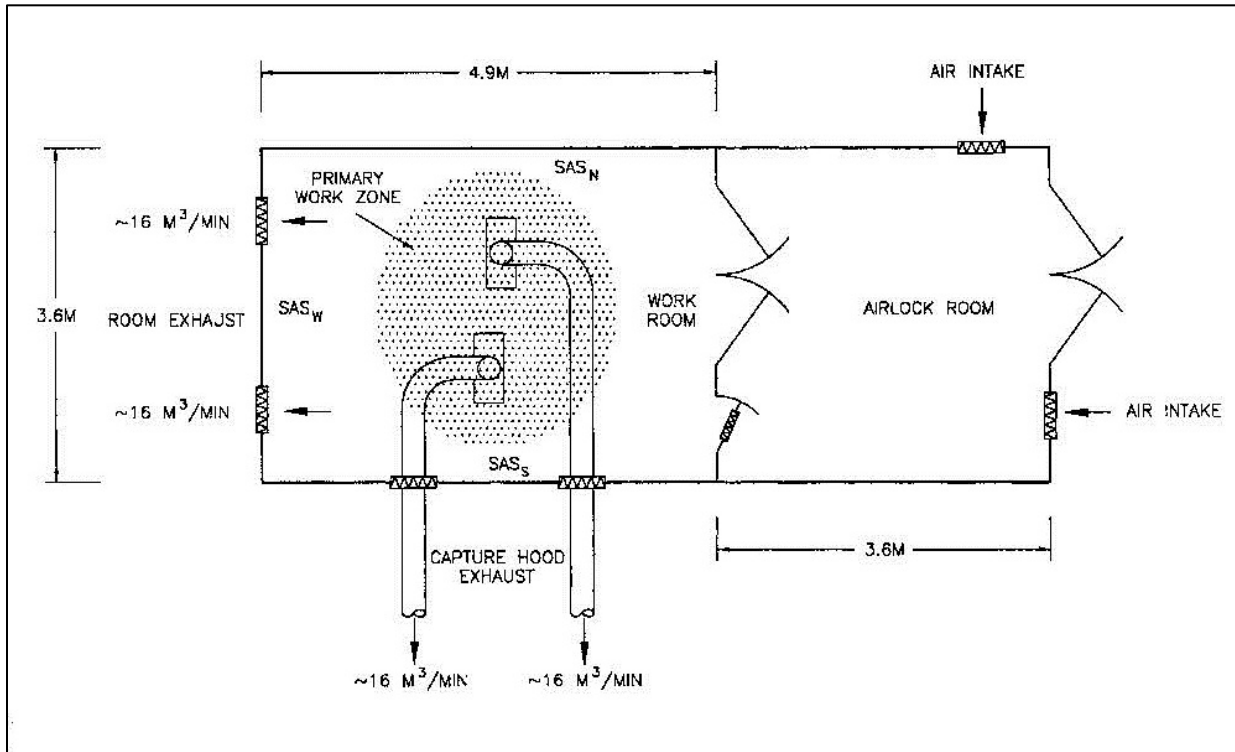
Figure 6-1. Containment enclosure floorplan (Munyon and Lee 2002, p. 3).

Figure 6-2. Exterior view of containment enclosure (Munyon and Lee 2002, p. 3).

Figure 6-3. Interior view of workroom for containment enclosure (Munyon and Lee 2002, p. 3).

Independent of the other air samplers, a 10-stage cascade impactor was used to determine the particle size distribution of workplace aerosols during seven measurement periods. The cascade impactor samples were collected adjacent to the north wall SAS, which is depicted in Figure 6-1. Aerosols were separated on the basis of aerodynamic diameter over a range of 0.08 to 28 µm. The average activity median aerodynamic diameter for the set of seven measurements was 3.0 µm with a corresponding average GSD of 2.4 (Munyon and Lee 2002).

Figure 6-4 depicts the four histograms from Munyon and Lee (2002) that summarize the relative performance between the SASs and PASs. The cumulative response of workplace air samplers throughout the duration of the decontamination and decommissioning project is shown in Figures 6-5 and 6-6. These curves illustrate how well the samplers performed relative to one another. In each case the daily activity concentration was summed over the entire sampling period and then plotted on the basis of the fractional cumulative concentration for each sampler. The relative performance between each of the SAS locations is shown in Figure 6-5. It is interesting to note the general similarity in response between the north and west wall samplers as shown in Figure 6-5. The relative performance between the PASs and SASs is shown in Figure 6-6. Overall, the summed response of the three SASs agrees very well with that of the three corresponding PASs. The plotted data illustrate that the SASs, which were positioned a couple of meters away from the work crew, were indeed sensitive to changes in the activity concentration as measured by the SASs (Munyon and Lee 2002).
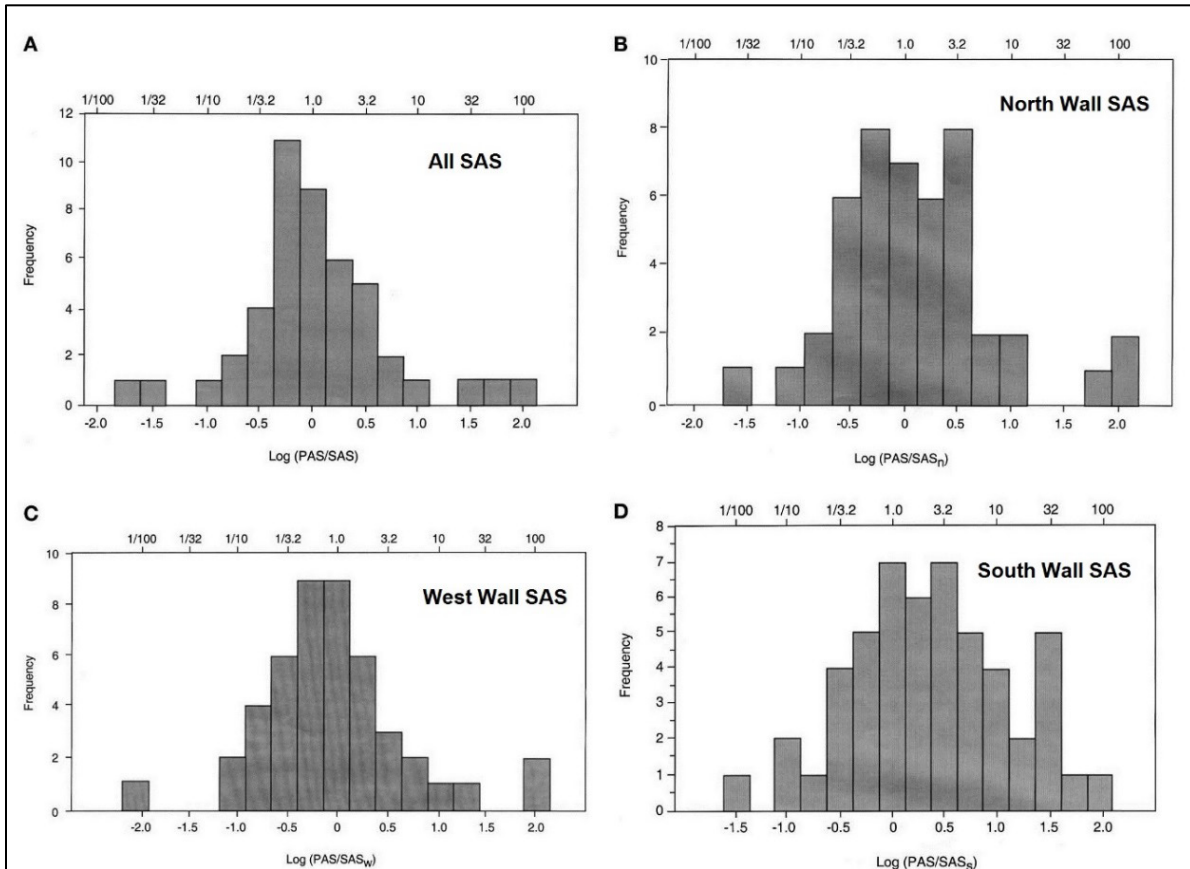
Figure 6-4. Relative performance between the BZ (PAS) and GA (SAS) air samplers (Munyon and Lee 2002, p. 5).
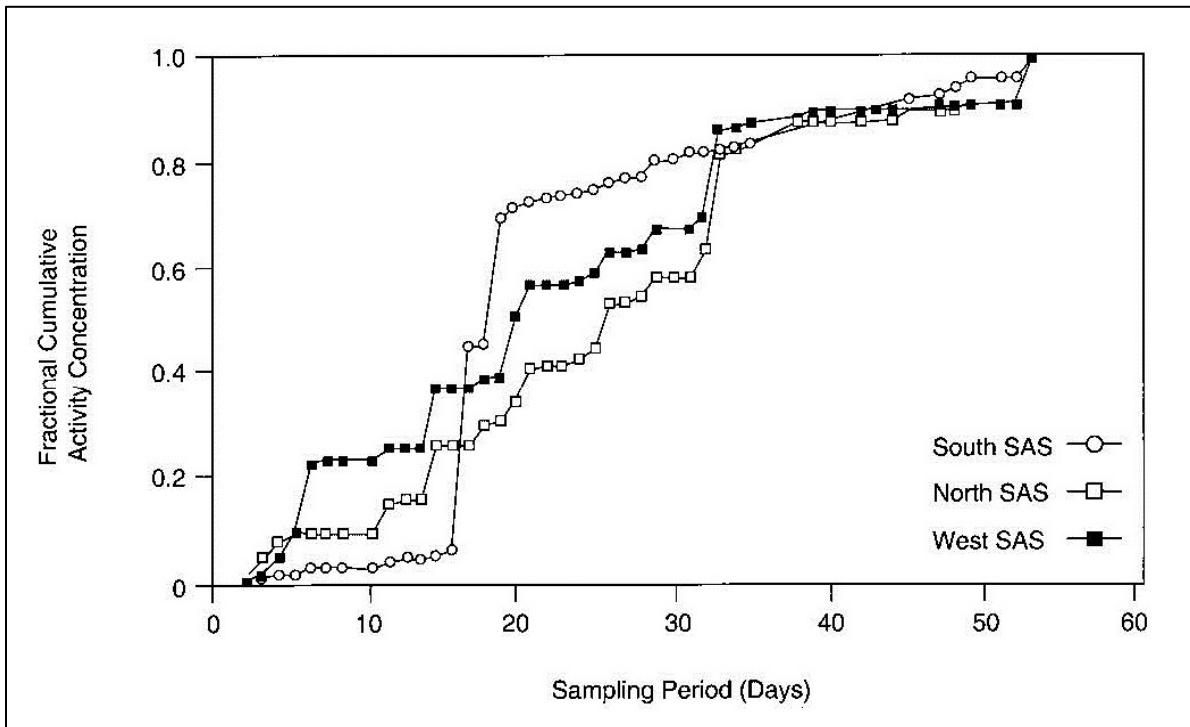
Figure 6-5. Normalized cumulative response functions for SAS data by SAS location (Munyon and Lee 2002, p. 6).
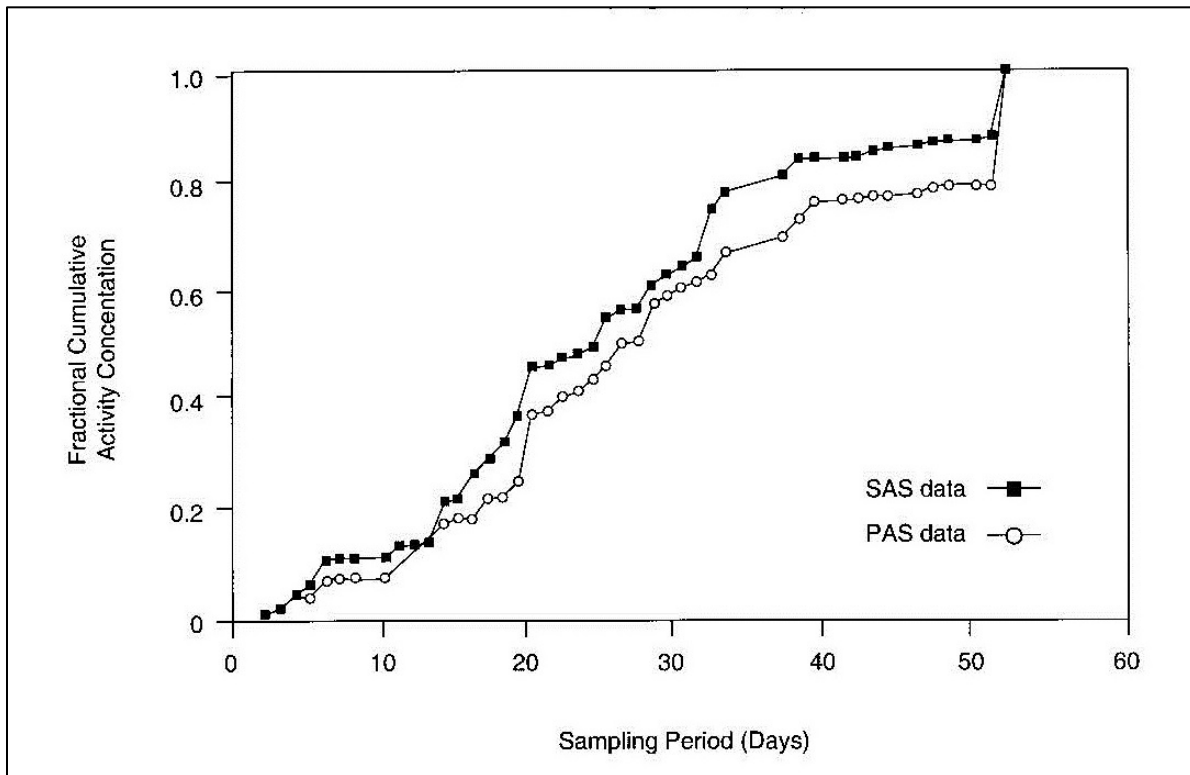
Figure 6-6. Normalized cumulative response functions for PAS versus SAS data (Munyon and Lee 2002, p. 6).

6.2   EVALUATION OF THE MUNYON AND LEE STUDY DATA

In Figure 6-4, Histogram A (i.e., the histogram labelled "All SAS") was thought to represent the sum of Histograms B to D, but an evaluation of the data determined that was not the case. Because Munyon and Lee (2002) only indicate that Histogram A depicts the PAS:SAS ratios with no further details, it could not be determined what Histogram A actually represented. Therefore, the data from Histograms B to D were retabulated to create a combined histogram and dataset for this evaluation.

Unlike the other studies evaluated in this report, Munyon and Lee (2002) is based on an actual work activity and the PAS data from actual workers rather than a simulated scenario. Because the workers likely moved around in the workroom, the data from this study are only representative of the BZ location in Scenario 2.

6.2.1   Statistical Evaluation of the Data

The data were presented in the original paper as a histogram of the frequencies of specified BZ:GA ratios. The data in each bin of the histogram were assigned a value equal to the midpoint of the respective bin. For example, there were five occurrences of a BZ:GA ratio in the bin with a midpoint of 0.1, which is represented in the dataset as {0.1, 0.1, 0.1, 0.1, 0.1}. Then a lognormal model was fit to the dataset using ROS, generating the GM and GSD shown in Figure 6-7. In the quantile-quantile plot below, the quantiles are from the fitted lognormal distribution, and the horizontal lines are the 50th, 84th, and 95th percentiles for the plotted data (ORAUT 2020).

Based on Figure 6-7, the BZ:GA ratio distribution for Scenario 2 (variable worker location relative to the release point) has a GM of 1.08 and a GSD of 5.40.
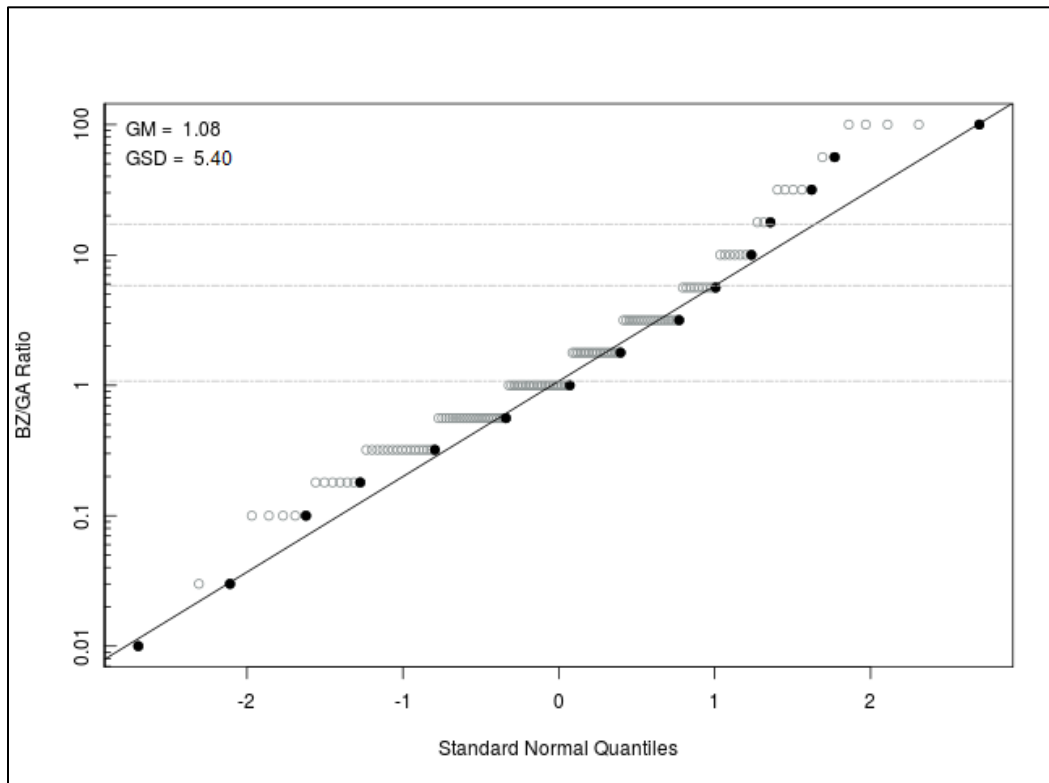
Figure 6-7. Model for Scenario 2 (ORAUT 2020).

7.0 SCRIPSICK ET AL. STUDY

In June 1978, the results of a study at the LANL were presented at the International Atomic Energy Agency Symposium on Advances in Radiation Protection Monitoring, and in August 1979 the paper for that presentation was published as part of the proceedings for that symposium (Scripsick et al. 1979a). Additional details about the LANL study are documented in Section I.A of LANL progress report LA-8153-PR (Scripsick et al. 1979b). The purpose of that study was to measure the dilution of contaminants between worker BZ and GA air concentrations.

7.1 DESCRIPTION OF THE STUDY

In Scripsick et al. (1979a, 1979b), releases were simulated from 20 potential release locations in a typical workroom inside a plutonium-handling facility. Facility operations involved research and development with various forms of plutonium, and all work was performed in gloveboxes.

The workroom dimensions were 9.0- by 6.3- by 4.1-m tall (30- by 21- by 13-ft tall), and the room layout was typical of workrooms dealing with toxic materials. Figure 7-1 provides a diagram of this workroom and depicts the fixed aerosol sampling locations along with the ventilation inlets and outlets. In Figure 7-1, the letters A through H identify the fixed air sampler locations. The asterisks in Figure 7-1 identify the two continuous air monitors (CAMs) locations for the room (locations NEC and SEC) and the locations of two additional air samplers that were used for the study (locations NEX and SEX). The ventilation inlet was near the ceiling, and the ventilation exhausts were on the floor at the opposite end of the room from the inlet. The ventilation rate for the room was approximately 12 AC/hr (Scripsick et al. 1979a, 1979b). Figure 7-2 provides a diagram of the workroom depicting the 20 release locations for this study.
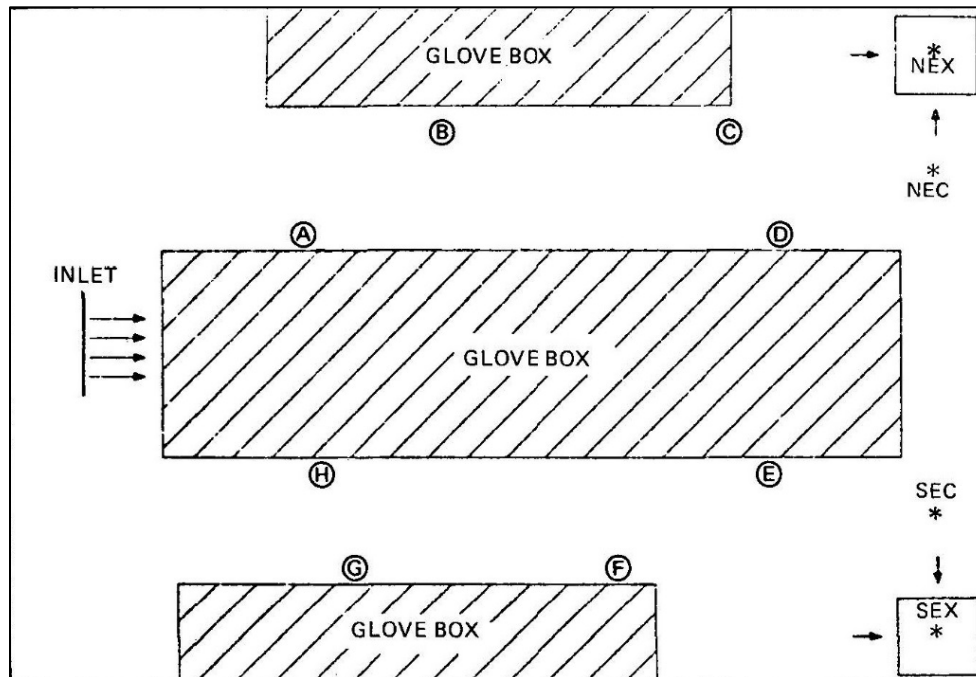
Figure 7-1. Workroom floorplan with ventilation system components and air sampler locations (Scripsick et al. 1979a, p. 319).
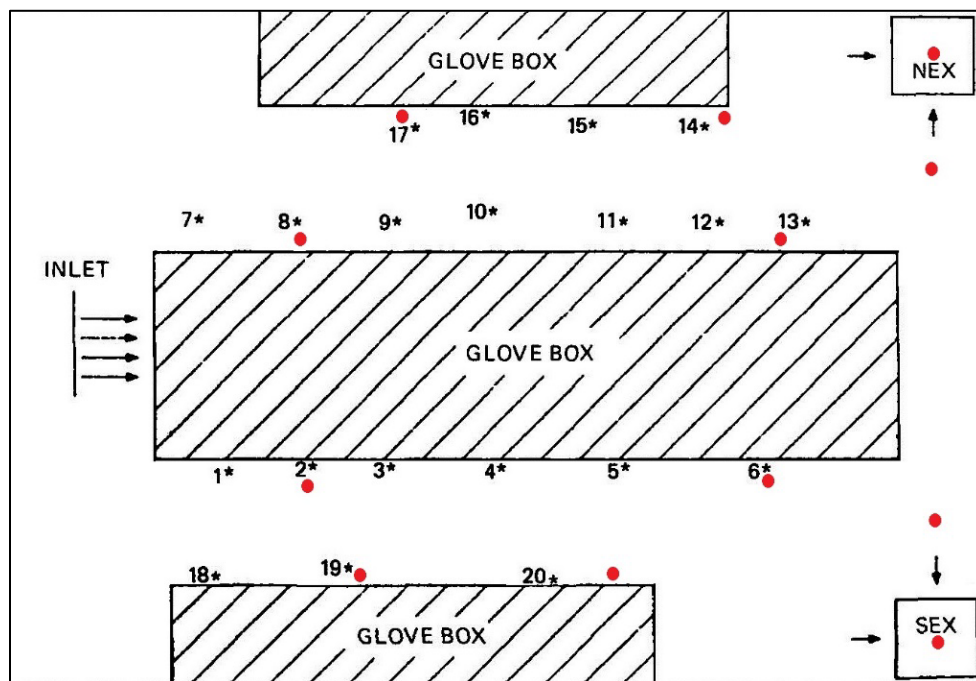
Figure 7-2. Numbered release locations used in the study (Scripsick et al. 1979a, p. 319).

The test aerosol was generated from a solution of fluorescein in NH_4OH, which was detectable at an air concentration of 0.1 µg/m^3 during this study. The generated aerosol had a count median aerodynamic diameter of 0.35 µm with a GSD of 2.1. The aerosol releases were made 1.3 m (4.3 ft) above the floor. Aerosol was generated during the first 15 minutes of each test. Collection of air samples was initiated when the aerosol generation started and continued for 15 minutes after the aerosol generation was stopped. Another test was started after the workroom was allowed to clear for 15 minutes (i.e., after 3 AC), and clean air sampling filters were placed on all samplers. Six releases

were made at each of the 20 locations in Figure 7-2 (Scripsick et al. 1979a, 1979b). Red dots were added to Figure 7-2 to depict the sampler locations from Figure 7-1 in relation to the release locations.

The study used a variable BZ location that was always 0.4 m (1.3 ft) above the release location (i.e., 1.7 m [5.6 ft] above the floor). Area samplers along the glovebox faces (Samplers A through H) were reported as being "~2 m above the floor," which is likely the same height of the BZ sampler rounded to the nearest meter. The CAMs at locations NEC and SEX were located at 1 m (3.2 ft) above the floor. The two additional air samplers at locations NEX and SEX were located immediately above each workroom ventilation exhaust, which was interpreted as being near floor level.

In Scripsick et al. (1979a, 1979b), BZ dilution factors (BDs) were calculated for each release location and sampler location combination by dividing the BZ air concentration at the release by the air concentration at the sampler, which makes the BD values in this study equivalent to BZ:GA ratios. As indicated above, six releases were made at each of the 20 release locations. For each release location and sampler location combination, the average BD value and standard deviation was calculated from the six releases and measurements made for that release location. The results of those measurements and average BD calculations were provided in Table I of Scripsick et al. (1979a, 1979b) and are represented in Table 7-1.

7.2 EVALUATION OF THE SCRIPSICK ET AL. STUDY DATA

To evaluate potential differences between BZ and GA air concentrations, the ORAU Team used the Scripsick et al. (1979a, 1979b) data to evaluate the two BZ location scenarios described at the end of Section 3.0. To evaluate the BZ location in Scenario 1, the data from Table 7-1 was used "as is" because the average BDs in that figure were equivalent to BZ:GA ratios for Scenario 1 (i.e., the BZ location was always at the release point for this study).

Because the actual BZ locations in Scripsick et al. (1979a, 1979b) were fixed for a given release location, the ratio of the BDs (i.e., BZ:GA ratios) in Table 7-1 could be used to generate additional sets of data to evaluate Scenario 2 for this study. By taking the ratio of two different samplers (i.e., two different rows) for the same release location (i.e., the same column) from Table 7-1, the original BZ result in the BDs will cancel out, resulting in the ratio of the concentrations at the two samplers. This can be used to produce a new set of BZ:GA ratios that can be used to evaluate Scenario 2. The following equations are being used to illustrate how the original BZ air concentration from the study can be cancelled out to produce a new BZ:GA ratio.

For release locations j = {1, 2,...,20}, and GA sampler locations i = {A, B,...,H, NEC, SEC, NEX, SEX}.

$$BD_{i,j} = \frac{C_{BZj}}{C_{GAi}} = \frac{BZ_j}{GA_i} = BZ{:}GA_{i,j} \qquad (7\text{-}1)$$

where

$BD_{i,j}$ = is the BD for GA sampler location i and release location j
C_{BZj} = breathing zone air concentration at release location j, which is also notated as BZ_j
C_{GAi} = GA air concentration at GA air sampler location i, which is also notated as GA_i
$BZ{:}GA_{i,j}$ = is the BZ:GA ratio when the GA sampler is at location i and the BZ is at release location j

Table 7-1. Average BDs by release location.[a]

Samplers	1	2	3	4	5	6	7	8	9	10
A	5.7 ±0.3[b]	7.1 ±2.1	7.5 ±2.3	16 ±5.8	40 ±11	151 ±55	13 ±5.2	2.6 ±0.3	7.3 ±3.6	26 ±11
B	6.0 ±0.7	9.4 ±3.9	6.5 ±0.3	10 ±3.6	28 ±5.5	132 ±89	22 ±0.9	15 ±3.3	9.4 ±1.3	15 ±4.6
C	8.0 ±0.3	11 ±2.3	5.1 ±0.4	8.5 ±1.2	33 ±9.0	45 ±15	29 ±2.7	28 ±4.5	24 ±5.7	32 ±4.4
D	7.4 ±4	15 ±7.6	6.3 ±1.0	6.9 ±0.8	25 ±5.6	54 ±25	18 ±4.0	17 ±5.6	11 ±2.3	18 ±2.9
E	6.6 ±0.2	7.4 ±1.3	19 ±12	12 ±2.3	22 ±0.6	23 ±23	35 ±8.7	41 ±3.9	38 ±7.0	41 ±8.6
F	6.0 ±0.6	6.4 ±1.1	34 ±14	15 ±3.8	34 ±30	338 ±128	40 ±9.2	49 ±2.8	43 ±2.7	48 ±10
G	4.9 ±0.1	5.9 ±0.8	6.0 ±0.7	15 ±6.3	71 ±46	466 ±190	36 ±13	50 ±6.6	44 ±2.2	49 ±12
H	2.6 ±0.9	2.9 ±1.3	5.7 ±1.1	20 ±8.7	119 ±54	1079 ±384	44 ±26	96 ±11	79 ±34	102 ±23
NEC	11 ±0.5	13 ±5.0	11 ±2.3	18 ±2.6	32 ±10	23 ±6.1	43 ±11	54. ±7.4	53 ±4.1	48 ±15
SEC	11 ±2.1	12 ±3.7	11 ±4.0	19 ±3.0	3.9 ±8.7	31 ±7.2	55 ±8.0	5.4 ±4.1	64 ±40	57 ±15
NEX	9.8 ±0.7	10 ±1.7	8.6 ±2.4	36 ±33	43 ±13	25 ±11	36 ±36	51 ±34	64 ±40	57 ±15
SEX	11 ±1.0	13 ±5.6	15 ±5.4	25 ±6.4	69 ±36	365 ±456	60 ±20	89 ±19	69 ±22	61 ±8.3

Samplers	11	12	13	14	15	16	17	18	19	20
A	68 ±39	168 ±64	148 ±60	102 ±49	41 ±24	46 ±21	63 ±15	8.6 ±2.5	19 ±10	68 ±20
B	33 ±8.2	78 ±31	55 ±18	46 ±25	24 ±13	31 ±10	1 ±0.2	8.4 ±1.4	1.3 ±3.2	50 ±21
C	31 ±13	38 ±5.2	104 ±142	32 ±16	23 ±8.1	41 ±4.7	28 ±4.6	8.9 ±0.7	6.4 ±0.6	24 ±7.1
D	13 ±2.0	1.6 ±2.0	6.3 ±19	23 ±9.2	11 ±2.4	13 ±2.0	24 ±3.3	9.0 ±1.3	6.2 ±0.4	22 ±10
E	63 ±26	150 ±25	215 ±18	62 ±18	61 ±22	66 ±12	59 ±11	15 ±2.7	12 ±1.7	23 ±0.7
F	83 ±32	194 ±36	236 ±25	76 ±21	72 ±20	83 ±41	68 ±13	16 ±1.0	13 ±1.2	26 ±7.0
G	118 ±45	240 ±51	256 ±45	110 ±38	86 ±22	79 ±16	73 ±13	12 ±2.1	12 ±1.4	46 ±18
H	224 ±83	469 ±114	546 ±125	194 ±90	196 ±39	165 ±34	124 ±37	6.7 ±1.9	10 ±0.7	61 ±33
NEC	58 ±27	41 ±34	87 ±61	85 ±25	42 ±28	84 ±29	9.6 ±1.4	14 ±2.1	11 ±1.1	8.5 ±1.9
SEC	84 ±41	217 ±43	268 ±98	80 ±25	92 ±35	90 ±23	88 ±19	54 ±78	18 ±2.2	20 ±7.2
NEX	45 ±49	66 ±73	47 ±30	28 ±8.9	23 ±9.6	21 ±6.9	11 ±3.5	13 ±4.6	8.5 ±3.7	23 ±12
SEX	200 ±252	208 ±46	356 ±128	83 ±25	86 ±18	162 ±166	143 ±146	17 ±1.8	12 ±1.3	18 ±12

a.   Sources: Scripsick et al. (1979a, 1979b).
b.   Standard deviation estimate over six releases.

For new BZ location x, which is a selected GA sampler location:

$$\frac{BZ{:}GA_{i,j}}{BZ{:}GA_{x,j}} = \frac{\left(\dfrac{BZ_j}{GA_i}\right)}{\left(\dfrac{BZ_j}{GA_x}\right)} = \frac{GA_x}{GA_i} = BZ{:}GA_{i,x} \tag{7-2}$$

Using the data for Release Location 1 as an example, the original BZ location was at Release Location 1, which is not depicted as an air sampler location in Figure 7-1. To redesignate GA sampler location A as the new BZ location and produce a new BZ:GA ratio from that data, one just needs to take the following ratio:

$$\frac{BZ{:}GA_{NEC,1}}{BZ{:}GA_{A,1}} = \frac{\left(\dfrac{BZ_1}{GA_{NEC}}\right)}{\left(\dfrac{BZ_1}{GA_A}\right)} = \frac{GA_A}{GA_{NEC}} = BZ : GA_{NEC,A} \tag{7-3}$$

7.2.1   Statistical Evaluation of the Data

The two BZ location scenarios described at the end of Section 3.0 were used to evaluate the potential differences between the BZ and GA air concentrations in the Scripsick et al. (1979a, 1979b) study. The following describes how Scenario 1 and Scenario 2 were evaluated using the data from Table 7-1. For each scenario, a lognormal model was fit to each dataset using ROS, generating a GM and GSD for each model. In the quantile-quantile plots below, the quantiles are from the fitted lognormal distribution, and the horizontal lines are the 50th, 84th, and 95th percentiles for the plotted data (ORAUT 2020).

7.2.1.1   Scenario 1 Results: Colocated Worker and Release Point

As indicated above, the raw data in Table 7-1 are BDs, which are equivalent to BZ:GA ratios when the BZ is always at the release location. Therefore, the BDs in Table 7-1 were used as is for evaluating Scenario 1. In Table 7-1, a BD is given for 10 retrospective samplers and 2 CAMs at each of the 20 release points. A lognormal model was fit to the 240 BZ:GA ratios in Table 7-1, which is shown in Figure 7-3 (ORAUT 2020).
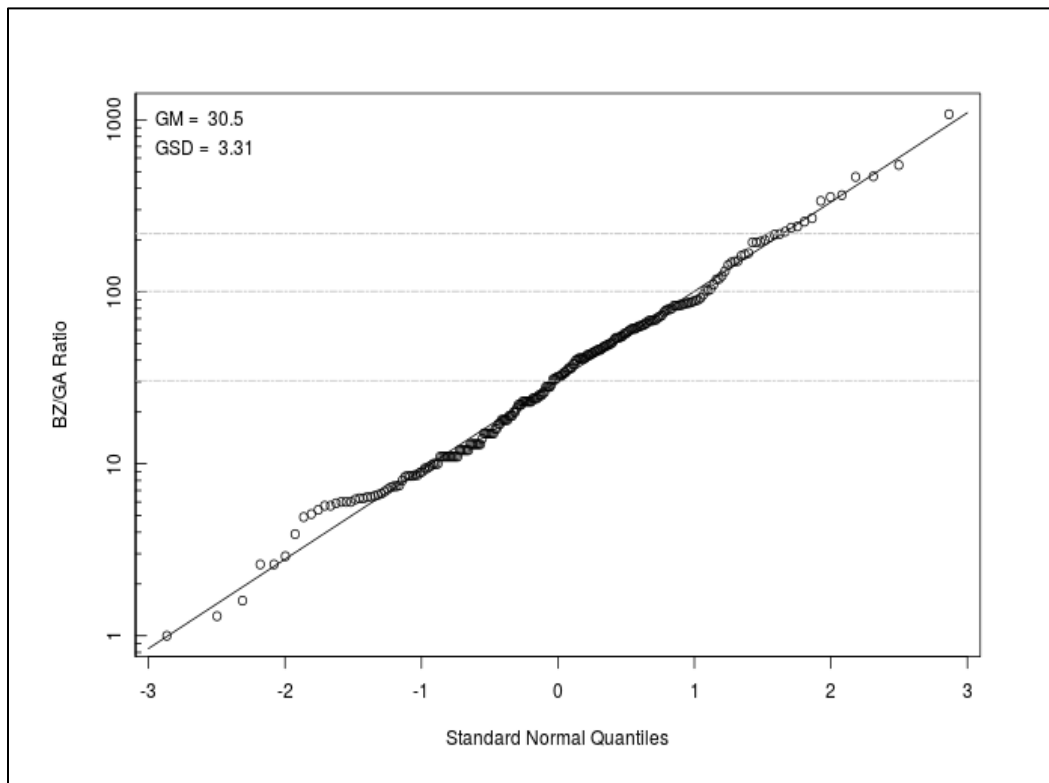
Figure 7-3. Model for Scenario 1 (ORAUT 2020).

7.2.1.2 Scenario 2 Results: Variable Worker Location Relative to the Release Point

For the Scenario 2 evaluation, additional BZ:GA ratio combinations were calculated from the Table 7-1 data using Equations 7-1 and 7-2. To produce the additional BZ:GA ratio combinations for the Scenario 2 evaluation, air sampler locations A through H were evaluated as other potential BZ locations. These additional BZ locations are in addition to the ones used for Scenario 1 (i.e., when the BZ location was always at the release location). Because the air samplers at locations NEC, SEC, NEX, and SEX were only 1 m (3.2 ft) above the floor or less, they were excluded as potential BZ locations for this evaluation. For each of the eight new BZ locations, all 12 air sampler locations were each designated in turn as the GA locations for all 20 release locations. For example, when the location A air sampler was designated as the BZ location (BZ-A), a BZ:GA ratio was calculated for each of the 12 potential GA locations and 20 release locations. This created a single BZ:GA ratio dataset consisting of 240 data points for the BZ-A location. Then a lognormal model fit was performed on the new dataset for the BZ-A location using ROS (ORAUT 2020). This process was then repeated for each of the remaining new BZ location designations until a new lognormal model was created for all eight of the new BZ locations (ORAUT 2020).

Because the GMs for the eight new lognormal models were significantly lower than the GM for the lognormal model for Scenario 1, the eight new lognormal models were combined to evaluate how well they fit a single lognormal distribution by themselves. The eight new lognormal models were combined using Monte Carlo simulation to create a single dataset for when the BZ location was at air sampler locations A through H. A lognormal model fit was then performed on the new dataset using ROS (ORAUT 2020). Figure 7-4 provides the results of this intermediate evaluation for Scenario 2. Based on Figure 7-4, the combination of the eight new lognormal models fit a single lognormal distribution reasonably well.
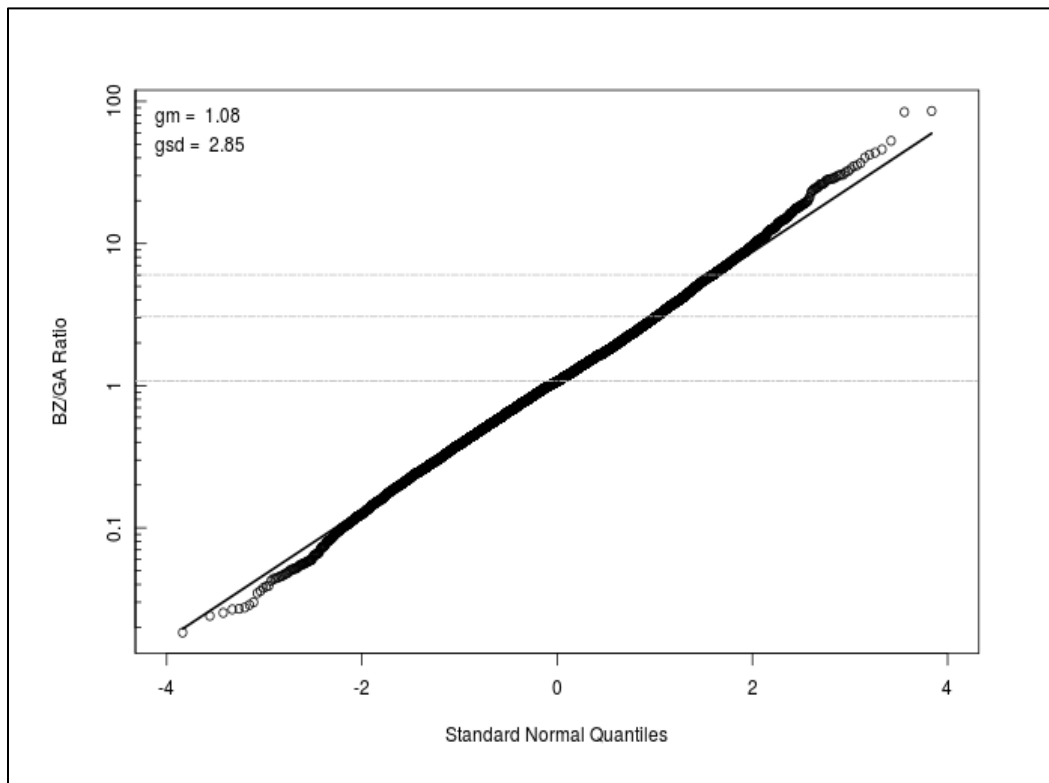
Figure 7-4. Intermediate model for Scenario 2 (ORAUT 2020).

For the Scenario 2 evaluation, the eight new lognormal models were combined with the lognormal model for Scenario 1 using Monte Carlo simulation to create a single dataset for Scenario 2. A lognormal model fit was then performed on the new dataset using ROS (ORAUT 2020). Figure 7-5 provides the results for the Scenario 2 evaluation. As indicated by Figure 7-5, this combination of lognormal models no longer fits a single lognormal distribution very well. Based on Figures 7-3, 7-4, and 7-5, the complete Scenario 2 dataset is clearly the product of two significantly different lognormal distributions. The lack of fit between the Scenario 1 model and the other eight models was tolerated for this report because it represents only one of nine different models that were combined to generate the Scenario 2 model. Fitting the Scenario 2 dataset to a different distribution other than a lognormal distribution was not considered, because it would have been impractical for this report and its intended uses. For practical reasons, the final models need to be lognormal distributions. Consideration was given to excluding the Scenario 1 model from this Scenario 2 evaluation. However, it was decided that it would be more appropriate to include it for the following reasons: (1) the scenario when the BZ location is at the release locations is a plausible scenario that should be included in the Scenario 2 evaluation, (2) the GM and GSD values would be lower if the Scenario 1 model was excluded, and (3) excluding the Scenario 1 model would make this Scenario 2 evaluation inconsistent with the Scenario 2 evaluations performed on the other studies that were evaluated in this report.
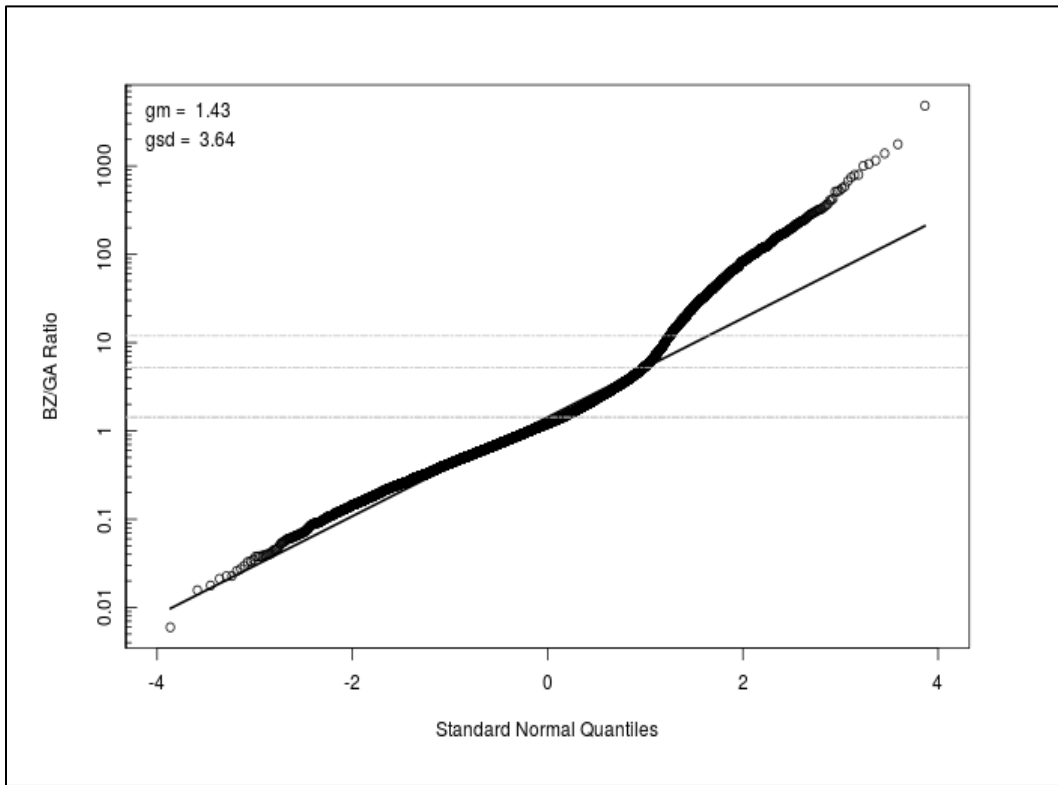
Figure 7-5. Model for Scenario 2 (ORAUT 2020).

7.2.1.3   Summary of Scenario 1 and Scenario 2 Results

Table 7-2 summarizes the results from Sections 7.2.1.1 and 7.2.1.2 for Scenarios 1 and 2.

Table 7-2. Summary of the BZ:GA ratio
distributions for Scripsick et al. (1979a, 1979b).

Scenario	BZ:GA ratio GM	BZ:GA ratio GSD
Scenario 1	30.5	3.31
Scenario 2	1.43	3.64

8.0   WHICKER AND MOXLEY STUDY

In 2001, the results of a study that was performed by LANL personnel at the Savannah River Site
(SRS) C-Lab were documented as LA-UR-01-4933 (Whicker and Moxley 2001). Additional details
about the study were also documented in a 2003 *Health Physics* journal article (Whicker, Rodgers,
and Moxley 2003). The specific goals of the Whicker and Moxley study were to measure fundamental
airflow characteristics (velocity, turbulence), aerosol lag times, dilution, and potential dose savings
given various arrangements of CAMs. From those measurements an evaluation of the adequacy of
the then-current CAM sampling location was performed, and the study also evaluated other possible
sampling locations to determine the optimal number of and placement of CAMs.

8.1   DESCRIPTION OF THE STUDY

In Whicker and Moxley (2001), releases were simulated from six potential release locations in the
C-Lab. At the time of the study, the SRS C-Lab was being used as a low-level plutonium chemistry
laboratory that contained multiple workstations, hoods, and gloveboxes. The laboratory dimensions
were approximately 6- by 4- by 3- m tall (20- by 13- by 10-ft tall). Figure 8-1 provides a diagram of the

C-Lab and depicts the release locations and air sampling locations. In Figure 8-1, the boxes with R1 to R6 in them identify the six release locations, and the numbers identify the fixed air sampler and CAM locations. Sampler location 8 is not depicted in Figure 8-1 because it represents the variable location of the BZ sample. The supply air for the workroom was introduced through a series of diffusers along a ceiling strip that ran through the middle of the room, and the room air was exhausted through the chemical hoods. The ventilation rate for the room was approximately 15 AC/hr.

Figure 2. Map of aerosol study with LPC sampling locations (1-15) and release locations (R1-R6). Number 15 is approximately at the same sampling location of the current CAM indicated by the shaded circle. Hallway is to the left of the room.
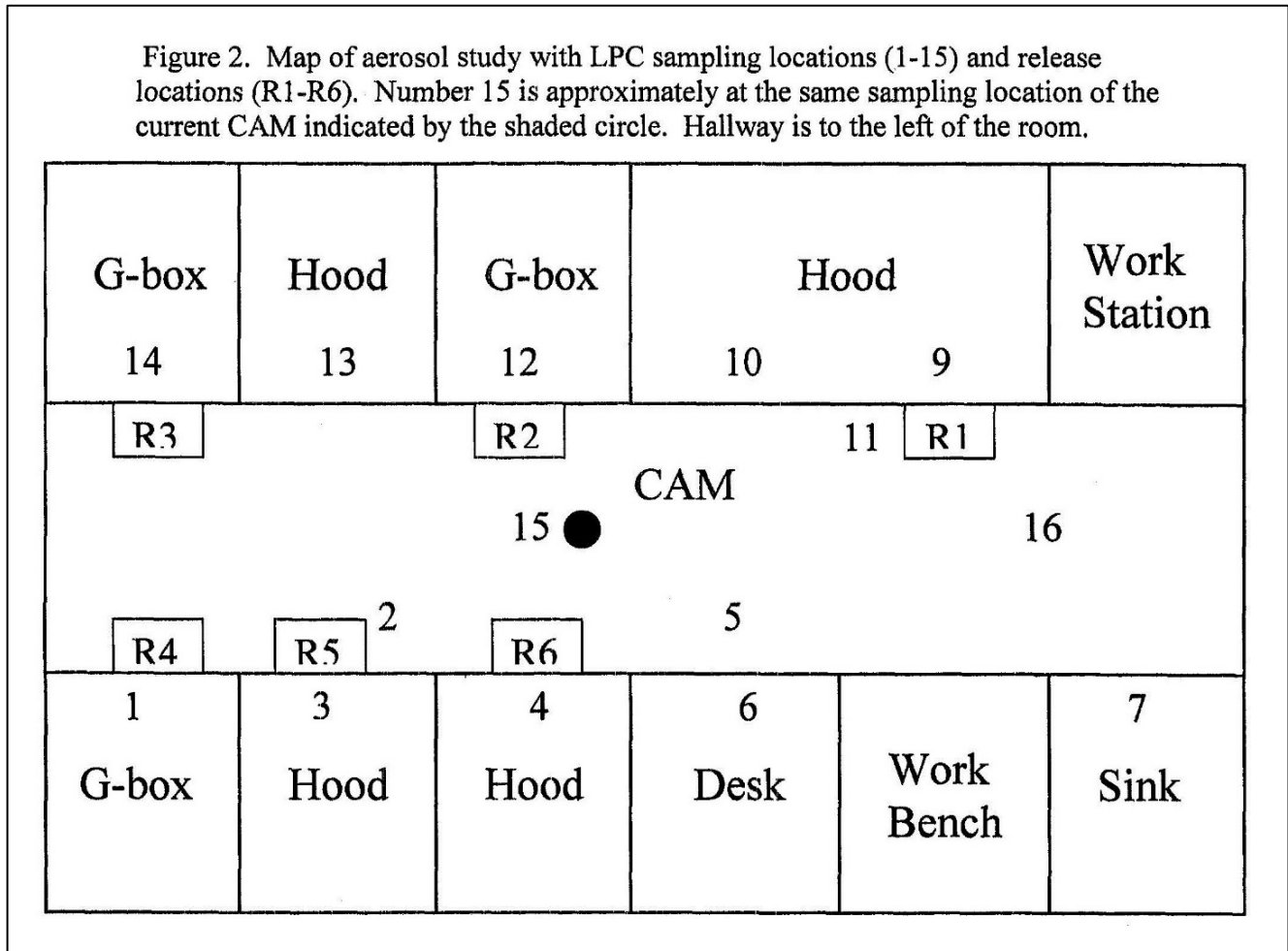
Figure 8-1. C-Lab floorplan with air sampler locations and release locations depicted (Whicker and Moxley 2001, p. 16).

The six different release locations used in the study were based on input from the C-Lab operations personnel, who indicated those six locations were the most probable locations for real releases. The simulated releases were in the form of 60-second "puff-type" releases at each of the six release locations in the workroom. Three separate releases were performed at each of the six locations to measure the variability of the aerosol dispersion, which resulted in a total of 18 simulated releases.

To simulate a radioactive aerosol release, a nontoxic oil (dioctyl sebacate) aerosol was released from an aerosol generator. The generated particles were polydispersable with a size range of 0.01 to 2 µm. The distribution of the particle size range had a GM of about 0.3 µm and a GSD of less than 2. Tracer releases at glovebox workstations (release locations R2 through R4) were conducted about 30 cm (~1 ft) in front of the glovebox face and at the height of the gloves, to simulate the breach of a glove. Tracer releases at chemical hood workstations (release locations R1, R5, and R6) were conducted in front of the hood and near the floor to simulate a dropped sample that breaks on the

floor and disperses the material into the air (Whicker and Moxley 2001; Whicker, Rodgers, and Moxley 2003).

Sixteen laser particle counters (LPCs), which were coupled to a multiplexer, were used to measure the concentrations at all of the sampling locations. The 16 LPCs were set up to provide concentration measurements in 10-second intervals to measure the aerosol migration through time and space. For this ORAU Team report, only the 9-minute average concentration data for each release location and sampler location combination were used. In Whicker, Rodgers, and Moxley (2003), the 9-minute average concentration was defined as the tracer aerosol concentration measurements averaged over a 9-minute interval.

For the simulated releases, it was assumed the cause of release was the result of a worker's action and not a random event (i.e., the worker was always next to the aerosol release). To do that, the study used a variable BZ location designated as location 8. The BZ LPC was always positioned about 30 cm (~1 ft) over and behind the aerosol generator's release point (Whicker and Moxley 2001; Whicker, Rodgers, and Moxley 2003). For the chemical hood release locations, this put the BZ location only 30 cm (~1 ft) or so above the floor, which is an unlikely BZ location. One would also expect a release and BZ location combination that close to the floor to significantly bias the BZ air concentrations for release locations R2 through R4 high. However, a comparison of the measured concentrations for location 8 and the nearest fixed sampler that was closest to the BZ location indicates that was not the case. The fact that chemical hoods were the room's air exhaust points might have mitigated the potential bias. The LPC at location 15 was placed about 30 cm (~1 ft) directly below the existing CAM intake tube for evaluation and comparison with other CAM placement locations (Whicker and Moxley 2001). For LPC locations 1 through 7, 9 through 14, and 16, no sampling elevation was provided in the documentation. For this ORAUT Team report, it was assumed the sampling elevation for LPC locations 1 through 7, 9 through 14, and 16 was 1.7 m (5.6 ft), which was the sampler elevation in other LANL studies.

8.2 EVALUATION OF THE WHICKER AND MOXLEY STUDY DATA

As indicated above, only the 9-minute average concentration data generated for each release location and sampler location combination were used for this report. The 9-minute average concentration data are redepicted in Table 8-1.

Table 8-1. 9-min average air concentrations by release location (particles/ft^3) (Whicker and Moxley 2001).

Measurement location	R1	R2	R3	R4	R5	R6
1	14,406	423,751	828,070	929,484	60,554	74,831
2	75,033	450,019	559,933	547,856	62,260	411,195
3	No data	345,591	494,387	542,140	38,438	107,993
4	62,693	156,404	355,190	496,388	7,545	227,033
5	171,816	98,778	144,317	190,359	3,300	461,537
6	244,397	93,188	53,089	93,091	2,000	624,272
7	268,213	77,182	32,609	52,222	478	423,681
8[a]	350,699	205,203	504,657	544,960	42,109	485,956
9	200,578	89,125	43,691	75,236	454	435,768
10	147,222	70,434	92,680	118,969	1,525	388,079
11	215,446	437,992	261,424	289,824	6,039	458,991
12	34,089	151,648	320,713	358,358	7,874	183,370
13	10,678	276,646	470,217	494,661	29,715	69,539
14	10,385	291,385	549,856	594,946	42,683	65,453
15	128,326	198,547	371,092	421,902	15,141	333,763
16	22,348	592,443	968,702	989,134	56,281	107,379

a. Measurement location 8 was a variable location that represented the BZ location that was used in the C-Lab study.

To evaluate potential differences between BZ and GA air concentrations from the Whicker and Moxley (2001) study, the ORAU Team used the data in Table 8-1 to evaluate the two BZ location scenarios described at the end of Section 3.0.

8.2.1 Statistical Evaluation of the Data

The two BZ location scenarios described at the end of Section 3.0 were used to evaluate the potential differences between the BZ and GA air concentrations in the Whicker and Moxley (2001) study. The following describes how Scenario 1 and Scenario 2 were evaluated using the data from Table 8-1. For each scenario, a lognormal model was fit to the dataset for that scenario using ROS, generating a GM and GSD for each model. In the quantile-quantile plots below, the quantiles are from the fitted lognormal distribution, and the horizontal lines are the 50th, 84th, and 95th percentiles for the plotted data (ORAUT 2020).

For the Scenario 1 and Scenario 2 evaluations, BZ:GA ratios were calculated for each potential BZ location from the air concentration data in Table 8-1. To produce those BZ:GA ratios, all 16 air sampler locations were evaluated as potential BZ locations. Then, for each of the 16 BZ locations, all 16 air sampler locations were each designated in turn as the GA locations for all six release locations. For example, when the location 1 air sampler was designated as the BZ location (BZ-1), a BZ:GA ratio was calculated for each of the 16 potential GA locations and six release locations. This created a single BZ:GA ratio dataset consisting of 95 data points for the BZ-1 location. Because there was no air concentration result for the air sampler at location 3 for the first release location (R1), there were only 95 BZ:GA ratio combinations generated for each BZ location dataset. Then a lognormal model fit was performed on the new dataset for the BZ-1 location using ROS. This process was then repeated for each of the remaining BZ location designations until a new lognormal model was created for all 16 of the BZ locations (ORAUT 2020).

8.2.1.1 Scenario 1 Results: Colocated Worker and Release Point

Only the lognormal model that was generated for BZ-8 location dataset was used for the Scenario 1 evaluation. The location 8 air sampler represented the sampling location at each release point. As

indicated in Table 8-1, location 8 was a variable sampling location that was dependent on the location of the release point. The lognormal model for Scenario 1 is shown in Figure 8-2 (ORAUT 2020).
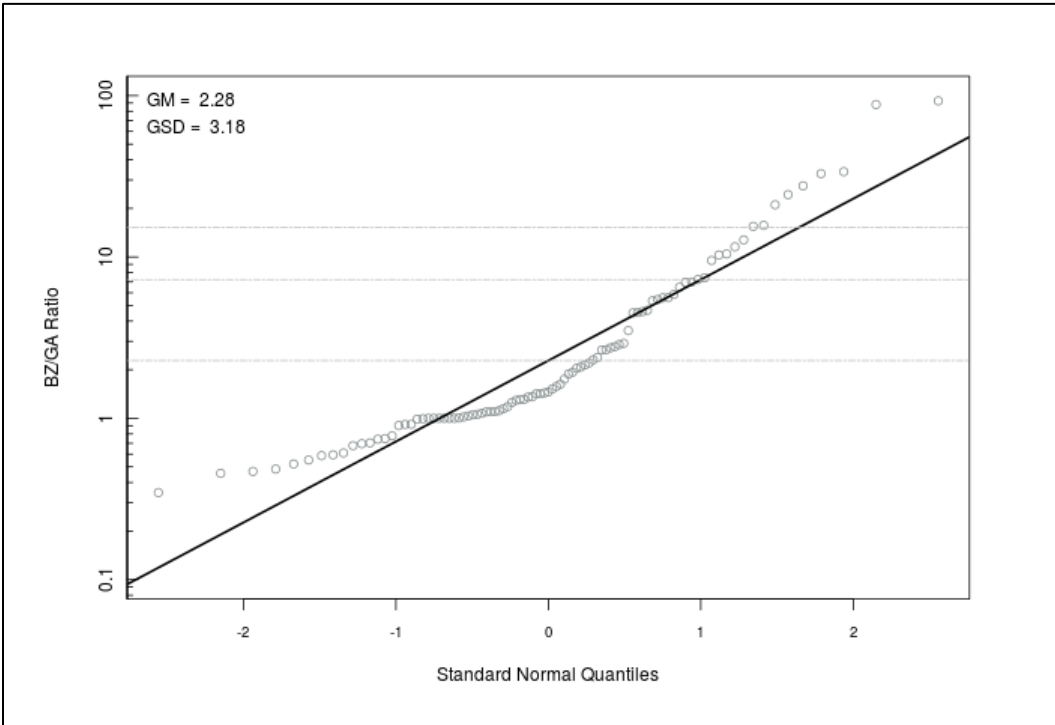
Figure 8-2. Model for Scenario 1 (ORAUT 2020).

8.2.1.2   Scenario 2 Results: Variable Worker Location Relative to the Release Point

For the Scenario 2 evaluation, the 16 lognormal models that were created for each BZ location designation were combined using Monte Carlo simulation to create a single dataset for Scenario 2. A lognormal model fit was then performed on the new dataset using ROS (ORAUT 2020). Figure 8-3 provides the results for the Scenario 2 evaluation.
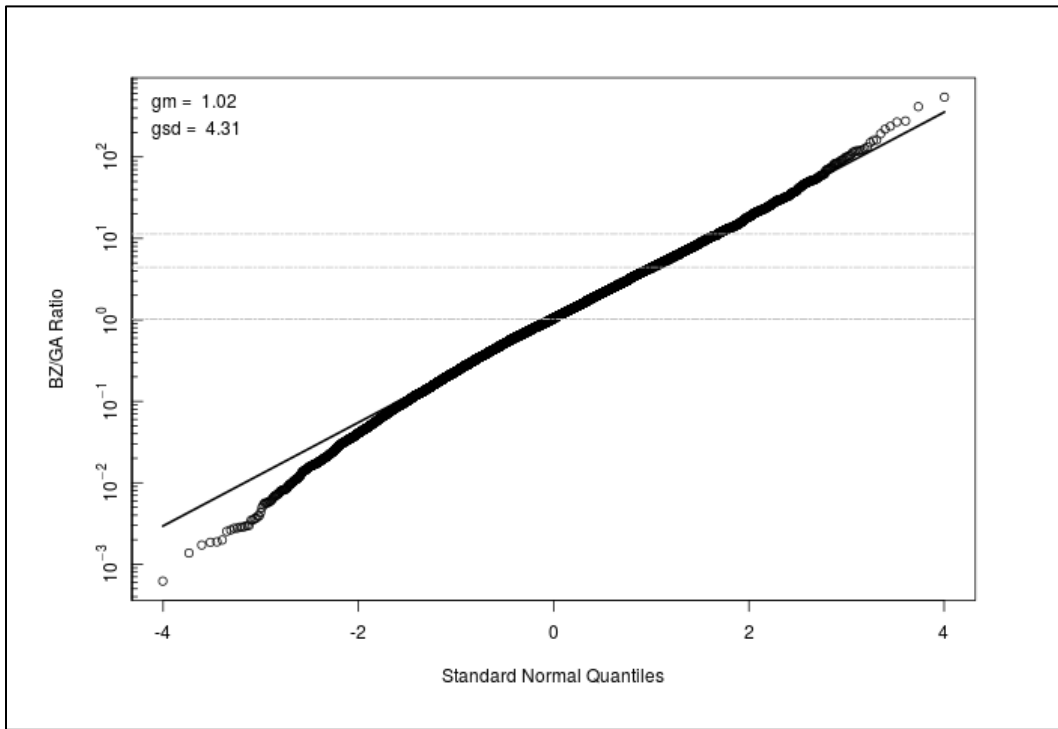
Figure 8-3. Model for Scenario 2 (ORAUT 2020).

8.2.1.3   Summary of Scenario 1 and Scenario 2 Results

Table 8-2 summarizes the results from Sections 8.2.1.1 and 8.2.1.2 for Scenarios 1 and 2.

Table 8-2. Summary of the BZ:GA ratio distributions for Whicker and Moxley (2001).

Scenario	BZ:GA ratio GM	BZ:GA ratio GSD
Scenario 1	2.28	3.18
Scenario 2	1.02	4.31

9.0   DISCUSSION

As indicated in Section 1.0, the purpose and scope of this report is to evaluate the differences between the GA and BZ air concentrations for small workrooms and to determine if any adjustment to the GA air concentrations is necessary to make them equivalent to the BZ air concentrations in a small workroom. Based on the evaluations for this report, adjustments to GA air concentrations are warranted, and those adjustments can be made by applying the appropriate BZ:GA ratio distribution below. The appropriate BZ:GA ratio distribution is dependent on the worker's exposure scenario and the type of workroom.

9.1   COMBINED RATIO DISTRIBUTIONS

The datasets from each study were combined using Monte Carlo simulations to create a single dataset for each BZ location scenario (i.e., Scenarios 1 and 2) and for each evaluated ventilation scheme. With the exception of Gonzales et al. (1974), the studies evaluated only had one ventilation scheme. As explained in Section 4.3.3, three ventilation schemes were evaluated in Gonzales et al. for the same test room, and it was decided to weight that data more heavily by generating separate BZ:GA ratio models for each ventilation scheme. For each scenario, a lognormal model was fit to each dataset using ROS, generating a GM and GSD for each model. In the quantile-quantile plots

below, the quantiles are from the fitted lognormal distribution, and the horizontal lines are the 50th, 84th, and 95th percentiles for the plotted data (ORAUT 2020).

9.1.1 Evaluations for Scenario 1

As defined in Section 3.0, Scenario 1 assumes the worker (BZ location) was always located at the same X,Y coordinates in the room as the release point. Table 9-1 summarizes the BZ:GA ratio distributions for each of the evaluated datasets for Scenario 1.

Table 9-1. Summary of BZ:GA ratio distributions for Scenario 1.

Study	BZ:GA ratio GM	BZ:GA ratio GSD
Gonzales et al. (1974) – 0° ventilation direction	1.35	3.37
Gonzales et al. (1974) – 90° ventilation direction	1.59	4.13
Gonzales et al. (1974) – 180° ventilation direction	0.852	2.00
Charuau (1987)	4.92	2.50
Scripsick et al. (1979a, 1979b)	30.5	3.31
Whicker and Moxley (2001)	2.28	3.18

The BZ:GA ratio distributions for Scenario 1 in Table 9-1 were combined to generate a single distribution that is representative of all of the evaluated studies for Scenario 1. This resulted in a combined BZ:GA ratio distribution with a GM of 2.95 and a GSD of 5.03 for Scenario 1 (Figure 9-1) (ORAUT 2020).
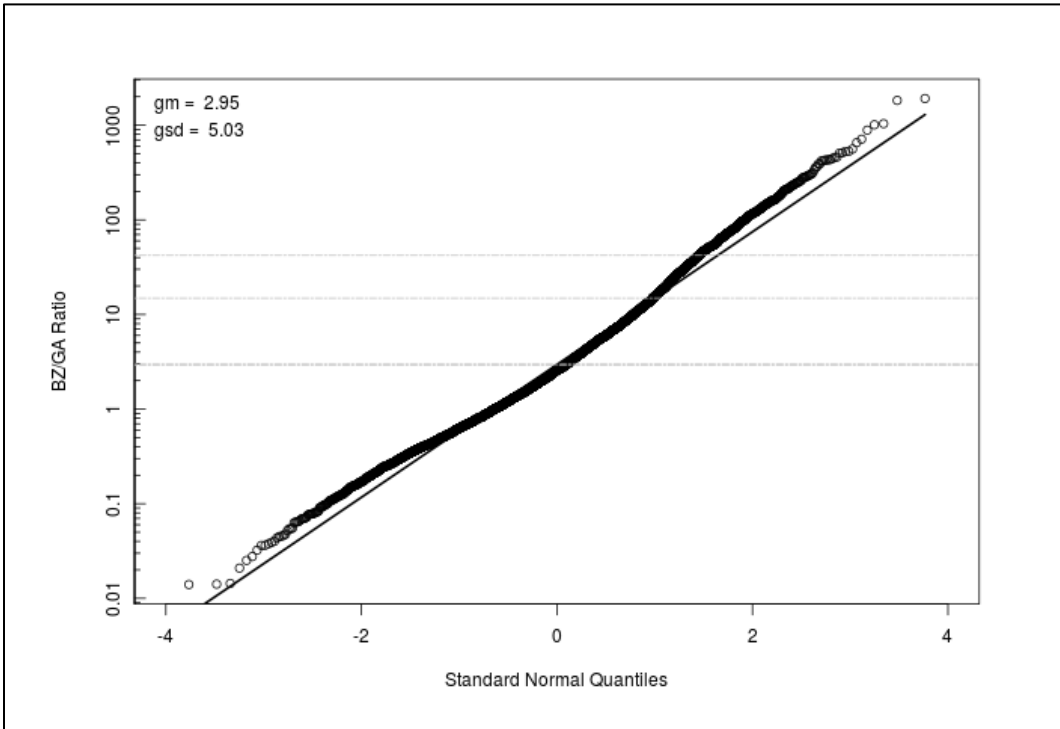
Figure 9-1. Combined model for all Scenario 1 models (ORAUT 2020).

The generated data for Scenario 1 also indicate there is a significant difference between the BZ:GA ratios when the workroom is generally open in the middle of the room rather than when the workroom has significant obstructions in the middle of the room. Because the data indicate the BZ:GA ratios can be significantly higher when the workroom has significant obstructions in the middle of the room, it might be more appropriate to use a BZ:GA ratio based only on the data from workrooms with obstructions in the middle of the room. Therefore, the BZ:GA ratio distributions in Table 9-1 were

divided into two groups and reevaluated. The grouping in Table 9-2 represents the scenario when the workroom is generally open in the middle of the room. The grouping in Table 9-3 represents the scenario when the workroom has significant obstructions in the middle of the room.

Table 9-2. Summary of BZ:GA ratio distributions when workroom is open in the middle.

Study	BZ:GA ratio GM	BZ:GA ratio GSD
Gonzales et al. (1974) – 0° ventilation direction	1.35	3.37
Gonzales et al. (1974) – 90° ventilation direction	1.59	4.13
Gonzales et al. (1974) – 180° ventilation direction	0.852	2.00
Whicker and Moxley (2001)	2.28	3.18

Table 9-3. Summary of BZ:GA ratio distributions when workroom has obstructions in the middle.

Study	BZ:GA ratio GM	BZ:GA ratio GSD
Charuau (1987)	4.92	2.50
Scripsick et al. (1979a, 1979b)	30.5	3.31

The same statistical process used to evaluate the Table 9-1 distributions was used to evaluate the Table 9-2 distributions for Scenario 1. Based on this process, the combined BZ:GA ratio has a GM of 1.39 and a GSD of 3.27 for Scenario 1 when the workroom is open in the middle of the room (Figure 9-2) (ORAUT 2020).
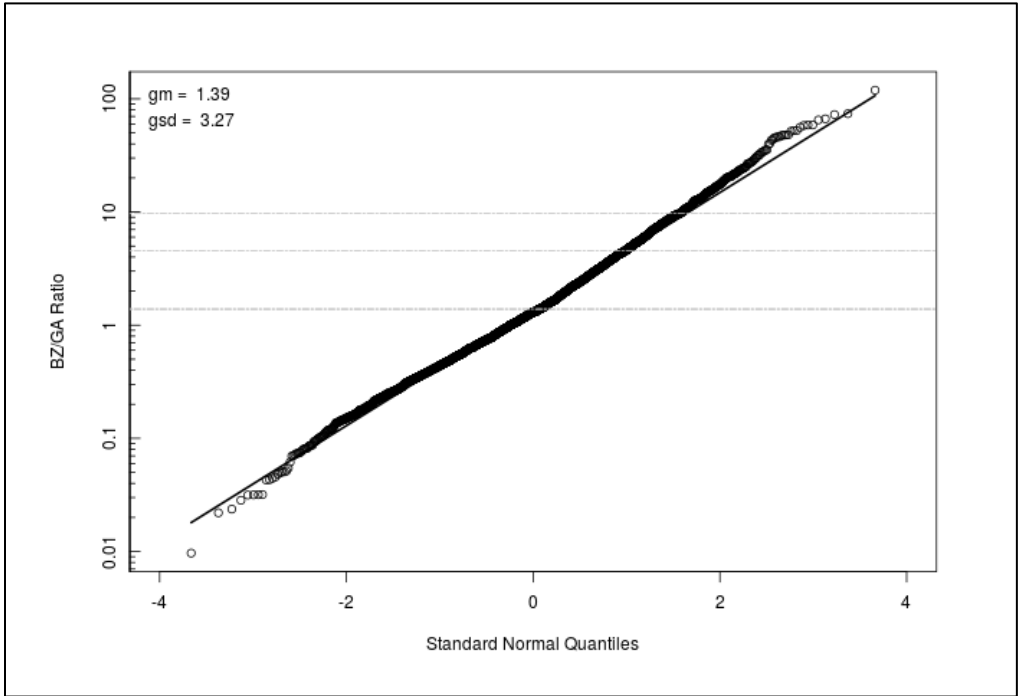
Figure 9-2. Combined model for Scenario 1 models that were for open workspaces (ORAUT 2020).

The same statistical process used to evaluate the Table 9-1 distributions was used to evaluate the Table 9-3 distributions for Scenario 1. Based on this process, the combined BZ:GA ratio has a GM of 12.0 and a GSD of 4.11 for Scenario 1 when the workroom has significant obstructions in the middle of the room (Figure 9-3) (ORAUT 2020).
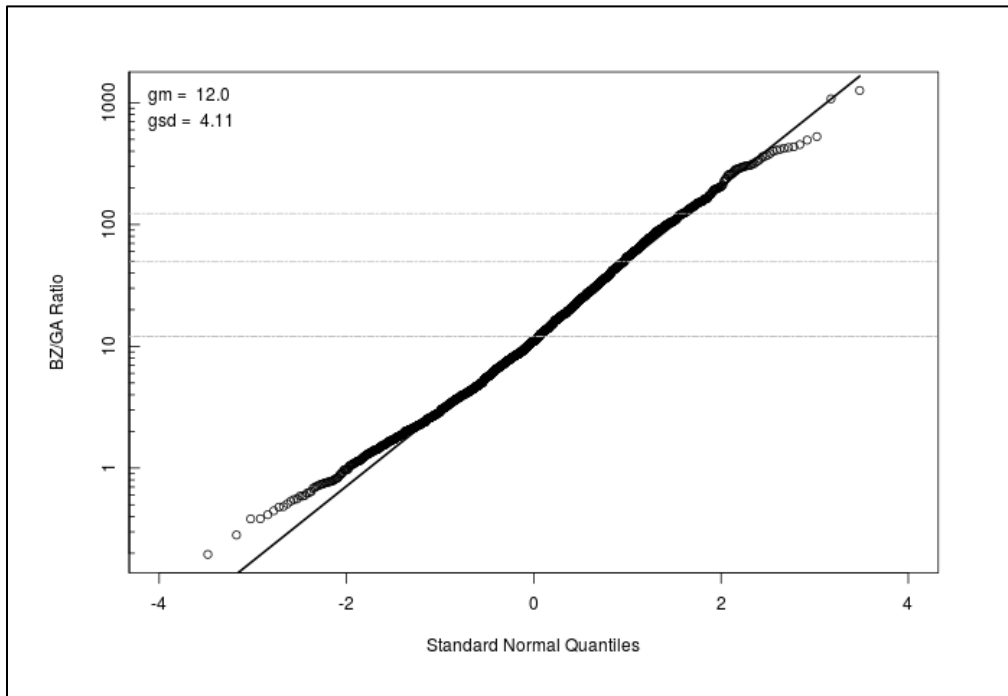
Figure 9-3. Combined model for all Scenario 1 models that were for obstructed work spaces (ORAUT 2020).

9.1.2   Evaluations for Scenario 2

As defined in Section 3.0, Scenario 2 assumes the worker (BZ location) was not necessarily at the same X, Y coordinates in the workroom as the release point. Table 9-4 summarizes the BZ:GA ratio distributions for each of the evaluated datasets for Scenario 2.

Table 9-4. Summary of BZ:GA ratio distributions for Scenario 2.

Study	BZ:GA ratio GM	BZ:GA ratio GSD
Gonzales et al. (1974) – 0° ventilation direction	1.06	3.86
Gonzales et al. (1974) – 90° ventilation direction	1.04	6.80
Gonzales et al. (1974) – 180° ventilation direction	1.08	2.28
Charuau (1987)	1.00	2.94
Munyon and Lee (2002)	1.08	5.40
Scripsick et al. (1979a, 1979b)	1.43	3.64
Whicker and Moxley (2001)	1.02	4.31

The BZ:GA ratio distributions for Scenario 2 in Table 9-4 were combined to generate a single distribution that is representative of all of the studies evaluated for Scenario 2. This resulted in a combined BZ:GA ratio distribution having GM of 1.08 and a GSD of 4.02 for Scenario 2 (Figure 9-4) (ORAUT 2020).
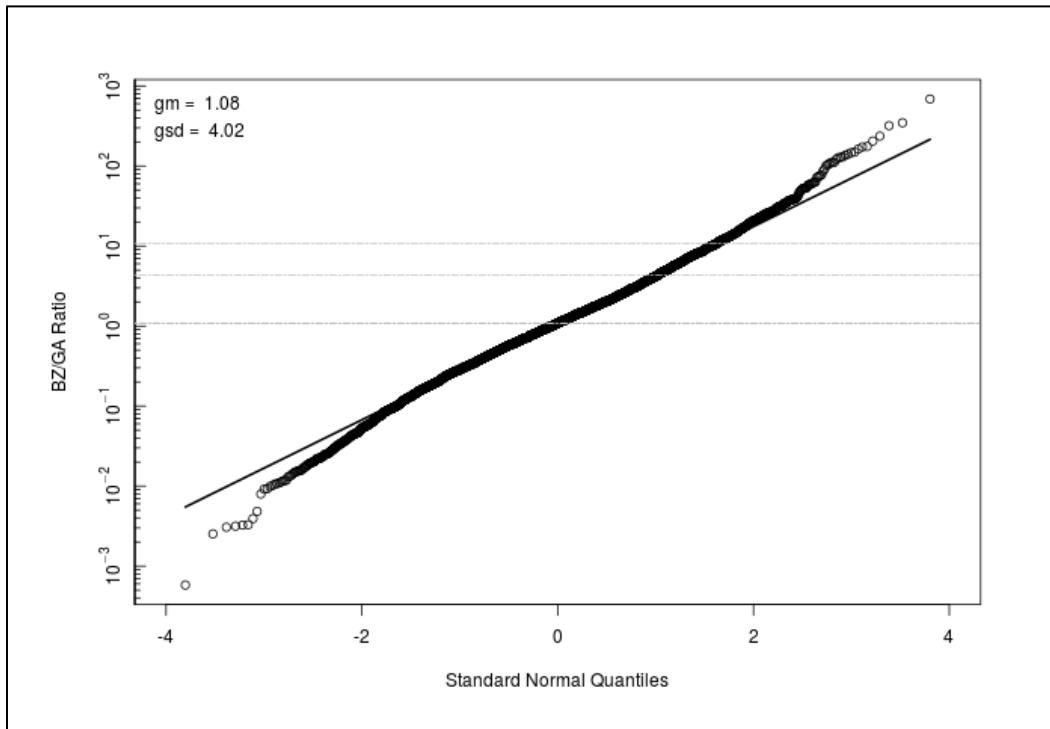
Figure 9-4. Combined model for all Scenario 2 models (ORAUT 2020).

The generated data for Scenario 2 did not indicate a significant difference between the BZ:GA ratios when the workroom is generally open in the middle of the room versus when the room has a lot of obstructions in the middle of the room. Therefore, no special consideration is warranted for Scenario 2 when there are obstructions in the middle of the room.

9.2   OTHER OBSERVATIONS

As indicated in Section 2.0, the ventilation rate and room complexity were two of the six parameters that were thought to affect the level of mixing the most. However, comparisons of the individual BZ:GA ratio distributions and the combined BZ:GA ratio distributions indicate that ventilation rate and room complexity had less of an effect on the level of mixing than expected. An indicator of the level of mixing in a room is the BZ:GA ratio distribution. Mixing is likely more complete, as the GM and GSD for that distribution both approach unity.

9.2.1   Ventilation Rate

As indicated in Section 2.1.3, the ventilation rate is usually only evaluated in terms of air change rate, specifically AC/hr. In the studies evaluated for this report, there were six different air change rates (i.e. 6, 9, 10, 12, 15, and 90 AC/hr). To determine if the air change rates affected the BZ:GA ratio distributions for a specific scenario (i.e., Scenario 1 and Scenario 2), each of the BZ:GA ratio distributions from the evaluated studies were graphed in a scatter plot for each scenario. Because the 9- and 10-AC/hr air change rates are nearly equal and because there were not many data points for them, they were combined into a single air change rate to simplify the scatter plots. As discussed in Section 4.3, in addition to Scenarios 1 and 2, the Gonzales et al. (1974) study data were evaluated for the two additional scenarios (Scenarios A and B). Scatter plots of the results of those scenario evaluations are depicted in Figures 4-5 through 4-7. Those scatter plots indicate that the differences between the Scenario A and Scenario B results are typically limited to a slightly higher GM for Scenario B. Because of that and because Scenario A is an unrestricted scenario (i.e., the GA

sampler could be anywhere in the test room), only the Scenario A data were used in the scatter plots to compare the air changes rates.

The uncombined BZ:GA ratio distributions for Scenario 1 were obtained from ORAUT (2020) and are presented in Table 9-5. Figure 9-5, is a scatter plot of the uncombined BZ:GA ratio distributions for Scenario 1.

Table 9-5. Summary of uncombined BZ:GA ratio distributions for Scenario 1.[a]

Study[b]	Air change rate (AC/hr)	BZ:GA ratio GM	BZ:GA ratio GSD
Gonzales et al. (1974) – 0° v.d., 1-ft elevation	6	0.869	2.88
Gonzales et al. (1974) – 90° v.d., 1-ft elevation	6	1.52	3.49
Gonzales et al. (1974) – 180° v.d., 1-ft elevation	6	0.952	1.57
Gonzales et al. (1974) – 0° v.d., 2-ft elevation	6	0.687	2.24
Gonzales et al. (1974) – 0° v.d., 2-ft elevation	9	1.27	2.77
Charuau (1987) – 2.3 µm aerosol	10	3.02	1.88
Charuau (1987) – 10.5 µm aerosol	10	7.79	2.54
Gonzales et al. (1974) – 0° v.d., 1-ft elevation	12	3.05	3.33
Gonzales et al. (1974) – 90° v.d., 1-ft elevation	12	1.38	4.51
Gonzales et al. (1974) – 180° v.d., 1-ft elevation	12	0.674	2.44
Gonzales et al. (1974) – 90° v.d., 2-ft elevation	12	1.44	4.21
Scripsick et al. (1979a, 1979b)	12	30.5	3.31
Whicker and Moxley (2001)	15	2.28	3.18

a.   Values in this table were obtained from ORAUT (2020) and rounded to 3 significant figures.
b.   v.d. = ventilation direction.
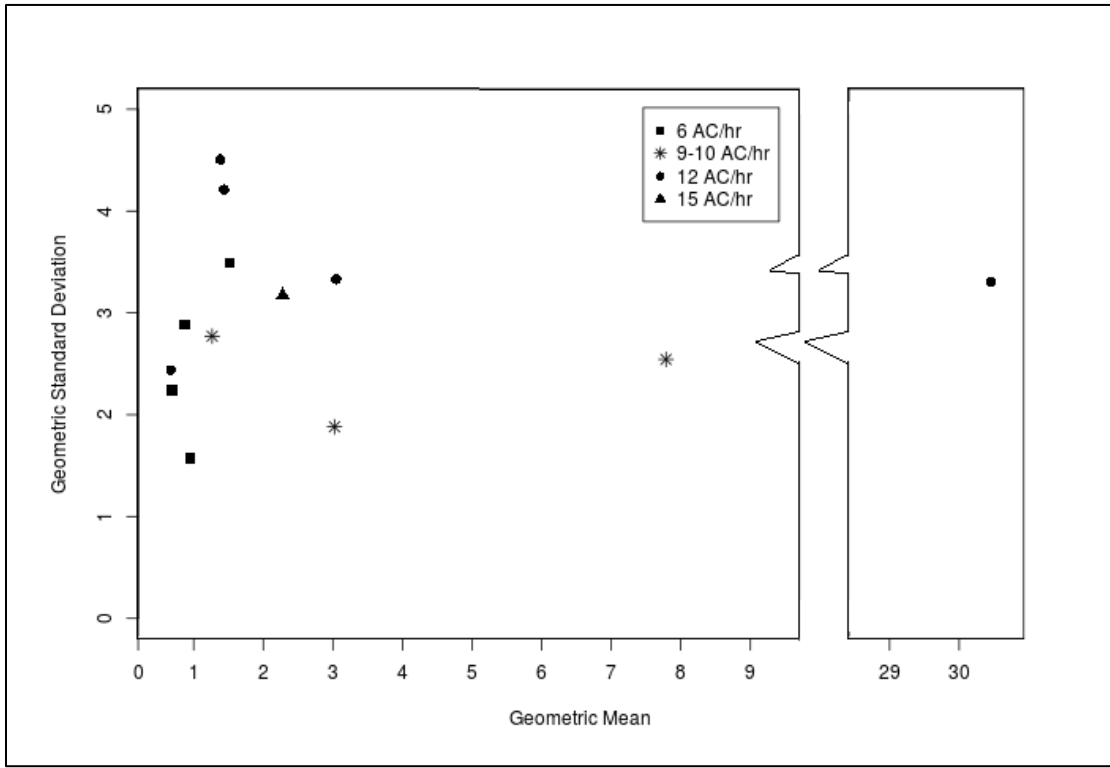
Figure 9-5. Scatter plot of uncombined BZ:GA ratio distributions for Scenario 1 (ORAUT 2020).

The uncombined BZ:GA ratio distributions for Scenario 2 were obtained from ORAUT (2020) and are presented in Table 9-6. Figure 9-6 is a scatter plot of the uncombined BZ:GA ratio distributions for Scenario 2.

Table 9-6. Summary of uncombined BZ:GA ratio distributions for Scenario 2.[a]

Study[b]	Air change rate (AC/hr)	BZ:GA ratio GM	BZ:GA ratio GSD
Gonzales et al. (1974) – 0° v.d., 1-ft elevation	6	1.03	4.10
Gonzales et al. (1974) – 90° v.d., 1-ft elevation	6	1.01	5.26
Gonzales et al. (1974) – 180° v.d., 1-ft elevation	6	0.984	1.88
Gonzales et al. (1974) – 0° v.d., 2-ft elevation	6	0.997	2.74
Gonzales et al. (1974) – 0° v.d., 2-ft elevation	9	1.00	3.78
Charuau (1987) – 2.3 µm aerosol	10	1.02	2.32
Charuau (1987) – 10.5 µm aerosol	10	1.01	3.67
Gonzales et al. (1974) – 0° v.d., 1-ft elevation	12	1.00	4.78
Gonzales et al. (1974) – 90° v.d., 1-ft elevation	12	1.01	7.88
Gonzales et al. (1974) – 180° v.d., 1-ft elevation	12	1.02	2.98
Gonzales et al. (1974) – 90° v.d., 2-ft elevation	12	0.995	7.29
Scripsick et al. (1979a, 1979b)	12	1.43	3.64
Whicker and Moxley (2001)	15	1.02	4.31
Munyon and Lee (2002)	90	1.08	5.40

a. Values in this table were obtained from ORAUT (2020) and rounded to 3 significant figures.
b. v.d. = ventilation direction.
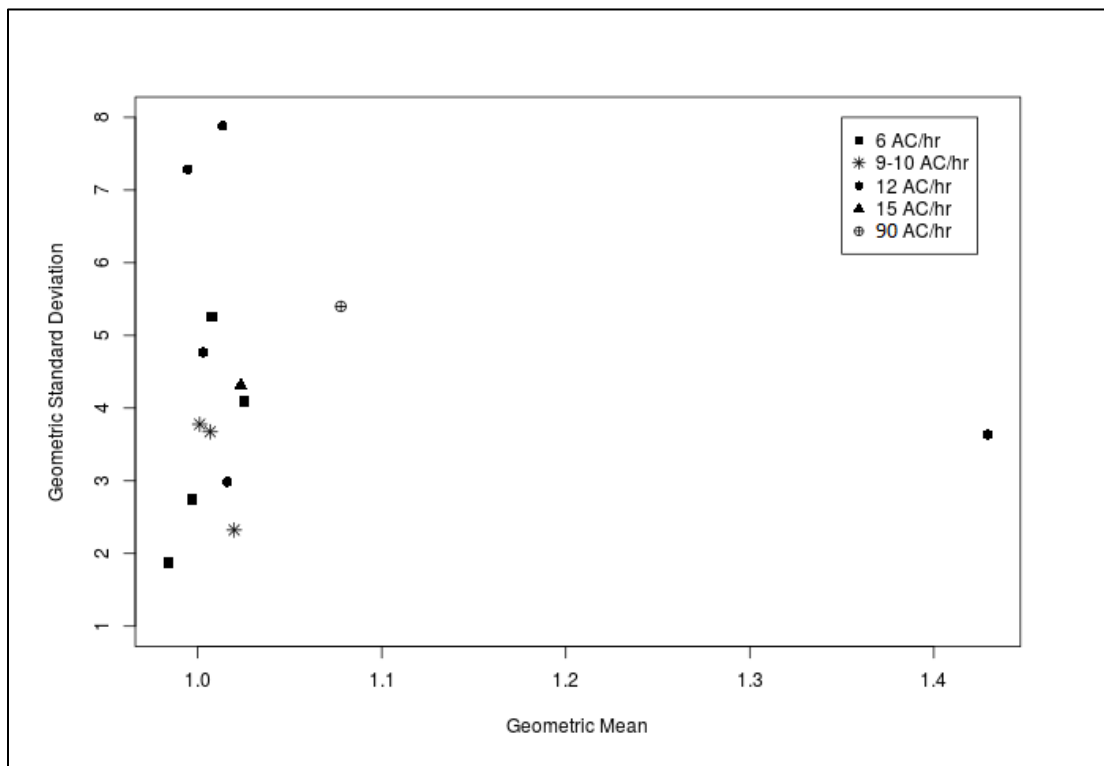
Figure 9-6. Scatter plot of uncombined BZ:GA ratio distributions for Scenario 2 (ORAUT 2020).

Based on the scatter plots in Figures 9-5 and 9-6, the different air change rates appear to have less of an effect on the BZ:GA ratio distribution than expected. In these plots, the different air change rates do not appear to have any noticeable effect on the BZ:GA ratio distributions.

9.2.2 Room Complexity

Because the level of complexity of a room cannot be readily quantified, a qualitative review of the BZ:GA ratios and their respective room complexities was performed. In regards to room complexity, the room in Charuau (1987) had the most complex room configuration and likely the most complex ventilation flow patterns of the evaluated studies. The room in Scripsick et al. (1979a, 1979b) had the next most complex room. As anticipated, the two most complex rooms in the evaluated studies generated significantly higher GM values for their BZ:GA ratio distributions for Scenario 1. However, for Scenario 2, the GM values for their BZ:GA ratio distributions were much closer to unity. Therefore, room complexity does not appear to have a significant effect on exposure scenarios similar to Scenario 2.

10.0 CONCLUSIONS

As indicated in Section 2.0, when the median of the BZ:GA ratio distribution becomes significantly greater than 1 or the GSD becomes large, the GA air concentration should be adjusted to account for the increased uncertainty in the BZ air concentration. Based on that and the combined BZ:GA ratio distributions presented above, the GA air concentrations in most small workrooms should be adjusted to make them equivalent to BZ air concentrations. Table 10-1 summarizes the results from Sections 9.1.1 and 9.1.2 for Scenarios 1 and 2. For the scenarios in Table 10-1, the appropriate BZ:GA ratio distribution can be applied to the GA air concentrations to make them equivalent to BZ air concentrations.

Table 10-1. Summary of the combined BZ:GA ratio distributions.

Scenario	BZ:GA ratio GM	BZ:GA ratio GSD
Scenario 1	2.95	5.03
Scenario 1 – open in the middle	1.39	3.27
Scenario 1 – obstructions in the middle	12.0	4.11
Scenario 2	1.08	4.02

For acute exposure scenarios, the decision to use the results from Scenario 1 or Scenario 2 will be dependent on whether or not the worker was present at the release locations. Because it is unlikely that a worker would be located at the release location for every release event, the results from Scenario 1 would normally just be applicable to acute exposure scenarios, such as when the worker was at the release location during a radiological accident or excursion. Therefore, the results from Scenario 2 would usually be the more appropriate BZ:GA ratio distribution to use for assessing chronic exposure scenarios. However, in the rare instances when a chronic exposure scenario is more consistent with the description for Scenario 1, the results from Scenario 1 should be used.

For convenience, the Worker Location Scenario definitions from Section 3.0 are represented below:

- Scenario 1. Assumes the worker (BZ location) was always located at the same X,Y coordinates in the room as the release point (i.e., colocated worker and release point).

- Scenario 2. Assumes the worker (BZ location) was not necessarily located at the same X,Y coordinates in the room as the release point (i.e., variable worker location relative to the release point).

11.0 ANTICIPATED USE OF THE BZ:GA RATIO DATA

The use of the BZ:GA ratio information in this report is primarily intended for radiological workrooms with relatively long-lived radionuclides. Because short-lived radionuclides (i.e., having half-lives of

only a few hours or less) can affect the BZ:GA ratios in a workroom, the BZ:GA ratio information in this report is not intended to be used with short-lived radionuclides. As indicated in Sections 1.0 and 2.0, all uses of the BZ:GA ratio information in this report will need to be justified on a case-by-case basis. Because all potential uses of the data in this report cannot be foreseen, it will be the responsibility of the users of this report's BZ:GA ratio information to justify the use of it and the appropriateness of how they choose to apply it. As indicated in Section 2.0, there are five potential key parameters that should be considered when justifying the application of the generic BZ:GA ratio distributions in Table 10-1 to site-specific GA air sample results. Those parameters include: (1) room size, (2) particle size distribution for the airborne radioactivity, (3) ventilation rate for the room, (4) room complexity, and (5) the presence of dominant particles.

1. As indicated in Section 1.0, the BZ:GA ratio information in this report is intended to be applicable to small workrooms. However, "small workroom" is an undefined and potentially highly variable term.

    The room sizes in the evaluated studies ranged from 17.6 to 105.0 m^2 (190 to 1,130 ft^2). The room sizes that the BZ:GA ratio information is being used for should be reasonably comparable to those room sizes, and should not be used for rooms that are significantly larger than 105.0 m^2 (1,130 ft^2). As the workroom size increases beyond 105.0 m^2 (1,130 ft^2), it will become progressively more difficult to justify using the BZ:GA ratio information in this report for that workroom.

    In addition, because the studies evaluated for this report did not include any elevated releases, the BZ:GA information in this report might not be applicable to scenarios with elevated releases. As indicated in Section 2.0, elevated releases are considered to be above the BZ elevation and can include releases originating at a lower elevation that are propelled above the BZ elevation (e.g., jet releases, over pressurization releases, aerosol plumes lofted by heat sources, etc.) for the purposes of this report.

2. In the rare event that the particle size distribution is known for the air being sampled by the GA air samplers, one should consider adjusting the workroom's GA air sample results to exclude the nonrespirable fraction before applying a BZ:GA ratio.

3. The BZ:GA ratios in this report are based on the data from rooms with a wide range of ventilation rates, which were expressed in terms of room air change rates in the evaluated studies. Those air change rates included 6, 9, 10, 12, 15, and 90 AC/hr. Based on the results generated from the evaluated studies, the air change rate appears to have less of an effect on the BZ:GA ratio distribution than one would expect. Therefore, the BZ:GA ratio information in this report is considered applicable to rooms with all but the most extreme air change rates.

4. The complexity of the rooms and ventilation flow patterns appear to have the largest effect on BZ:GA ratio distribution, but that is mostly limited to Scenario 1 when there are obstructions in the middle of the room. In terms of complexity, the room in Charuau (1987) has the most complex room configuration and likely the most complex ventilation flow patterns of the evaluated studies. For exposure scenarios similar to Scenario 2, the complexity of the rooms and ventilation flow patterns do not appear to have much of an effect on BZ:GA ratio distribution. When evaluating Scenario 2 types of exposures, the BZ:GA ratio data in this report is likely applicable to all small workrooms.

5. As indicated in Section 2.2.2, air sample data from workrooms with dominant particles are very unreliable. Therefore, using that data to assess worker exposures should be avoided when possible. However, when that is not avoidable, intake distributions should be calculated

instead of point estimates to account for the stochastic nature associated with sampling and inhaling those particles (Scott and Fencl 1999).

After justifying the use of this BZ:GA ratio information for a workroom, the next step would be to select the most appropriate BZ:GA ratio distribution from Table 10-1 in Section 10.0, which will depend on whether the exposure scenario is best represented by Scenario 1 or Scenario 2. Section 10.0 also provides some guidance that might help with choosing between Scenarios 1 and 2. If best represented by Scenario 1, the user will then need to decide and justify which of the three Scenario 1 ratio options is most appropriate for the workroom for which the BZ:GA ratio distribution is being used.

The following describes one of the anticipated ways to use the BZ:GA ratio information in this report. The initial anticipated use of the BZ:GA ratio information provided in Section 10.0 is to multiply the appropriate BZ:GA ratio distribution from Table 10-1 to the GA air sample results for a workroom to make the measured air concentrations equivalent to BZ air concentrations in that workroom.

To illustrate the application of BZ:GA ratio information in this document, this section uses Scenario 2 as an example on how to use the various BZ:GA ratio distributions to convert GA air concentrations into BZ air concentrations. In Section 10.0, the Scenario 2 models for all five studies are combined into a single BZ:GA ratio distribution for the Scenario 2 model, which has a $GM_{BZ:GA}$ = 1.08 and $GSD_{BZ:GA}$ = 4.02. Three examples are described below, which represent the three types of GA air concentrations that might be encountered.

Example 1

When the GA air concentration has a lognormal distribution with a GM_{GA} and GSD_{GA}, the BZ:GA ratio distribution can be used to make it equivalent to the probability distribution for the BZ air concentration by using the following equations:

$$GM_{BZ} = \exp\left(\ln\left(GM_{GA}\right) + \ln\left(GM_{BZ:GA}\right)\right) \tag{11-1}$$

$$GSD_{BZ} = \exp\left(\sqrt{\ln\left(GSD_{GA}\right)^2 + \ln\left(GSD_{BZ:GA}\right)^2}\right) \tag{11-2}$$

where

GM_{BZ}	=	GM of the BZ air concentration distribution
GSD_{BZ}	=	GSD of the BZ air concentration distribution
$GM_{BZ:GA}$	=	GM of the applicable BZ:GA ratio distribution
$GSD_{BZ:GA}$	=	GSD of the applicable BZ:GA ratio distribution
GM_{GA}	=	GM of the GA air concentration distribution
GSD_{GA}	=	GSD of the GA air concentration distribution

Based on Equation 11-2, the GSD of the BZ air concentration distribution will always be larger than the GSD of the GA air concentration distribution. For example, if GM_{GA} = 10 µCi/cm³ and GSD_{GA} = 4.0, the GM_{BZ} and GSD_{BZ} would equal the following:

$$GM_{BZ} = \exp\left(\ln\left(10\right) + \ln\left(1.08\right)\right) = 11 \text{ µCi/cm}^3 \tag{11-3}$$

$$GSD_{BZ} = \exp\left(\sqrt{\ln\left(4.0\right)^2 + \ln\left(4.02\right)^2}\right) = 7.1 \tag{11-4}$$

Example 2
When the GA air concentration is a constant, the BZ:GA ratio distribution can be used to make it equivalent to the probability distribution for the BZ air concentration by using the following equations:

$$GM_{BZ} = C_{GA} \times GM_{BZ:GA} \qquad (11\text{-}5)$$

$$GSD_{BZ} = GSD_{BZ:GA} \qquad (11\text{-}6)$$

where

$\qquad C_{GA}$ = is the GA air concentration

For example, if the GA air concentration is a constant with a value of 10 µCi/cm^3, the GM_{BZ} and GSD_{BZ} would equal the following:

$$GM_{BZ} = 10 \times 1.08 = 11 \ \mu\text{Ci/cm}^3 \qquad (11\text{-}7)$$

$$GSD_{BZ} = 4.02 \qquad (11\text{-}8)$$

Example 3
When the GA air concentration is not a constant and has a distribution other than a lognormal distribution (e.g., a normal distribution with an arithmetic mean and standard deviation), the BZ:GA ratio distribution can be used to make it equivalent to the probability distribution for the BZ air concentration by multiplying the two distributions together using Monte Carlo techniques.

REFERENCES

Aden, J., and B. R. Scott, 2003, "Modeling Variability and Uncertainty Associated with Inhaled Weapons-Grade PuO$_2$," *Health Physics*, volume 84, number 6, pp. 726–736. [SRDB Ref ID: 179244]

Charuau, J., 1987, "Design and Assessment of a Personal Monitor to Optimize the Occupational Monitoring in Plutonium Laboratories," PNL-SA-14225*, Proceedings of the Department of Energy Workshop on Workplace Aerosol Monitoring, Held in Napa, California, October 28-30, 1985*, Battelle Memorial Institute, Pacific Northwest Laboratory, Richland, Washington, February. [SRDB Ref ID: 172408, p. 172]

Gonzales, M., H. J. Ettinger, R. G. Stafford, and C. E. Breckinridge, 1974, *Relationship Between Air Sampling Data from Glove Box Work Areas and Inhalation Risk to the Worker*, LA-5520-MS, University of California, Los Alamos Scientific Laboratory, Los Alamos, New Mexico, March. [SRDB Ref ID: 172405]

Hinds, W. C, 1982, "Aerosol Technology: Properties, Behavior, and Measurement of Airborne Particles," Wiley, New York. [SRDB Ref ID: 177004]

ICRP (International Commission on Radiological Protection), 2015, *Occupational Intakes of Radionuclides: Part 1*, Publication 130, Sage Publishing, London, England. [SRDB Ref ID: 168251]

Jones, E. W., R. G. Hopkins, D. L. E. Smith, and D. M. Wallace, 1983, "Experience in the Use of Lapel Air Samplers at A.W.R.E," *Journal of the Society for Radiological Protection*, volume 3, number 3, pp. 11–17. [SRDB Ref ID: 168445]

Lister, B. A. J., 1967, "Development of Air Sampling Technology by the Atomic Energy Research Establishment, Harwell," pp. 37–54, *Proceedings of a Symposium on Instruments and Techniques for the Assessment of Airborne Radioactivity in Nuclear Operations, International Atomic Energy Agency, Held in Vienna, 3-7 July 1967*, IAEA Report No. SM-95/30, International Atomic Energy Agency, Vienna, Austria. [SRDB Ref ID: 168202]

Munyon, W. J., and M. B. Lee, 2002, "Summary of Stationary and Personal Air Sampling Measurements Made During a Plutonium Glovebox Decommissioning Project," *Health Physics*, volume 82, number 2, pp. 244–253. [SRDB Ref ID: 91597]

ORAUT (Oak Ridge Associated Universities Team), 2019a, "Determining Certain Dimensions in Fig. 1 in Gonzales et al. (1974)," Oak Ridge, Tennessee, December 6. [SRDB Ref ID: 178684]

ORAUT (Oak Ridge Associated Universities Team), 2019b, "Modified Figure 4 in Gonzales Supporting ORAUT-RPRT-0097," Rev. 0, Oak Ridge, Tennessee, May 6. [SRDB Ref ID: 176654]

ORAUT (Oak Ridge Associated Universities Team), 2019c, "Probabilities and Graphical Areas for Selected Figures from LA-5520-MS," Rev. 0, Oak Ridge, Tennessee, April 25. [SRDB Ref ID: 176121]

ORAUT (Oak Ridge Associated Universities Team), 2019d, "Modified Figure 12 in Gonzales Supporting ORAUT-RPRT-0097," Rev. 0, Oak Ridge, Tennessee, May 6. [SRDB Ref ID: 176333]

ORAUT (Oak Ridge Associated Universities Team), 2020, "Supporting Documentation for the Statistical Evaluations in ORAUT-RPRT-0097 Rev 00," Rev. 0, Oak Ridge, Tennessee, July 20. [SRDB Ref ID: 176881]

Scripsick, R. C., R. G. Stafford, R. J. Beckman, M. I. Tillery, and P. O. Romero, 1979a, "Evaluation of a Radioactive Aerosol Surveillance System," IAEA-SM-229/62, Proceedings of an International Symposium on Advances in Radiation Protection Monitoring, Held in Stockholm, Sweden, June 26-30, 1978, International Atomic Energy Agency, Vienna, Austria, August. [SRDB Ref ID: 175373, p. 318]

Scripsick, R. C., M. I. Tillery, R. G. Stafford, and P. O. Romero, 1979b, Aerosol Sampling and Characterization for Hazard Evaluation, LA-8153-PR, University of California, Los Alamos Scientific Laboratory, Los Alamos, New Mexico, November. [SRDB Ref ID: 175374]

Scott, B. R., M. D. Hoover, and G. J. Newton, 1997, "On Evaluating Respiratory Tract Intake of High Specific Activity Alpha Emitting Particles for Brief Occupational Exposure," *Radiation Protection Dosimetry*, volume 69, number 1, pp. 43–50. [SRDB Ref ID: 184520]

Scott, B. R., and A. F. Fencl, 1999, "Variability in PuO_2 Intake by Inhalation: Implications for Worker Protection at the U.S. Department of Energy," *Radiation Protection Journal*, volume 83, number 3, pp. 221–232. [SRDB Ref ID: 179236]

Scott, B. R., Y. S. Cheng, M. D. Hoover, H. Schöllnberger, Y. Zhou, G. J. Newton, R. E. Neft, M. Ménache, J. H. Diel, N. D. Okladnikova, Z. B. Tokarskaya, S. V. Osovets, V. L. Peterson, and S. S. Yaniv, 2001, *Interim Report – Improved Radiation Dosimetry/Risk Estimates to Facilitate Environmental Management of Plutonium Contaminated Sites*, Lovelace Respiratory Research Institute, Albuquerque, New Mexico, September. [SRDB Ref ID: 33817]

Sherwood, R. J., 1966, "On the Interpretation of Air Sampling for Radioactive Particles," *American Industrial Hygiene Association Journal*, March-April, pp. 98–109. [SRDB Ref ID: 28046]

Skrable, K. W., 1974, "Systems Described by Linear First Order Kinetics," *Health Physics*, volume 27, pp. 155–157. [SRDB Ref ID: 165844]

Strong, R., 1988, "A Review of Experience with Plutonium Exposure Assessment Methodologies at the Nuclear Fuel Reprocessing Site of British Nuclear Fuels PLC," pp. 106–116, ORNL/TM-10971, *Proceedings of the Second Conference on Radiation Protection Dosimetry, Held in Orlando, Florida, October 31-November 3, 1988*, Oak Ridge National Laboratory, Oak Ridge, Tennessee. [SRDB Ref ID: 172406, p. 121]

Whicker, J. J., and J. Moxley, 2001, Quantitative Air Migration Study at the Savannah River Site C-Lab, LA-UR-01-4933, University of California, Los Alamos Scientific Laboratory, Los Alamos, New Mexico. [SRDB Ref ID: 175376]

Whicker, J. J., J. C. Rodgers, and J. S. Moxley, 2003, "A Quantitative Method for Optimized Placement of Continuous Air Monitors," Health Physics, volume 85, number 5, pp. 599–609. [SRDB Ref ID: 175375]

ATTACHMENT A
GRAPHS FROM GONZALES ET AL.

LIST OF FIGURES

ATTACHMENT A
GRAPHS FROM GONZALES ET AL. (continued)

As indicated in Section 4.2, of the 44 graphs depicting iso-concentration curves for Gonzales et al. (1974), only the 18 most representative graphs were presented in that study. For the purposes of this ORAU Team report, those 18 graphs (Figures 5 through 19 of Gonzales et al.) have been reorganized and provided below as Figures A-1 through A-8. The concentrations in the graphs are presented as a percentage of the measured air concentrations at the aerosol release point.

In relation to these figures, it should be noted that they do not depict the entire area of the test room in Figure 4-1 above. The dimensions of the test room were 20- by 20-ft (6.10- by 6.10-m), but Figures 5 through 19 only depict a 16- by 14-ft (4.88- by 4.27-m) area in that room. In addition, Figures 5 through 19 only provide iso-concentration data for a 10- by 14-ft (3.05- by 4.27-m) area (the monitored area).

ATTACHMENT A
GRAPHS FROM GONZALES ET AL. (continued)
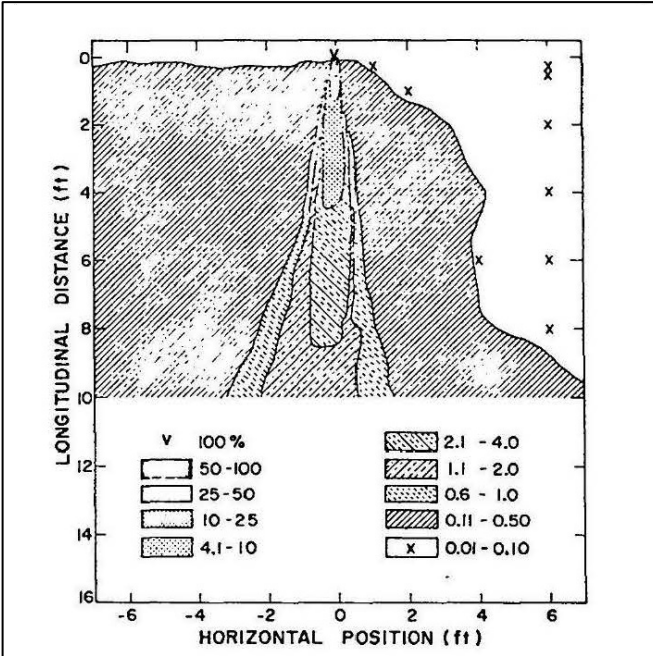
Fig. 4. Iso-concentration curves within horizontal plane at leak level, 6 room air changes per hour, 0° angle air direction.
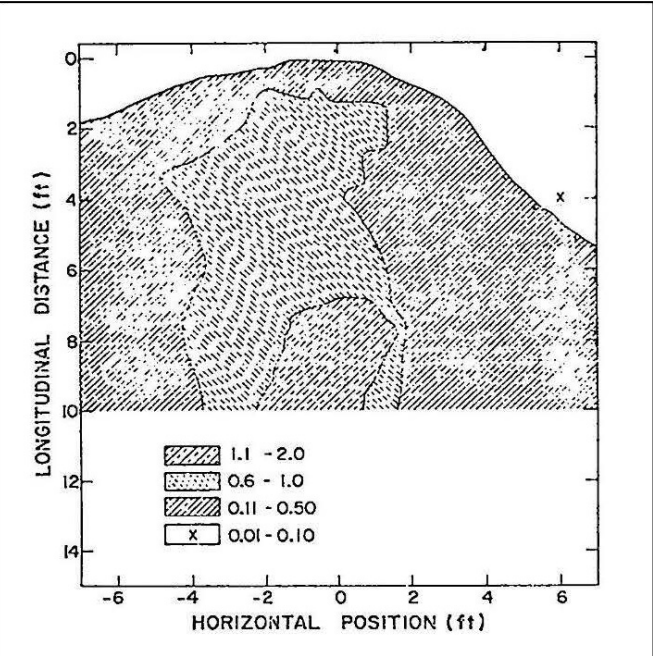
Fig. 6. Iso-concentration curves within horizontal plane 1 ft above leak level, 6 room air changes per hour, 0° angle air direction.
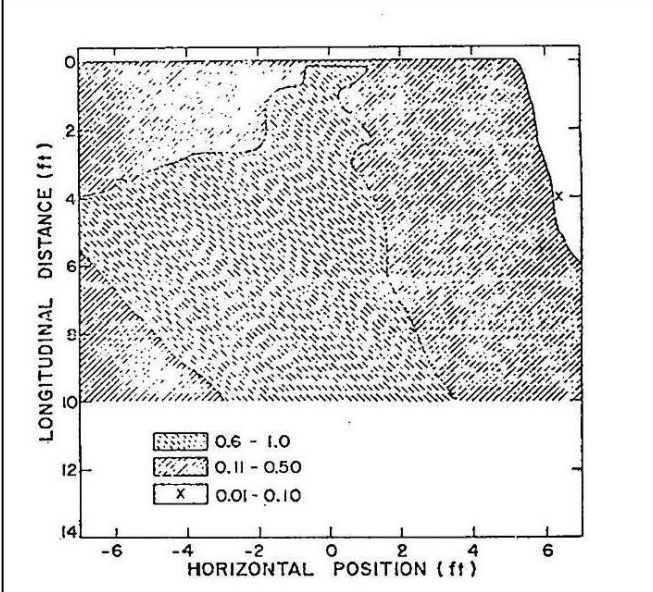
Fig. 7. Iso-concentration curves within horizontal plane 2 ft above leak level, 6 room air changes per hour, 0° angle air direction.

Intentionally Blank

Figure A-1. Graphs of iso-concentration curves for a 0° angle air direction and 6 AC/hr (Gonzales et al. 1974, p. 9-10).

ATTACHMENT A
GRAPHS FROM GONZALES ET AL. (continued)
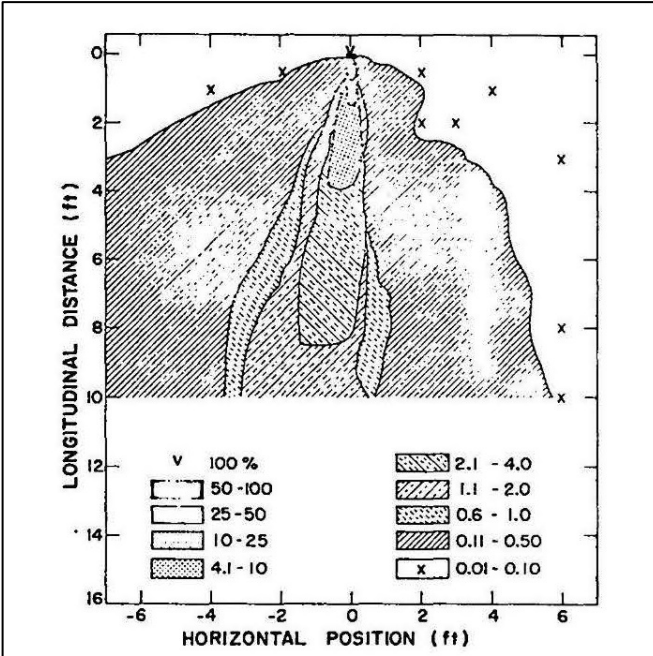
Fig. 3. Iso-concentration curves within horizontal plane at leak level, 9 room air changes per hour, 0° angle air direction.

Graph for
1 ft above leak level
Not Provided in LA-5520-MS
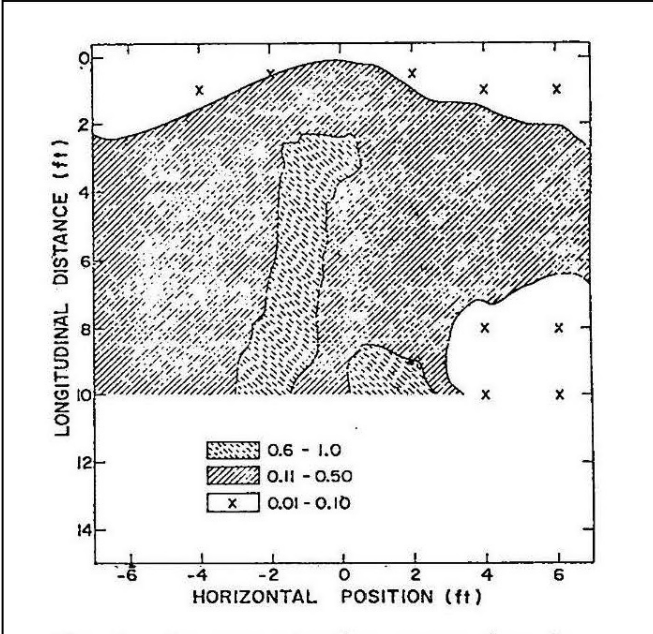
Fig. 8. Iso-concentration curves through horizontal plane 2 ft above leak level, 9 room air changes per hour, 0° angle air direction.

Intentionally
Blank

Figure A-2. Graphs of iso-concentration curves for a 0° angle air direction and 9 AC/hr (Gonzales et al. 1974, p. 9-10).

ATTACHMENT A
GRAPHS FROM GONZALES ET AL. (continued)
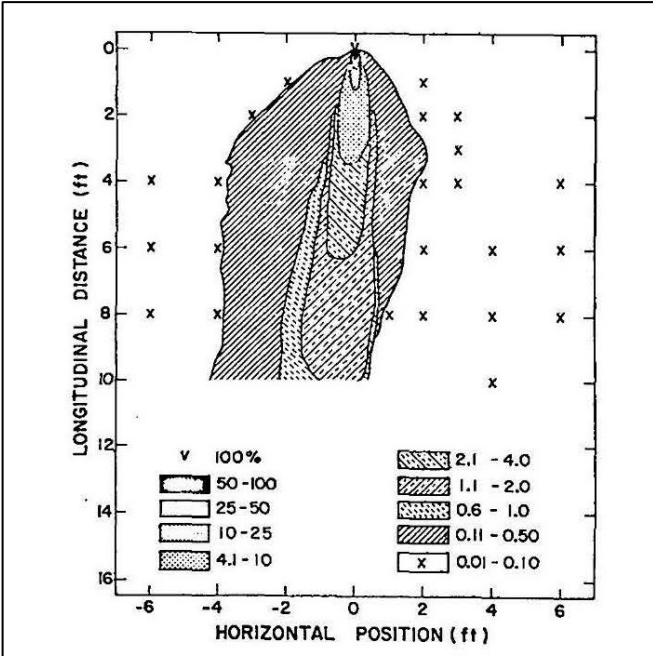
Fig. 2. Iso-concentration curves within horizontal plane at leak level, 12 room air changes per hour 0° angle air direction.
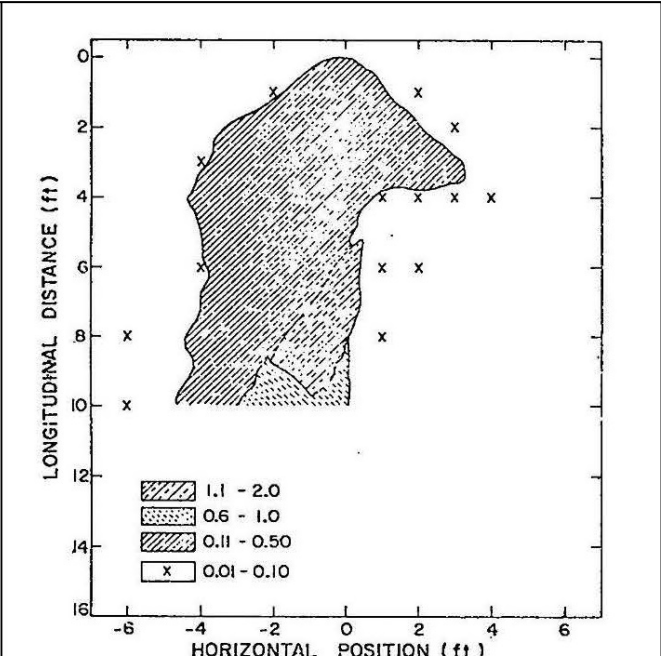
Fig. 5. Iso-concentration curves within horizontal plane 1 ft above leak level, 12 room air changes per hour, 0° angle air direction.

Graph for
2 ft above leak level
Not Provided in LA-5520-MS

Intentionally
Blank

Figure A-3. Graphs of iso-concentration curves for a 0° angle air direction and 12 AC/hr (Gonzales et al. 1974, p. 8 and 10).

ATTACHMENT A
GRAPHS FROM GONZALES ET AL. (continued)
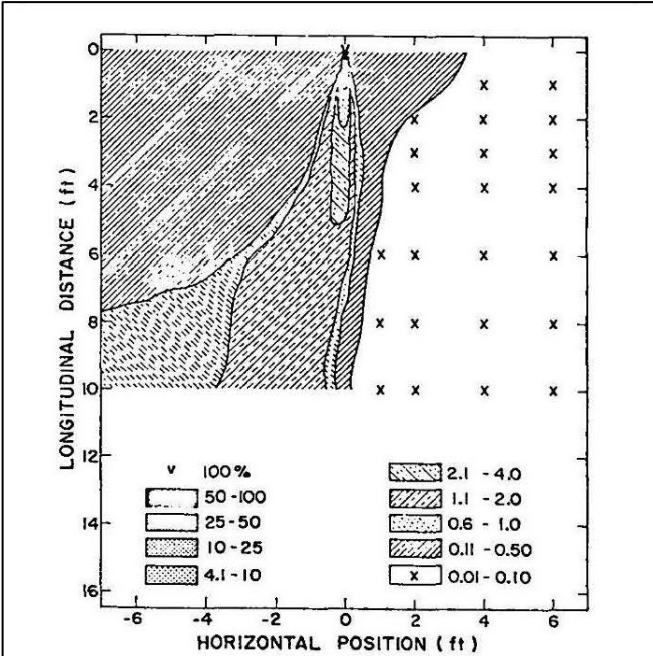
Fig. 11. Iso-concentration curves within horizontal plane at leak level, 6 room air changes per hour, 90° angle air direction.
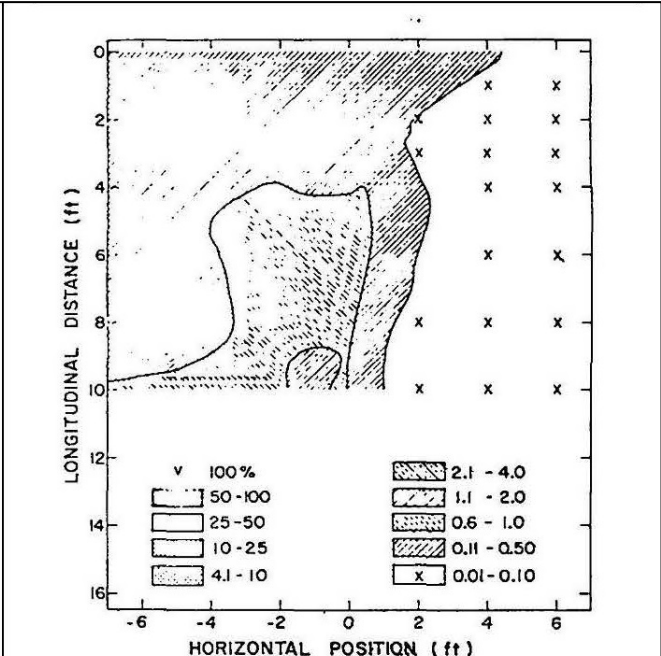
Fig. 13. Iso-concentration curves through horizontal plane 1 ft above leak level, 6 room air changes per hour, 90° angle air direction.

Graph for
2 ft above leak level
Not Provided in LA-5520-MS

Intentionally
Blank

Figure A-4. Graphs of iso-concentration curves for a 90° angle air direction and 6 AC/hr (Gonzales et al. 1974, p. 11-12).

ATTACHMENT A
GRAPHS FROM GONZALES ET AL. (continued)
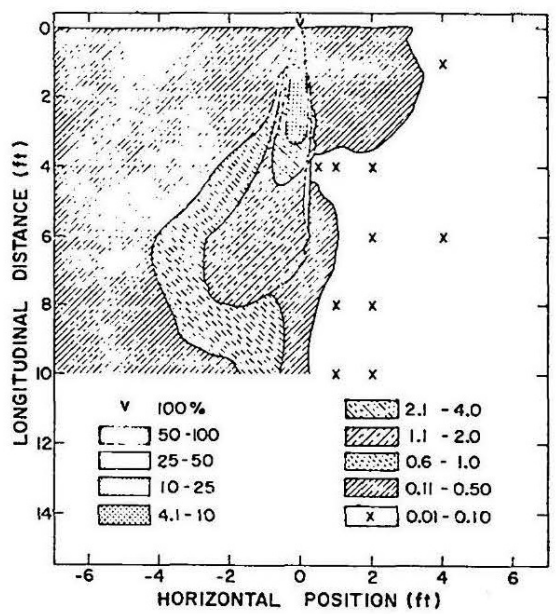
Fig. 10. Iso-concentration curves within horizontal plane at leak level, 9 room air changes per hour, 90° angle air direction.

Graph for
1 ft above leak level
Not Provided in LA-5520-MS

Graph for
2 ft above leak level
Not Provided in LA-5520-MS

Intentionally
Blank

Figure A-5. Graphs of iso-concentration curves for a 90° angle air direction and 9 AC/hr (Gonzales et al. 1974, p. 11).

ATTACHMENT A
GRAPHS FROM GONZALES ET AL. (continued)
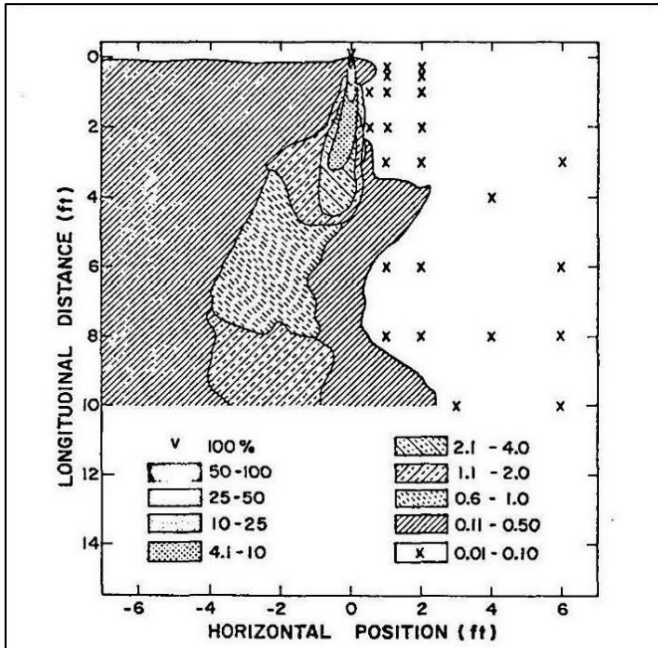
Fig. 9. Iso-concentration curves within horizontal plane at leak level, 12 room air changes per hour, 90° angle air direction.
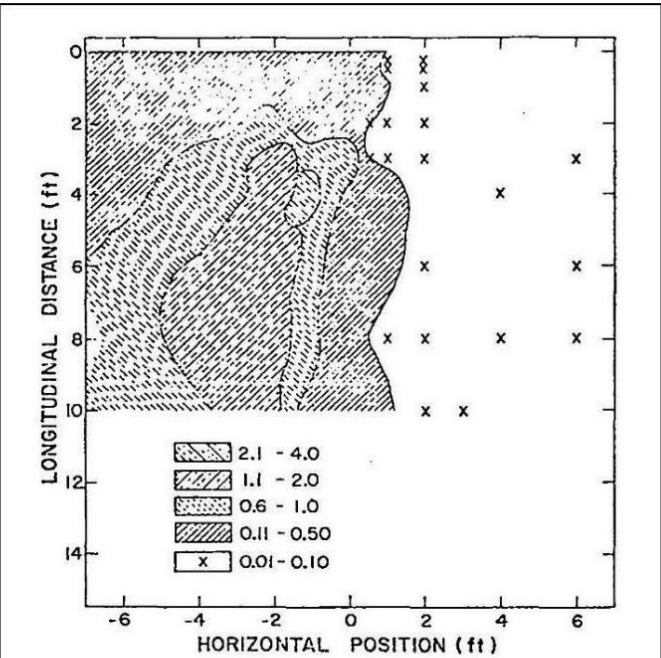
Fig. 12. Iso-concentration curves through horizontal plane 1 ft above leak level, 12 room air changes per hour, 90° angle air direction.
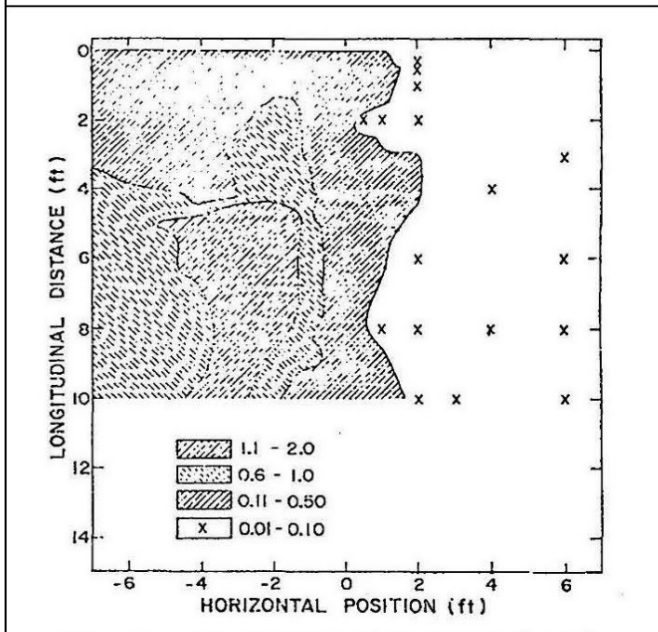
Fig. 14. Iso-concentration curves through horizontal plane 2 ft above leak level, 12 room air changes per hour, 90° angle air direction.
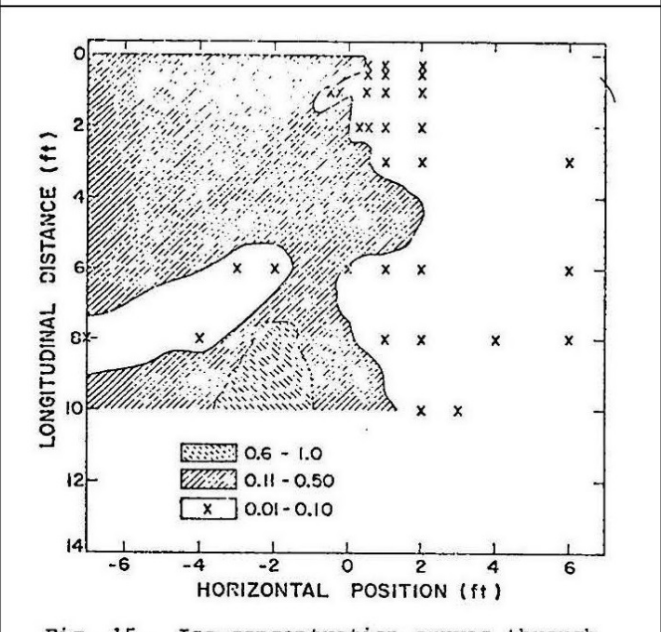
Fig. 15. Iso-concentration curves through horizontal plane 1 ft below leak level, 12 room air changes per hour, 90° angle air direction.

Figure A-6. Graphs of iso-concentration curves for a 90° angle air direction and 12 AC/hr (Gonzales et al. 1974, p. 11-13).

ATTACHMENT A
GRAPHS FROM GONZALES ET AL. (continued)
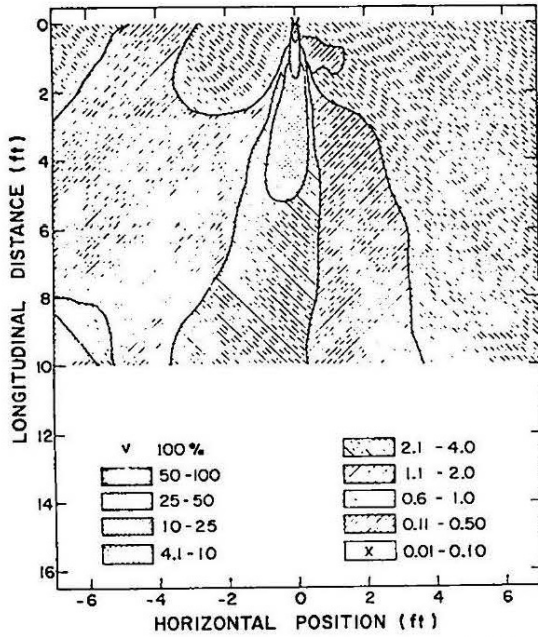
Fig. 17. Iso-concentration curves within horizontal plane at leak level, 6 room air changes per hour, 180° angle air direction.
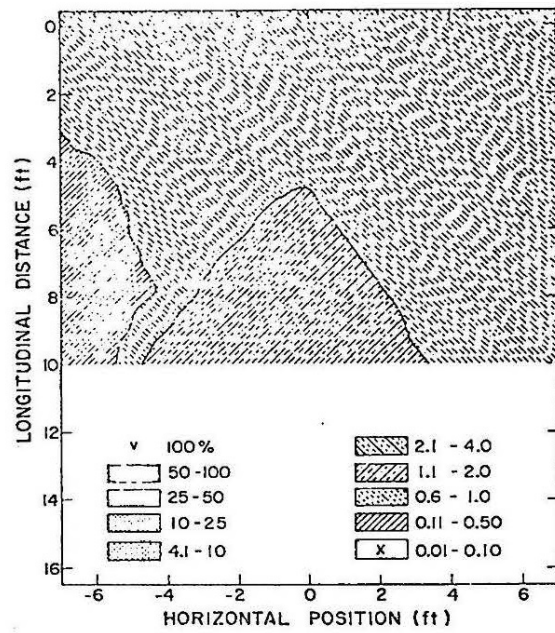
Fig. 19. Iso-concentration curves through horizontal plane 1 ft above leak level, 6 room air changes per hour, 180° angle air direction.

Graph for
2 ft above leak level
Not Provided in LA-5520-MS

Intentionally
Blank

Figure A-7. Graphs of iso-concentration curves for a 180° angle air direction and 6 AC/hr (Gonzales et al. 1974, p. 14).

ATTACHMENT A
GRAPHS FROM GONZALES ET AL. (continued)
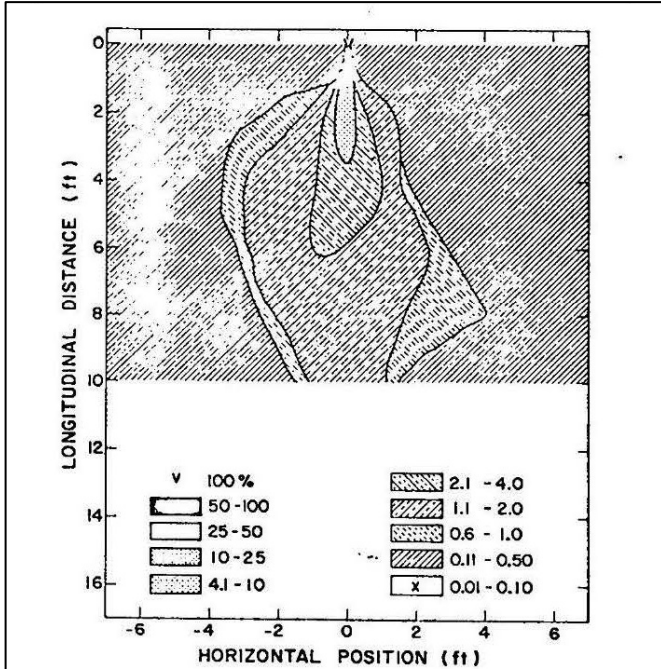
Fig. 16. Iso-concentration curves within horizontal plane at leak level, 12 room air changes per hour, 180° angle air direction.
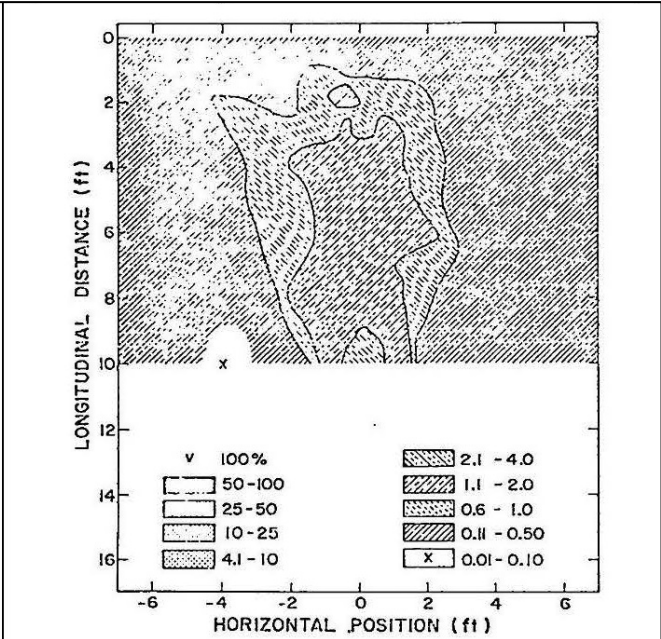
Fig. 18. Iso-concentration curves through horizontal plane 1 ft above leak level, 12 room air changes per hour, 180° angle air direction.

Graph for
2 ft above leak level
Not Provided in LA-5520-MS

Intentionally
Blank

Figure A-8. Graphs of iso-concentration curves for a 180° angle air direction and 12 AC/hr (Gonzales et al. 1974, p. 13-14).

ATTACHMENT B
REGION AREA FRACTIONS FROM ORAUT (2019c)

LIST OF FIGURES

ATTACHMENT B
REGION AREA FRACTIONS FROM ORAUT (2019c) (continued)

Figures B-1 through B-4 provide summaries of the calculated area fractions for Scenarios 1A, 1B, 2A, and 2B, which were calculated in ORAUT (2019c).

Figure 5:

Conc. Region	BZ Area Fractions by Region	GA Area Fractions by Region
R1	0.00000	0.67219
R2	1.00000	0.27075
R3	0.00000	0.03688
R4	0.00000	0.02018
R5	0.00000	0.00000
Sum	1.00000	1.00000

Figure 6:

Conc. Region	BZ Area Fractions by Region	GA Area Fractions by Region
R1	0.00000	0.14584
R2	1.00000	0.53461
R3	0.00000	0.25852
R4	0.00000	0.06103
R5	0.00000	0.00000
Sum	1.00000	1.00000

Figure 7:

Conc. Region	BZ Area Fractions by Region	GA Area Fractions by Region
R1	0.00000	0.04298
R2	1.00000	0.53396
R3	0.00000	0.42306
R4	0.00000	0.00000
R5	0.00000	0.00000
Sum	1.00000	1.00000

Figure 8:

Conc. Region	BZ Area Fractions by Region	GA Area Fractions by Region
R1	0.00000	0.21221
R2	1.00000	0.67218
R3	0.00000	0.11561
R4	0.00000	0.00000
R5	0.00000	0.00000
Sum	1.00000	1.00000

Figure 12:

Conc. Region	BZ Area Fractions by Region	GA Area Fractions by Region
R1	0.00000	0.42071
R2	1.00000	0.25476
R3	0.00000	0.18699
R4	0.00000	0.13053
R5	0.00000	0.00701
Sum	1.00000	1.00000

Figure 13:

Conc. Region	BZ Area Fractions by Region	GA Area Fractions by Region
R1	0.00000	0.35451
R2	1.00000	0.46100
R3	0.00000	0.17217
R4	0.00000	0.01232
R5	0.00000	0.00000
Sum	1.00000	1.00000

Figure 14:

Conc. Region	BZ Area Fractions by Region	GA Area Fractions by Region
R1	0.00000	0.41274
R2	1.00000	0.28525
R3	0.00000	0.20210
R4	0.00000	0.09991
R5	0.00000	0.00000
Sum	1.00000	1.00000

Figure 18:

Conc. Region	BZ Area Fractions by Region	GA Area Fractions by Region
R1	0.00000	0.00909
R2	1.00000	0.67210
R3	0.00000	0.16259
R4	0.00000	0.15622
R5	0.00000	0.00000
Sum	1.00000	1.00000

Figure 19:

Conc. Region	BZ Area Fractions by Region	GA Area Fractions by Region
R1	0.00000	0.00000
R2	0.00000	0.08790
R3	1.00000	0.74014
R4	0.00000	0.17196
R5	0.00000	0.00000
Sum	1.00000	1.00000

Figure B-1. Calculated region area fractions for Scenario 1A (ORAUT 2019c).

ATTACHMENT B
REGION AREA FRACTIONS FROM ORAUT (2019c) (continued)

Figure 5:

Conc. Region	BZ Area Fractions by Region	GA Area Fractions by Region
R1	0.00000	0.74665
R2	1.00000	0.19585
R3	0.00000	0.04501
R4	0.00000	0.01249
R5	0.00000	0.00000
Sum	1.00000	1.00000

Figure 6:

Conc. Region	BZ Area Fractions by Region	GA Area Fractions by Region
R1	0.00000	0.17644
R2	1.00000	0.57297
R3	0.00000	0.17913
R4	0.00000	0.07146
R5	0.00000	0.00000
Sum	1.00000	1.00000

Figure 7:

Conc. Region	BZ Area Fractions by Region	GA Area Fractions by Region
R1	0.00000	0.05252
R2	1.00000	0.57346
R3	0.00000	0.37403
R4	0.00000	0.00000
R5	0.00000	0.00000
Sum	1.00000	1.00001

Figure 8:

Conc. Region	BZ Area Fractions by Region	GA Area Fractions by Region
R1	0.00000	0.25659
R2	1.00000	0.65987
R3	0.00000	0.08354
R4	0.00000	0.00000
R5	0.00000	0.00000
Sum	1.00000	1.00000

Figure 12:

Conc. Region	BZ Area Fractions by Region	GA Area Fractions by Region
R1	0.00000	0.44980
R2	1.00000	0.24790
R3	0.00000	0.19601
R4	0.00000	0.10629
R5	0.00000	0.00000
Sum	1.00000	1.00000

Figure 13:

Conc. Region	BZ Area Fractions by Region	GA Area Fractions by Region
R1	0.00000	0.39581
R2	1.00000	0.47130
R3	0.00000	0.11800
R4	0.00000	0.01489
R5	0.00000	0.00000
Sum	1.00000	1.00000

Figure 14:

Conc. Region	BZ Area Fractions by Region	GA Area Fractions by Region
R1	0.00000	0.44662
R2	1.00000	0.26459
R3	0.00000	0.20526
R4	0.00000	0.08353
R5	0.00000	0.00000
Sum	1.00000	1.00000

Figure 18:

Conc. Region	BZ Area Fractions by Region	GA Area Fractions by Region
R1	0.00000	0.01095
R2	1.00000	0.79487
R3	0.00000	0.11320
R4	0.00000	0.08097
R5	0.00000	0.00000
Sum	1.00000	0.99999

Figure 19:

Conc. Region	BZ Area Fractions by Region	GA Area Fractions by Region
R1	0.00000	0.00000
R2	0.00000	0.10589
R3	1.00000	0.73310
R4	0.00000	0.16101
R5	0.00000	0.00000
Sum	1.00000	1.00000

Figure B-2. Calculated region area fractions for Scenario 1B (ORAUT 2019c).

ATTACHMENT B
REGION AREA FRACTIONS FROM ORAUT (2019c) (continued)

Figure 5:

Conc. Region	BZ Area Fractions by Region	GA Area Fractions by Region
R1	0.67219	0.67219
R2	0.27075	0.27075
R3	0.03688	0.03688
R4	0.02018	0.02018
R5	0.00000	0.00000
Sum	1.00000	1.00000

Figure 6:

Conc. Region	BZ Area Fractions by Region	GA Area Fractions by Region
R1	0.14584	0.14584
R2	0.53461	0.53461
R3	0.25852	0.25852
R4	0.06103	0.06103
R5	0.00000	0.00000
Sum	1.00000	1.00000

Figure 7:

Conc. Region	BZ Area Fractions by Region	GA Area Fractions by Region
R1	0.04298	0.04298
R2	0.53396	0.53396
R3	0.42306	0.42306
R4	0.00000	0.00000
R5	0.00000	0.00000
Sum	1.00000	1.00000

Figure 8:

Conc. Region	BZ Area Fractions by Region	GA Area Fractions by Region
R1	0.21221	0.21221
R2	0.67218	0.67218
R3	0.11561	0.11561
R4	0.00000	0.00000
R5	0.00000	0.00000
Sum	1.00000	1.00000

Figure 12:

Conc. Region	BZ Area Fractions by Region	GA Area Fractions by Region
R1	0.42071	0.42071
R2	0.25476	0.25476
R3	0.18699	0.18699
R4	0.13053	0.13053
R5	0.00701	0.00701
Sum	1.00000	1.00000

Figure 13:

Conc. Region	BZ Area Fractions by Region	GA Area Fractions by Region
R1	0.35451	0.35451
R2	0.46100	0.46100
R3	0.17217	0.17217
R4	0.01232	0.01232
R5	0.00000	0.00000
Sum	1.00000	1.00000

Figure 14:

Conc. Region	BZ Area Fractions by Region	GA Area Fractions by Region
R1	0.41274	0.41274
R2	0.28525	0.28525
R3	0.20210	0.20210
R4	0.09991	0.09991
R5	0.00000	0.00000
Sum	1.00000	1.00000

Figure 18:

Conc. Region	BZ Area Fractions by Region	GA Area Fractions by Region
R1	0.00909	0.00909
R2	0.67210	0.67210
R3	0.16259	0.16259
R4	0.15622	0.15622
R5	0.00000	0.00000
Sum	1.00000	1.00000

Figure 19:

Conc. Region	BZ Area Fractions by Region	GA Area Fractions by Region
R1	0.00000	0.00000
R2	0.08790	0.08790
R3	0.74014	0.74014
R4	0.17196	0.17196
R5	0.00000	0.00000
Sum	1.00000	1.00000

Figure B-3. Calculated region area fractions for Scenario 2A (ORAUT 2019c).

ATTACHMENT B
REGION AREA FRACTIONS FROM ORAUT (2019c) (continued)

Figure 5:

Conc. Region	BZ Area Fractions by Region	GA Area Fractions by Region
R1	0.67219	0.74665
R2	0.27075	0.19585
R3	0.03688	0.04501
R4	0.02018	0.01249
R5	0.00000	0.00000
Sum	1.00000	1.00000

Figure 6:

Conc. Region	BZ Area Fractions by Region	GA Area Fractions by Region
R1	0.14584	0.17644
R2	0.53461	0.57297
R3	0.25852	0.17913
R4	0.06103	0.07146
R5	0.00000	0.00000
Sum	1.00000	1.00000

Figure 7:

Conc. Region	BZ Area Fractions by Region	GA Area Fractions by Region
R1	0.04298	0.05252
R2	0.53396	0.57346
R3	0.42306	0.37403
R4	0.00000	0.00000
R5	0.00000	0.00000
Sum	1.00000	1.00001

Figure 8:

Conc. Region	BZ Area Fractions by Region	GA Area Fractions by Region
R1	0.21221	0.25659
R2	0.67218	0.65987
R3	0.11561	0.08354
R4	0.00000	0.00000
R5	0.00000	0.00000
Sum	1.00000	1.00000

Figure 12:

Conc. Region	BZ Area Fractions by Region	GA Area Fractions by Region
R1	0.42071	0.44980
R2	0.25476	0.24790
R3	0.18699	0.19601
R4	0.13053	0.10629
R5	0.00701	0.00000
Sum	1.00000	1.00000

Figure 13:

Conc. Region	BZ Area Fractions by Region	GA Area Fractions by Region
R1	0.35451	0.39581
R2	0.46100	0.47130
R3	0.17217	0.11800
R4	0.01232	0.01489
R5	0.00000	0.00000
Sum	1.00000	1.00000

Figure 14:

Conc. Region	BZ Area Fractions by Region	GA Area Fractions by Region
R1	0.41274	0.44662
R2	0.28525	0.26459
R3	0.20210	0.20526
R4	0.09991	0.08353
R5	0.00000	0.00000
Sum	1.00000	1.00000

Figure 18:

Conc. Region	BZ Area Fractions by Region	GA Area Fractions by Region
R1	0.00909	0.01095
R2	0.67210	0.79487
R3	0.16259	0.11320
R4	0.15622	0.08097
R5	0.00000	0.00000
Sum	1.00000	0.99999

Figure 19:

Conc. Region	BZ Area Fractions by Region	GA Area Fractions by Region
R1	0.00000	0.00000
R2	0.08790	0.10589
R3	0.74014	0.73310
R4	0.17196	0.16101
R5	0.00000	0.00000
Sum	1.00000	1.00000

Figure B-4. Calculated region area fractions for Scenario 2B (ORAUT 2019c).